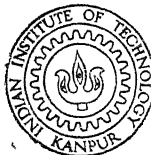


STUDIES OF LATERALLY LOADED PILE IN ELASTO-PLASTIC SOIL

BY
MIHIR BARAN ROY

TH
CE/1970/m
R 8/25
CE
1970
M
ROY
STU



DEPARTMENT OF CIVIL ENGINEERING
INDIAN INSTITUTE OF TECHNOLOGY KANPUR
JUNE 1970

STUDIES OF Laterally Loaded Pile in ELASTO-PLASTIC SOIL

A Thesis Submitted
In Partial Fulfilment of the Requirements
for the Degree of
MASTER OF TECHNOLOGY



BY
MIHIR BARAN ROY

POST GRADUATE OFFICE
This thesis has been approved
for the award of the Degree of
Master of Technology (M.Tech.)
in accordance with the
regulations of the Indian
Institute of Technology Kanpur
Dated. 3/7/71

to the

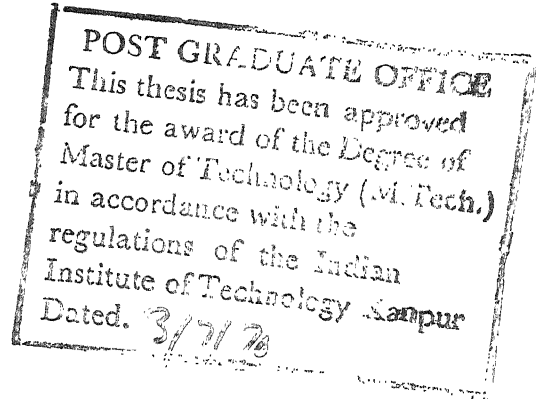
CE-1970-M-ROY-STU

DEPARTMENT OF CIVIL ENGINEERING
INDIAN INSTITUTE OF TECHNOLOGY KANPUR
JUNE 1970

CERTIFICATE

Certified that the work presented in this thesis has been carried out by Shri M.B. Roy under my supervision and has not been submitted elsewhere for a degree.

(M. R. Madhav)
Asst. Professor
Department of Civil Engineering
Indian Institute of Technology, Kanpur



ACKNOWLEDGEMENT

The author is sincerely grateful to Dr. M.R. Madhav for suggesting the problem, his expert advice and patient counsel throughout the progress of the work.

The author gratefully acknowledges the service and cooperation extended by the members of the staff of Computer Center, I.I.T., Kanpur.

In addition, the author wishes to acknowledge all the faculty members in Soil Mechanics for their inspiring, invaluable advice and constant encouragement throughout the author's stay at I.I.T., Kanpur.

The author also gratefully acknowledges Mr. Lakshmidhar, Mr. Goyal, Mr. Hark Singh and Mr. Verma for their help in the experimental set-up.

The author gratefully acknowledges the following.

Mr. A.K. Mandal and Mr. P. Basudhar for their help in writing the manuscripts.

Mr. R. P. Trivedi for his nice and careful typing.

TABLE OF CONTENTS

	Page
CERTIFICATE	ii
ACKNOWLEDGEMENT	iii
TABLE OF CONTENTS	iv
LIST OF TABLES	vi
LIST OF FIGURES	vii
LIST OF SYMBOLS	x
ABSTRACT	xii
CHAPTER I INTRODUCTION	
1.1 General	1
1.2 Soil-Pile Interaction	2
1.3 Modulus of Sub-grade Reaction 'k'	3
1.4 The existing solutions	7
1.5 Variation of 'k' with depth	9
1.6 Non-dimensional Solutions	11
1.7 Experimental study of Laterally Loaded Piles	13
CHAPTER II ELASTO-PLASTIC BEHAVIOR OF LATERALLY LOADED PILES.	
2.1 Pile Behavior	17
2.2 Soil Behavior	17
2.3 Model proposed	20
2.4 Formulation of the Problem	27
2.5 Non-dimensionalising the equations	30
2.6 Solutions	32

CHAPTER	III	FREE-FREE AND FIXED-FREE PILES	
		3.1 Introduction	40
		3.2 Free-free pile	40
		3.3 Fixed-free pile	42
		3.4 Discussion of results	44
CHAPTER	IV	OVERHANG PILE	
		4.1 Introduction	74
		4.2 Pile Behavior	74
		4.3 Soil Behavior	74
		4.4 Formulation of the problem	76
		4.5 Solution	80
		4.6 Discussion of results	84
CHAPTER	V	EXPERIMENTAL VERIFICATION	
		5.1 Introduction	95
		5.2 Soil Behavior	96
		5.3 Experimental set-up	97
		5.4 Calibration of test pile	103
		5.5 Data collection	103
		5.6 Discussion of results	105
CHAPTER	VI	DISCUSSION AND CONCLUSION :	112
		APPENDIX A	115
		APPENDIX B	117
		REFERENCES	120

LIST OF TABLES

Table No.		Page
2.1	Non-dimensional co-efficients	33
3.1	Boundary & continuity conditions Type I, Free-free pile	41
3.2	Boundary & continuity conditions Type II, fixed-free pile	43
4.1	Boundary & continuity conditions Free-free pile with overhang	81
5.1	Calibration of the test pile for moment.	104
B-1	Values of α_2 for α_1 ($d=0$)	119

LIST OF FIGURES

Figure		Page
1.1	Variation of k with depth for different types of soils	5
1.2 a	Variation of k with depth	10
1.2 b	Variation of m with depth	10
2.1	Deflected shape of laterally loaded pile	18
2.2	Different stages of pile soil interaction.	21
2.3	Model for elasto-plastic behavior of soil	22
2.4	Proposed model for elasto-plastic behavior of pile.	24
2.5	Stress-strain response of soil	25
2.6	Four stages of the pile in action	28
2.7	Pressure distribution for ultimate load (free-free pile, load at top).	36
2.8	Deflected shape of fixed-free pile	37
3.1	Load-deflection curve for various Z_m	46
3.2(a&b)	Load-deflection curve for short pile.	47
3.3(a&b)	Load-deflection curve for long pile	48
3.4(a)	Relation between α_1 and top deflection.	49
3.4(b)	Relation between α_1 and γ	49
3.5	Effect of r_0 and m_0 on pile deflection and shear distribution	50
3.6	Variation of deflection, BM, SF and soil pressure with α_1 - short pile.	51
3.7	Variation of deflection, BM, SF and soil pressure with α_1 - long pile.	52

3.8(a&b)	Moment-deflection relation for different Z_m .	56
3.9	Moment-deflection relation for different Z_m .	57
3.10(a&b)	Moment-deflection relation for different m_o and r_o .	58
3.11(a&b)	Effect of r_o and m_o on deflection and bending moment.	59
3.12	Variation of deflection, BM, SF and soil pressure with α_1 - short pile.	60
3.13	Variation of deflection, BM, SF and soil pressure with α_1 - short pile (for $d=1$).	61
3.14	Variation of deflection, BM, SF and soil pressure with α_1 - long pile.	62
3.15(a&b)	Effect of r_o on load-deflection relationship.	66
3.16(a&b)	Effect of m_o on load-deflection relationship.	67
3.17(a&b)	Effect of d on load-deflection relationship.	68
3.18	Effect of r_o on deflection, BM, SF and soil pressure - long pile.	69
3.19	Deflection, BM, SF and soil pressure Distribution - short pile	70
3.20	Deflection, BM, SF and soil pressure distribution - long pile (stage 2)	71
3.21	Deflection, BM, SF and soil pressure distribution - long pile (stage 3).	72
3.22	Ultimate load-free-free pile.	73
4.1	Deflected shape of overhang pile	75
4.2	Four stages of overhang pile	77
4.3	Model for overhang pile	78
4.4	Pressure distribution for ultimate load overhang pile.	82

4.5 (a&b)	Effect of r_0 on load deflection relation	87
4.6 (a&b)	Effect of m_0 on load deflection relation	88
4.7 (a&b)	Effect of d on load deflection relation	89
4.8 (a&b)	Effect of r_0 and m_0 on deflection and shear distribution.	90
4.9	Variation of α_3 with α_2 for different α_1	91
4.10	Variation of deflection, BM, SF and soil pressure with α_2 - short pile	92
4.11	Variation of deflection, BM, SF and soil pressure with α_2 - long pile	93
4.12(a&b)	Ultimate load - overhang pile	94
5.1	Results of shear box test.	98
5.2	Experimental set-up	99
5.3 (a&b)	Model pile assembly.	101
5.4	Shape of soil surface after failure.	108
5.5	Load-deflection relations for different pile lengths	109
5.6	Load-deflection cycle for aluminium pile	110
5.7	Bending moment distribution along the pile length for different loads	111

LIST OF SYMBOLS

A_y	Non-dimensional deflection coefficient for load.
A_s, A_m, A_v, A_p	Non-dimensional coefficients relating to applied load P_t , for slope, moment, shear and soil reaction respectively.
a	Constant for variation of soil property.
B	Pile width
B_y, B_s, B_m, B_v, B_p	Non-dimensional co-efficients relating to applied moment M_t , for deflection, slope, moment, shear and soil reaction respectively.
d	Non-dimensional constant for variation of soil property with depth.
e	Void ratio of soil
EI	Flexural stiffness of pile, the product of modulus of elasticity and moment of inertia of pile cross-section, in pound inch ² .
G	Specific gravity of soil
h	Total height of pile.
k	Modulus of sub-grade reaction.
K	Modulus of sub-grade reaction at the bottom of pile.
k_0, k_1, k_2	Constants of soil modulus variation.
L	Total length of pile
M	Moment.
M_t	Moment at top of pile.
m	Non-dimensional ultimate resistance of soil.
m_o	Non-dimensional ultimate soil-resistance at the top of soil surface.

N	Shear
n	Real positive constant used as exponent.
P_t	Load at top of pile.
P_u	Ultimate load of pile.
p	Soil reaction per unit length of pile
q, q_0	Ultimate soil resistance.
r_0	Stiffness ratio.
T	Chracteristic length.
t	Pile width
x	Depth below the point of load application.
y	Lateral deflection of pile
Z	Depth coefficient.
Z_{\max} or Z_m	Maximum value of depth coefficient = $\frac{L}{T}$.
$\gamma, \alpha_1, \alpha_2, \alpha_3$	The ratio of Z_1, Z_2 and Z_3 to Z_{\max} , being the depth, at which soil behavior changes from plastic to elastic or the reverse.
ϵ	Strain.

ABSTRACT

This thesis incorporates some studies carried out on the behavior of a laterally loaded pile. A brief review of existing literature on the problem is reported. Only behavior under static load is studied in this work.

The behavior of a pile in elasto-plastic soil is analysed. The soil is considered to behave elastically upto a certain limit of pile deflection, giving rise to a Winkler type of model. After the particular limit is exceeded, the soil flows plastically and the pile behavior changes. Accordingly, a laterally loaded pile behavior is divided into four distinct stages, starting from fully elastic to fully plastic soil behavior. A model is proposed to represent the elasto-plastic behavior of a given soil.

Non-dimensional closed form solutions are obtained for a variety of cases of pile behavior, like, free-free, fixed-free and piles with overhang with load and moment applied at top, for plastic yield occurring at the top and bottom of the pile. The effect of soil and pile parameters viz., the modulus of sub-grade reaction, the yield strength of soil, the modulus of elasticity, moment of inertia of the pile and pile length are brought out. Attempts have made to find the ultimate load capacity of a pile from the principle of statics. Lastly, experiments with model pile has been conducted which show agreement with the theory developed, assuming the soil to behave as elasto-plastic medium.

CHAPTER I

INTRODUCTION

1.1 GENERAL:

Piles, in general are used to transfer load from a Civil Engineering construction to earth. For the safety and proper functioning of the structure, certain restriction regarding load capacity, deflection, settlement etc. are to be taken into consideration for the design of a pile. Uptil now, attention was mostly paid for the study and design of piles carrying vertical load and/or moment only. Sandeman observed the deflection of laterally loaded pile as early as 1880. The need for the study of the behavior of laterally loaded pile, and the investigations for the design criteria, came about very recently with the development of on-shore structures and oil drilling rigs etc (26)*. Lateral loads from wind and wave are frequently the most critical factors in the design of such structures. Analysis of laterally loaded piles also apply to a variety of off-shore structures; such as poles of high tension power cables, pile support for earthquake restraint structures etc. A few industrial building foundations, receiving horizontal loads, or blasting thrust, need laterally loaded piles (19).

The problem of laterally loaded pile is closely related to the familiar problem of a beam on an elastic

*The numbers in the bracket represent the reference number given at the end.

foundation; however in one respect, it represents a specialised case. All external forces and moments are applied at one point i.e. at the top of the pile. On the other hand, if a pile suffers large deflection or rotation due to applied load, the problem is much more complicated due to the nonlinear characteristics of the soil and this needs generalisation of the beam-on-elastic-foundation theory.

1.2 SOIL-PILE INTERACTION:

Flexural and axial stresses of a pile are to be correctly analysed to design a safe and economic pile. So, the interaction between the soil and the pile is to be carefully analysed when the lateral load is acting. Since the problem deals with the soil, as well as the pile, a knowledge of the behavior of both is necessary.

The soil characteristics are to be determined first. A soil medium is not perfectly elastic at all values of strain. At small strains, soil behaviour can be approximated to be elastic. A laterally loaded pile, suffers the maximum displacement near the top and it is quite likely that the soil in this zone behaves inelastically. If the pile is a short-pile deflection near the bottom of the pile will also be quite high, in comparison to that at the middle zone. So the soil at the bottom of the pile may behave inelastically depending upon the

length, load and moment applied on the pile. Deflection being comparatively small in the middle zone of the pile, the soil is assumed to behave elastically.

1.3 MODULUS OF SUBGRADE REACTION 'k':

The modulus of subgrade reaction 'k' plays an important role in the soil-pile interaction. This is defined as "the pressure required per unit deformation calculated at 0.05 inch of deformation". According to Terzaghi (46), 'k' is defined as the pressure required per unit area of the surface of contact between a loaded beam or a slab and the subgrade on which it rests and onto which it transfers the load, and he named it as the "coefficient of subgrade reaction" 'k'.

In most cases, the soil modulus values tend to increase with depth. The principal reasons are:

(1). soils frequently increase their strength parameters with depth as a result of overburden pressure, and (2). pile deflections decrease with depth for any given loading, and the corresponding equivalent elastic moduli of soil reaction tend to increase at small deflection.

'k' is usually expressed as a function of depth of the pile.

$$k = K\left(\frac{x}{L}\right)^n \quad \dots \quad (1.1)$$

where

x = depth along the pile

L = total length of the pile.

' k ' is constant for stiff clay and it varies linearly for sand. The value of ' n ' is zero for ~~clay~~ and unity, for sand. For any other type of soil the value of ' n ' is chosen between zero and one. Fig. (1.1) shows the variation of ' k ' with depth for different types of soils (44).

Broms (3) has defined ' k ' as

$$k = n_h \left(\frac{x}{B} \right) \quad \dots \quad (1.2)$$

where ' n_h ' varies with relative density of the soil and also with the location of the water-table. ' B ' is the width of the pile.

Siva Reddy and Valsangkar (41) assumed ' k ' to be of the form

$$k = k_0 + k_1 x^2 \quad \dots \quad (1.3)$$

where k_0 = value of k at surface

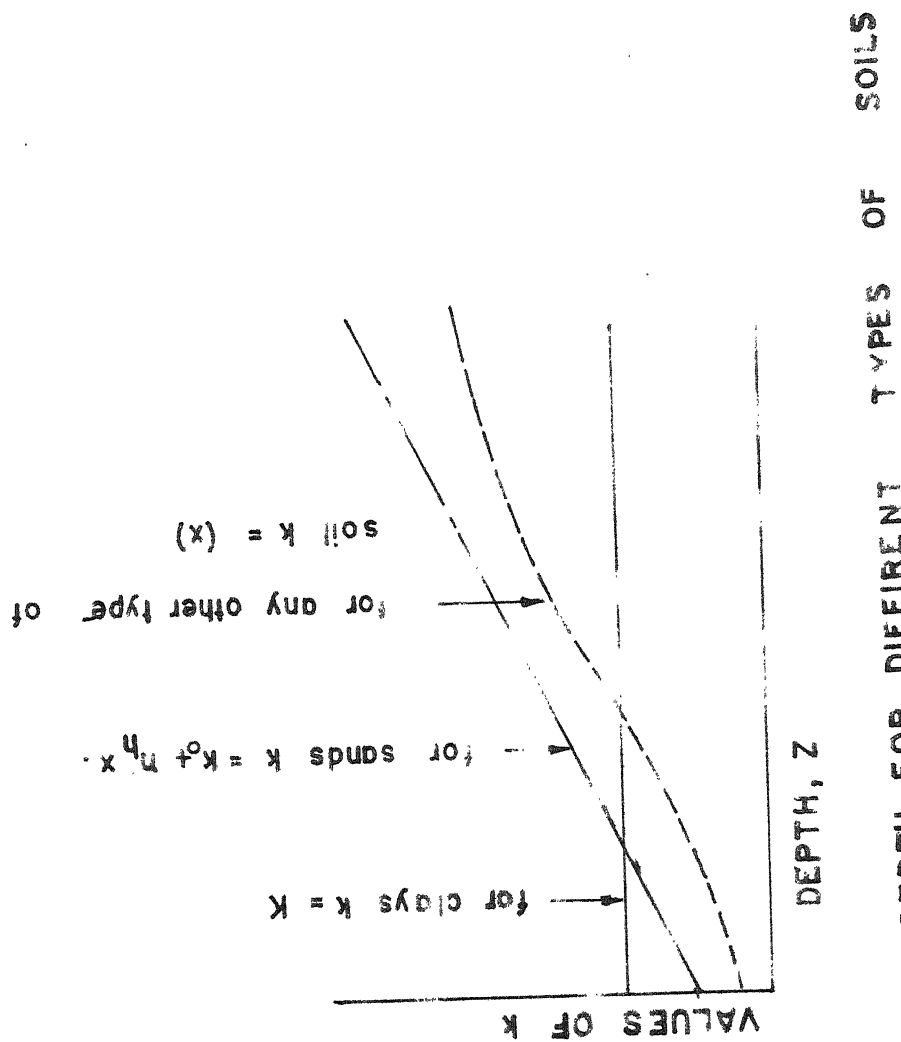
k_1 = value of k at the bottom of pile.

Snitko (43) chose the variation of ' k ' with depth as;

$$k(x) = k_h \left[1 - \text{Exp.}(-Ex) \right] \text{ in exponential form } \dots (1.4)$$

$$k(x) = k_h \left(\frac{x}{h} \right)^n, \quad n < 1 \text{ in power function } \dots (1.5)$$

The above expressions are valid only for small displacements, for large displacement i.e. in the zone



FIG(1-1) VARIATION OF k WITH DEPTH FOR DIFFERENT TYPES OF SOILS

of plastic deformation,

$$k(x) = k_h \left(\frac{x}{h}\right)^2 \quad \dots (1.6)$$

These relations have been verified by experiments.

Broms (3) calculated the ultimate lateral resistance of the pile by assuming the piles are transformed into a mechanism through the formation of plastic hinges. The ultimate resistance of a short pile is governed by the ultimate lateral resistance of the surrounding cohesive soil and that for long piles are governed by the yield resistance of the pile sections.

Two serious limitations of his analysis are:

(a) the deflection at working loads of a laterally loaded pile should not be so excessive as to impair the proper function of the member,

(b) its ultimate strength should be sufficiently high as to guard against complete collapse even under the most unfortunate combination of factors.

Kubo (23) from his study of model sheet piles concluded that the co-efficient of soil reaction 'k' decreases with the increase of pile width, but becomes almost constant when the pile width exceeds 20 cms. He has also shown that the soil pressure and pile deflection is connected by:

$$p = k x \cdot y^{0.5} \quad \dots (1.7)$$

In this work, it is assumed that the value of horizontal coefficient of subgrade reaction is the same as that in the vertical direction.

From the above discussion, it is apparent that, no soil can be uniquely represented by a mathematical expression or polynomial, which is valid for the whole length of the pile.

1.4 THE EXISTING SOLUTIONS:

The problem of laterally loaded pile is closely related to the problem of a beam on an elastic foundation, where the pile acts as a beam, the load and moment being applied at top and the soil behaves as the elastic medium.

Chang (6) has given the analytical solution for the static lateral loading. He solved the equation:

$$EI \frac{d^4 y}{d x^4} = p \quad \dots (1.8)$$

where $p = \text{soil pressure} = ky$

and presented the solution as:

$$y = C e^{-\beta x} (\cos \beta x + \sin \beta x)$$

the constants are to be found by using the boundary conditions.

Timoshenko (47) expressed the governing equation for beam deflection as:

$$EI \frac{d^4 y}{d x^4} = -ky \quad \dots (1.9)$$

and using the notation

$$\sqrt[4]{\frac{k}{4EI}} = \beta$$

The general solution, he represented as follows:

$$y = e^{\beta x} (A \cos \beta x + B \sin \beta x) + e^{-\beta x} (C \cos \beta x + D \sin \beta x) \dots (1.10)$$

The constants are determined from known boundary conditions.

Palmer and Brown (52) have given the solution of the basic differential equation in the form of difference equation, which is given for any point 'm' of the pile as follows:

$$\left(\frac{d^4 y}{dx^4} \right)_m = \frac{y_{m-2} - 4y_{m-1} + 6y_m - 4y_{m+1} + y_{m+2}}{\lambda^4} = \Delta^4 (y_m) \dots (1.11)$$

Siva Reddy and Valsangkar (42) have given the generalised solutions of laterally loaded piles with polynomial variation of soil modulus. The basic differential equation they suggested is

$$EI \frac{d^4 y}{dx^4} + \frac{d}{dx} \left[P(x) \frac{dy}{dx} \right] + k(x) y = 0 \dots (1.12)$$

where $P(x)$ is the axial force and the solutions are:

for cohesive soil: $y = C_0 \phi(\eta) + C_1 \phi_1(\eta) + C_2 \phi_2(\eta) + C_3 \phi_3(\eta)$

where $\phi(\eta)$ are polynomials.

for cohesionless soil: $y = F_0 f(Z) + F_1 f_1(Z) + F_2 f_2(Z) + F_3 f_3(Z)$

where $f(Z)$ are also polynomials. The constants

C and F are to be found from known boundary conditions.

1.5 VARIATION OF k WITH DEPTH:

These are some of the basic solutions for the problem. Improvements of the problem have been done by many engineers considering different parameters and their variations. One such important improvement is the variation of 'k' with depth.

Palmer and Brown (52) assumed the variation of 'k' with depth as:

$$k' = k \left(\frac{x}{L}\right)^n \quad \dots \quad (1.13)$$

where k' is the value of the soil modulus at any depth and ' k ' being the fixed value at the lower end of the pile. This is not an elastic modulus but corresponds to the Westerguard's ' k ' which is based on the assumption that the soil acts as a very dense liquid. They expressed the basic differential equation as:

$$EI \frac{d^4 y}{dx^4} = k \left(\frac{x}{L}\right)^n y \quad \dots \quad (1.14)$$

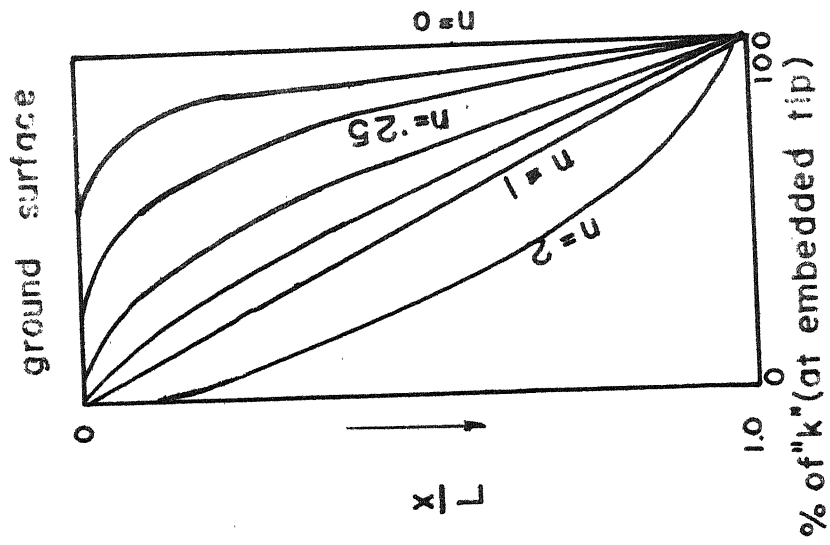
The values of percent of ' k ' at different depths for various values of n (ranging from zero to two) have been shown in Fig. (1.2(a)).

Palmer and Thompson (31) expressed ' k ' as

$$k' = k b \left[\frac{(t - m) L}{t} \right]^n \quad \dots \quad (1.15)$$

where,

b = width of the pile



FIG(1.2.a) VARIATION OF k WITH DEPTH
(after PALMER and BROWN)

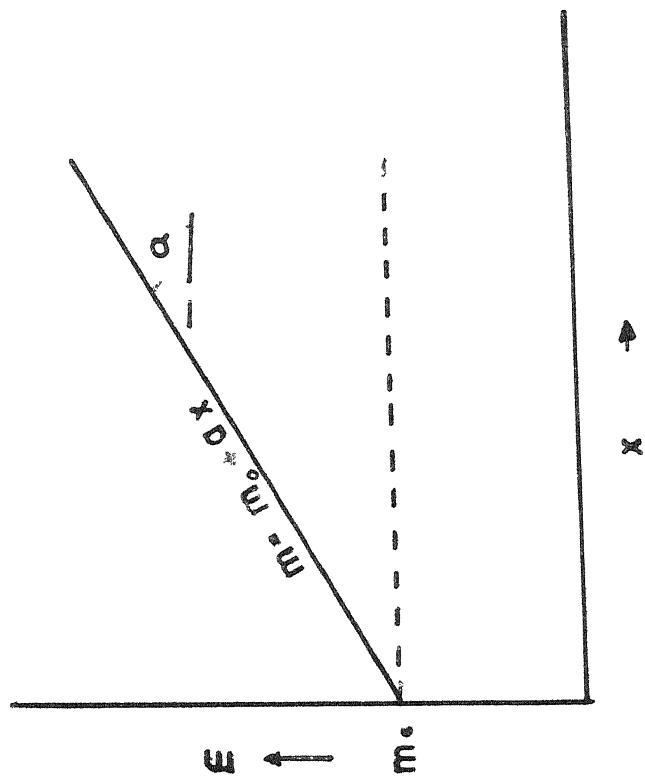


FIG (1.2b) VARIATION OF m WITH DEPTH

t = nos. of subdivisions of the pile

m = the point where 'k' value is desired

n = a positive constant between zero and one.

For homogeneous soil, this formula is quite appropriate.

MatLock and Reese (26) selected the form of soil modulus as:

$$\text{a power form: } k' = k x^n \quad \dots (1.16)$$

$$\text{and polynomial form: } k' = k_0 + k_1x + k_2x^2 \quad \dots (1.17)$$

The form $k' = kx$ is seen to be a special case of either of the above cases.

No unique value of 'k' can be attributed to a given soil. The pile deflection varies with the pile size, pile stiffness, the magnitude of the load, and the type of load (i.e. static or dynamic loading). So the soil modulus exists only as a mathematically convenient expression for the ratio of the soil reaction to the pile deflection.

1.6 NONDIMENSIONAL SOLUTIONS:

The principles of dimensional analyses may be used to establish the form of nondimensional relations for the laterally loaded pile. With the use of model theory, the necessary relations will be determined between a prototype, having any set of given dimensions and a similar model for which a solution may be available.

With the help of the principle of dimensional analysis, the equations of the laterally loaded pile can be reduced to a nondimensional form. The variables which have been dealt with, can be listed as:

- x = any depth of pile
- L = total length of pile
- k = soil modulus
- EI = of the pile
- P_t = load at top
- M_t = moment applied at top
- T = characteristic length.

The parameter T , which has the dimension of length, is a very useful tool to reduce all the parameters to a dimensionless form. Matlock and Reese (26) named this characteristic length as the "relative stiffness factor". But the definition of T vary with the form of the function of soil modulus. If ' k ' is expressed in lb/in²/in then

$$T = \sqrt[5]{\frac{EI}{k}} \quad \dots \quad (1.18)$$

and if ' k ' is expressed as lb/in², then

$$T = \sqrt[4]{\frac{EI}{k}} \quad \dots \quad (1.19)$$

For the case of applied shear P_t and moment M_t , the solution for the deflection may be expressed as

$$y = y(x, L, T, k, EI, P_t, M_t) \quad \dots \quad (1.20)$$

To satisfy the conditions of similarity, each of these groups must be equal for both model and prototype i.e.

$$\frac{x_p}{T_p} = \frac{x_m}{T_m} \quad \dots (1.21)$$

$$\frac{L_p}{T_p} = \frac{L_m}{T_m} \quad \dots (1.22)$$

$$\frac{k_p T_p^4}{EI_p} = \frac{k_m T_m^4}{EI_m} \quad \dots (1.23)$$

$$\frac{EI_p}{P_{tp} T_p} Y_{Ap} = \frac{EI_m}{P_{tm} T_m} Y_{Am} \quad \dots (1.24)$$

$$\frac{EI_p}{M_{tp} T_p^2} Y_{Bp} = \frac{EI_m}{M_{tm} T_m^2} Y_{Bm} \quad \dots (1.25)$$

where the suffix 'p' stands for prototype and 'm' stands for model pile. All these nondimensional parameters will be used to find the solutions for various cases in subsequent chapters.

1.7 EXPERIMENTAL STUDY OF LATERALLY LOADED PILES:

The settlement of piles under vertical loads during driving was observed for the first time by Personet in eighteenth century. The load-displacement study of laterally loaded pile was first done by Sandeman in 1880.

Feagin (12) conducted a number of lateral load tests on single and on group of timber and concrete piles. He concluded that for less than 6.5 tons of load per pile, the group effect is not significant. The

deflection was found to increase with repetition of load.

McCammon and Ascherman (29) tested a large number of hollow laterally loaded piles, driven into the bottom of Lake Maracaibo, Venezuela. They concluded that the soil acts as elastic medium when resisting lateral loads. The point of maximum bending moment occurs about 2-diameter below mud-line. One important conclusion they have drawn is that the effective point of fixation continues to move downwards as larger loads are applied, even though the point of maximum moment essentially remains at fixed elevation.

Based on the results of model tests, Tschebotarioff (51) concluded that resistance per pile to lateral loads decreases appreciably with an increasing number of piles in a group.

Wagner (51) conducted a large number of tests on laterally loaded timber piles and he concluded:

- 1..Overdriving reduces the lateral resistance of a pile..
- 2..Increase in length does not improve the lateral resistance appreciably, provided the pile is sufficiently embedded.
3. The strength and type of material within the first 20 ft.. of depth have considerable effect on the lateral resistance of the pile..

Gleser (51) on the basis of tests on hollow piles has drawn two important conclusions:

1. A pile with head so fixed as to constrain it to remain vertical, will assume an S or ogee shape, when subjected to lateral load.

2. Depending on the type of soil, some portion of the soil surrounding the pile undergoes an irreversible deformation.

Therefore, from the limited study of the present literature, it is quite evident that the problem of laterally loaded pile needs careful study of the different parameters. In this investigation, the soil behaviour is idealised on being elastic at small deflections. For large deflection (near the top) the soil behaves plastically and the soil resistance is assumed to vary as:

$$m = m_0 + ax \quad \dots\dots (1.26)$$

where, m_0 = maximum resistance offered by the soil at top.

x = depth at which pressure is required.

a = constant of proportionality.

This assumption enables one to choose the actual soil property by assuming a proper value of ' m_0 ' and ' a '. This form also takes care of overburden pressure. The equation (1.26) is represented in Fig. (1.2 (b)).

At present, there is no standard solution available for the calculation of bearing capacity of horizontally loaded piles for various types of soil. In this investigation

attempts have been made to study and analyse the behavior of laterally loaded piles under various loading and moment conditions and also for varying soil properties. Numerical values of closed form solutions have been worked out of IBM 7044 computer for extreme values of 'a'. Numerical solutions for pile deflection, bending moment, shear force and soil pressure have been worked out in non-dimensional forms, so that these results may be used as design charts. Attempts have also been made for the determination of the ultimate load capacity of the pile under various cases, considering ultimate resistance of the soil.

Chapter II, III and IV deal with free-free, fixed-free and piles with overhang. The experimental set-up and verification of the theory has been treated in chapter V. Discussion of the results and conclusions are presented in chapter VI.

Lastly, in appendix I, the procedure for non-dimensionalisation is given.

In appendix II, the solution for stage 4 for free-free and overhang cases are presented. The thesis ends with a list of references.

CHAPTER II

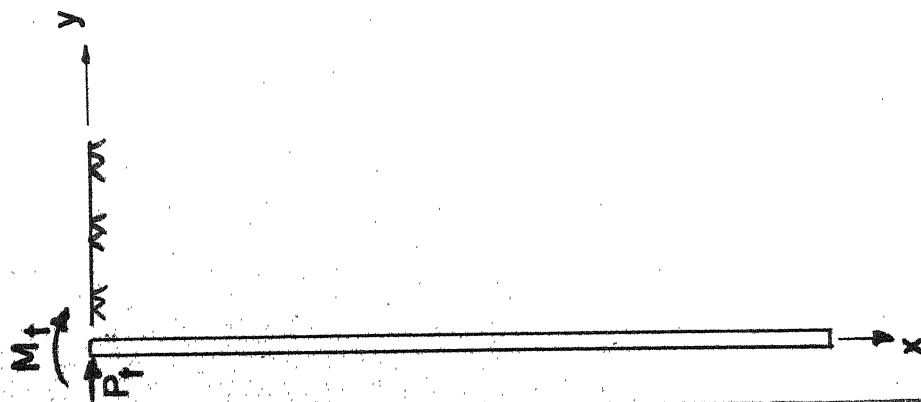
ELASTO-PLASTIC BEHAVIOR OF Laterally LOADED PILES

2.1 PILE BEHAVIOR:

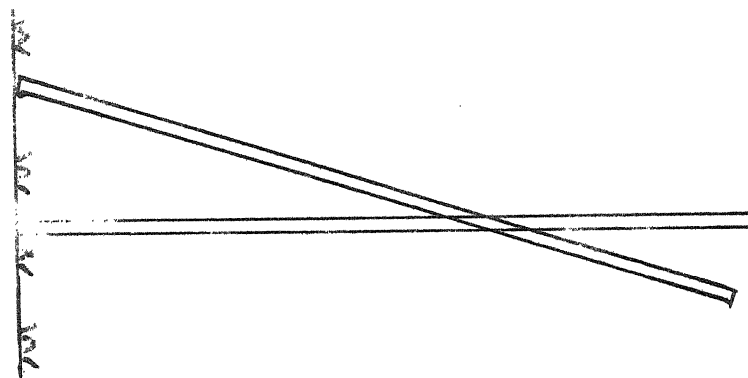
At working loads the deflection of a single pile can be considered to increase approximately linearly with the applied load. As stated earlier the pile is assumed as a beam on elastic foundation. The behavior of the pile under lateral loads can be described as follows. At small loads the ends of the pile will deflect elastically. As the load is increased, the top and bottom deflections will increase. At large loads the top and bottom of the pile will deflect by a large amount and the deflection of the central portion will be less in comparison to that at the ends. For long piles the deflection at the bottom will be relatively small (Fig. 2.1). True nature of pile deflections can be described as the deflection is maximum at the top, it gradually reduces with depth and at some point the pile deflection is zero and then the deflection again increases in a direction opposite to load applied and at the bottom of the pile, it reaches another maximum.

2.2 SOIL BEHAVIOR:

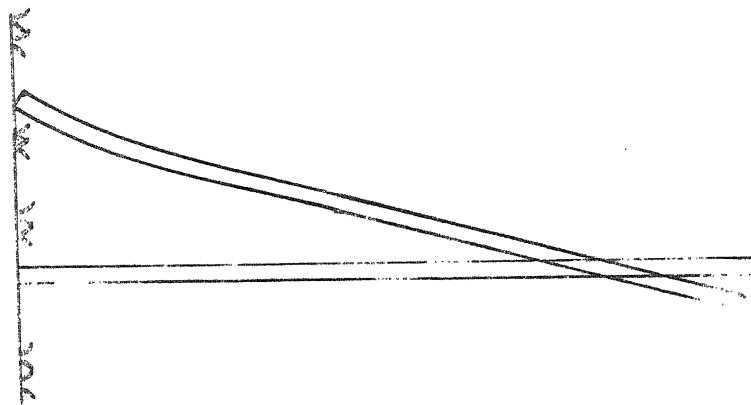
Corresponding to the different amounts of deflection at several depths suffered by the pile, as stated in section 2.1 the soil behavior also changes from point



(a) Original Pile



(b) Short Pile



(c) Long Pile

FIG(2-1) DEFLECTED SHAPE OF Laterally Loaded Pile

to point along the length of the pile. For different amount of pile deflection four distinct stages of soil response are possible.

In stage 1 when the load is small, the pile suffers moderate deflection both at the top and also at the bottom, so that the soil behaves as an elastic medium, throughout the length of the pile. In this case the deflections increase linearly with the increase of load (Fig. 2.2(b)).

When the load on the pile is increased further the deflection at the top increases such that the magnitude of the deflection exceeds q/k hence the soil pressure reaches the ultimate resistance of the soil (q). This zone is characterised as plastic zone. The deflection reduces with depth and when the deflection $y < q/k$, the elastic zone starts as in stage 1. The deflection at the bottom if less than q/k , the soil behaves as elastic medium. This condition is described as stage 2, which is the combination of a top plastic zone and stage 1 (Figure 2.2 (c)). Stage 3 of the pile is shown in (Fig. 2.2(d)). This stage is reached where the load exceeds a particular limit, deflection at the bottom increases and the plastic zone starts from the bottom also. This stage may be said to be the stage 1 sandwiched between two plastic zones at the top and also at the bottom. As the load increases

further the top plastic zone starts moving downwards and the bottom plastic zone moves upwards and the elastic zone shortens.

Stage 4 may be said to be a limiting case wherein the elastic zone completely disappears and only two plastic zones are formed. Stage 4 will give the ultimate load capacity of the pile (Fig. 2.2 (e)).

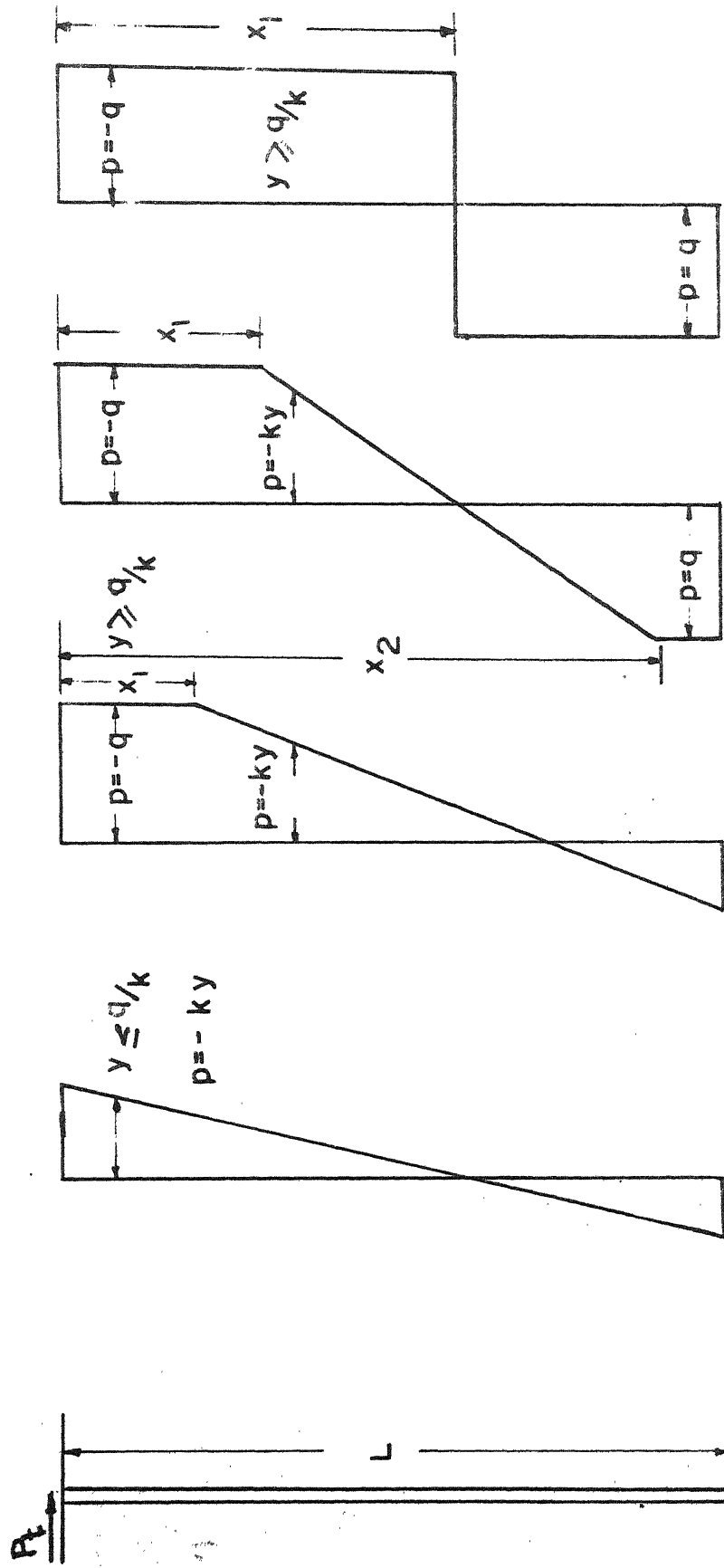
The above listed four stages define all the possible stages of pile-soil interaction under a lateral load. If a moment at the top is applied the behavior pattern will be same except in short pile where stage 2 may be skipped and soil behavior changes from stage 1 to stage 3.

2.3 MODEL PROPOSED:

So far, the problem of laterally loaded piles have been solved assuming the soil to be an ideal elastic medium and as Winkler type of foundation model.

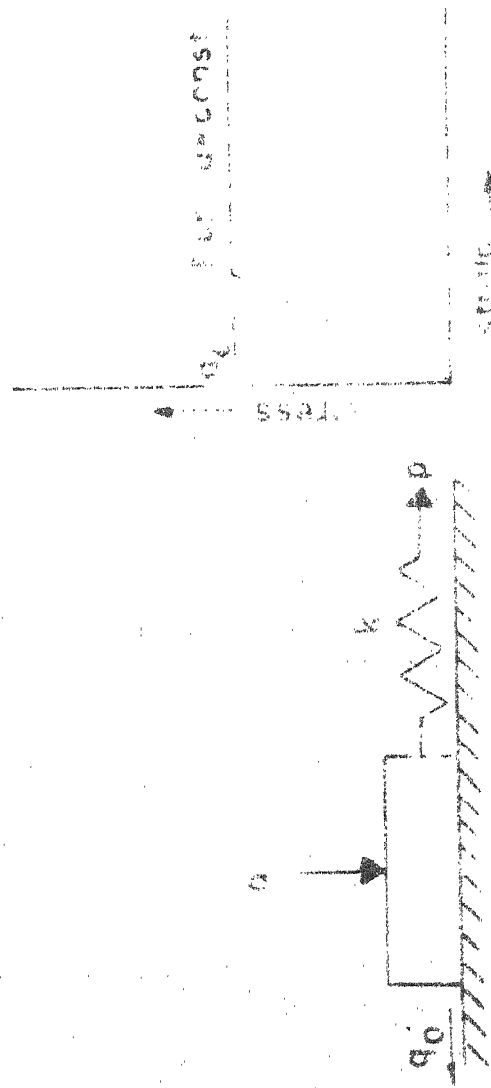
To overcome the limitation of the existing methods and also to explain the soil behavior in four stages as stated in section 2.2, a model for the laterally loaded pile is presented.

This model consists of a spring connected with a friction block in series to represent the actual soil behavior. In Winkler model only a Hookean spring is assumed to represent the soil. In this model a Hookean spring is



FIG(2.2)

STAGES OF PILE - SOIL INTERACTION



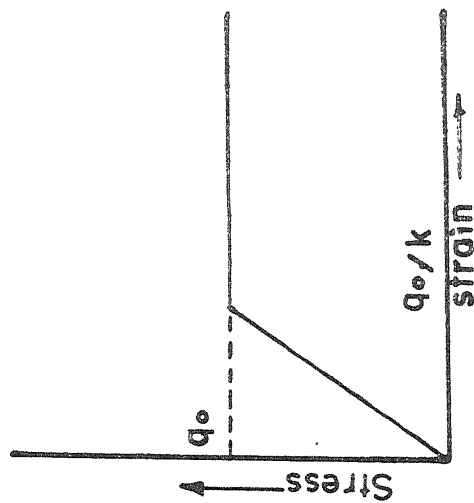
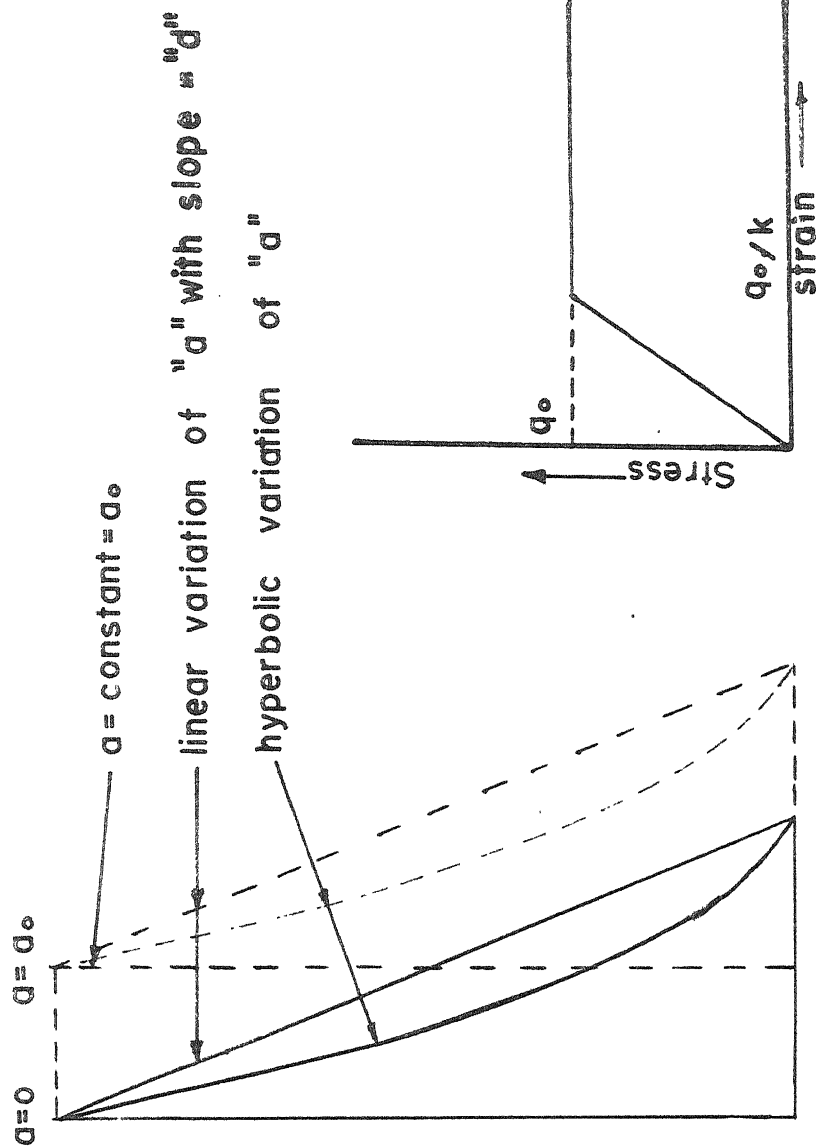
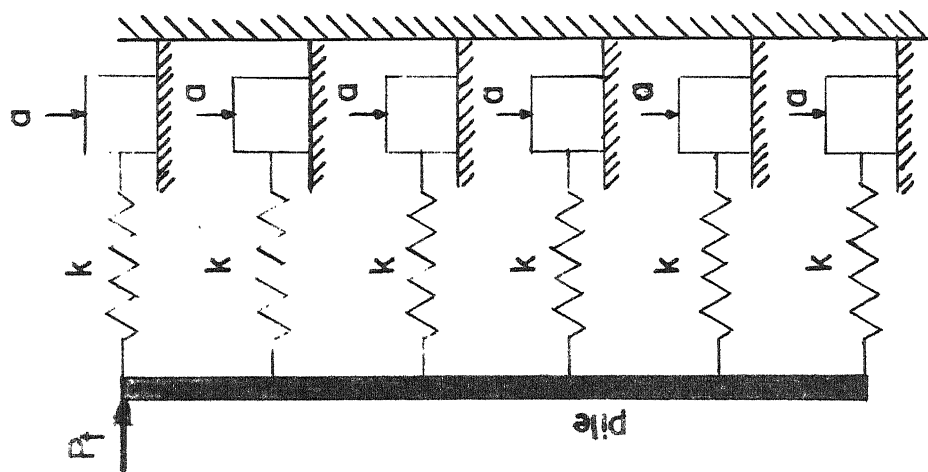
(a) Model For Elastic-Plastic Soil (b) Stress-Strain Response
for $p > p_{const}$

FIGURE 3: MODEL FOR ELASTO-PLASTIC BEHAVIOR

connected to a perfectly plastic material which gives rise to a perfect elastoplastic or St. Venant material to represent the complete soil behavior at all stages (Fig. 2.3(a)). The associated stress strain behavior is shown in (Fig. 2.3(b)). The normal load 'a' is introduced to take care of the variation of ultimate soil pressure (q) with depth. If this aspect is to be neglected then the value of a is assumed constant for all depth. For variation of ultimate pressure capacity with depth, any function for the variation of 'a' may be chosen.

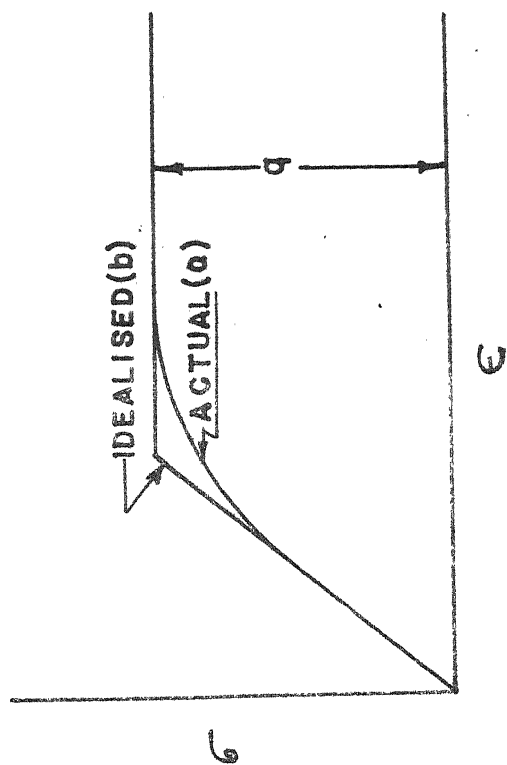
IDEALISATION OF THE SOIL BEHAVIOR:

The stress-strain behavior of a soil is in general nonlinear but commonly described by a hyperbolic type of stress-strain response (21). This is shown by curve (a) of fig. 2.5. The actual relationship can not be included in rigorous solutions, as it gives rise to nonlinear differential equation. It is felt reasonable to idealise the behavior by curve (b) in fig. 2.5. The idealised curve consists of a linear part upto a stress level q_0 , where the stress-strain ratio is constant leading to elastic behavior of the soil. The soil can not take up stresses higher than q_0 i.e. it behaves plastically, which is represented by the horizontal part of the idealised curve. This type of behavior can be described as



(a) Proposed Model (b) Possible Variations of "a" (c) Load-Deflection Curve (soil)

FIG (2-4) PROPOSED MODEL FOR ELASTO-PLASTIC BEHAVIOR OF PILE



FIG(2.5) STRESS-STRAIN RESPONSE OF A SOIL

"Elasto-Plastic" behavior. Mathematically the curve (b) can be represented as

$$p = ky \quad \text{for } y \leq q_0/k \quad \dots \quad (2.1)$$

$$\text{and } p = q_0 \quad \text{for } y > q_0/k \quad \dots \quad (2.2)$$

where p is the response and q_0 is the yield stress of the soil. A linear variation of 'a' is shown in fig. 2.3 (e). Based on these principles the model proposed is shown in fig. (2.4). For variation of 'k' with depth, suitable functions for variation of spring constants may be chosen. In stage 1, the friction blocks do not come into picture because the soil stress does not exceed the magnitude 'q' and so there is no plastic deformation and the soil behaves like Winkler model.

In stage 2, deflection at top exceeds ' q_0/k ', plastic deformation starts from the top, and it proceeds downwards. The rest of the soil behaves elastically.

In stage 3 the bottom deflection also exceeds q_0/k and the friction block suffers plastic movement representing the plastic behavior of the soil. The plastic behavior proceeds upwards with increasing load.

In stage 4, the deflection of the ends of the pile are so high that the soil behaves plastically throughout the whole depth, and all the friction blocks are activated.

It is clearly seen, that the proposed model is a unique and simple representation for the elasto-plastic behavior of the soil.

2.4 FORMULATION OF THE PROBLEM:

As stated earlier, the pile is assumed to be a beam on elastic foundation, and also based on the four stages of pile-soil behavior, the basic governing differential equation can be written as:

$$EI \frac{d^4 y}{dx^4} = -p \quad \dots \quad \dots \quad (2.3)$$

for stage 1, the soil being elastic throughout the length of the pile (Fig. 2.6(b)) and with the help of the equation (2.1) the final form of, the equation is given by:

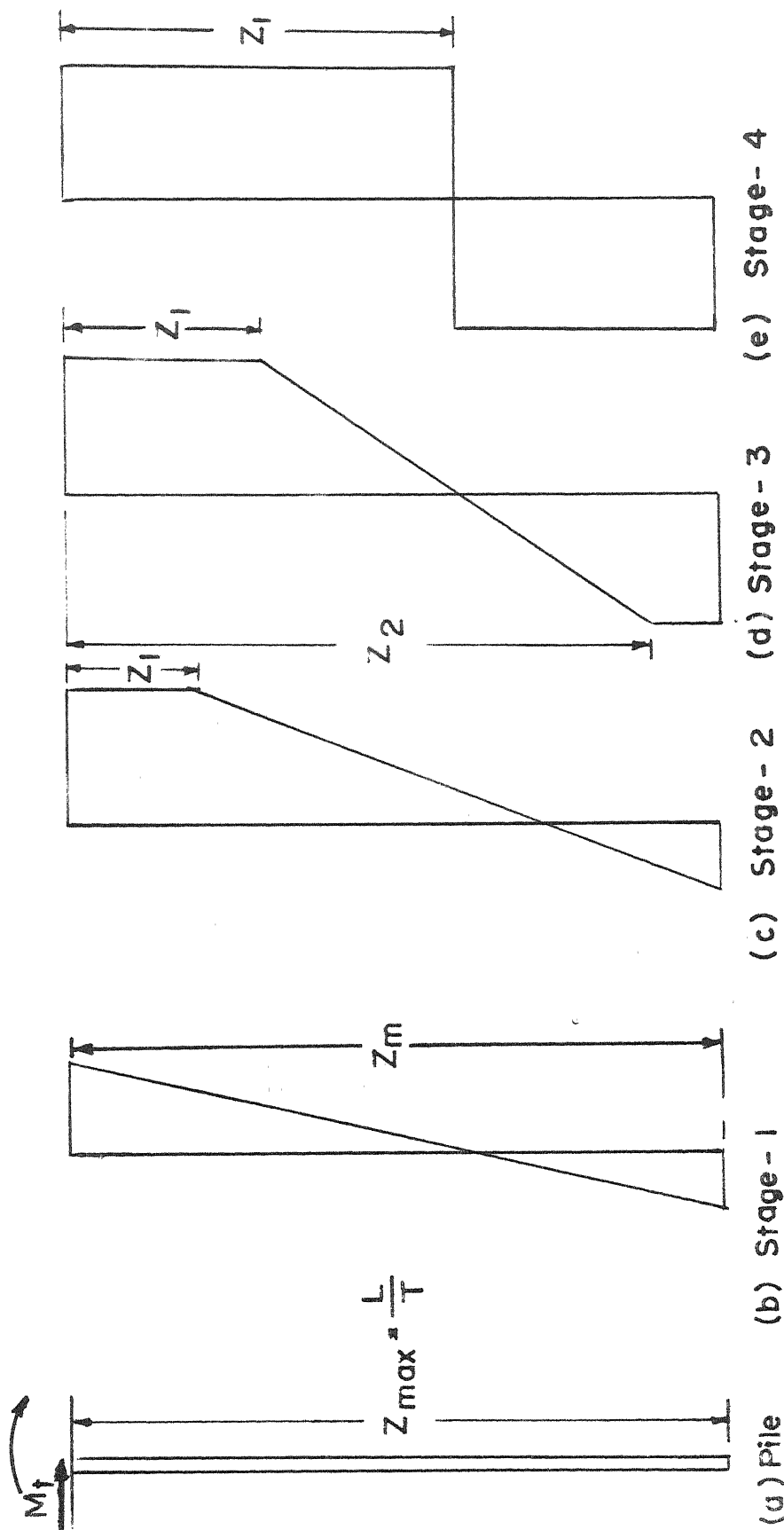
$$EI \frac{d^4 y}{dx^4} = -ky \quad \dots \quad \dots \quad (2.4)$$

For stage 2, the soil at the top portion being plastic and the rest of the portion of the soil remaining elastic, the governing set of differential equations using equations (2.1) and (2.2) may be written as

$$EI \frac{d^4 y}{dx^4} = -q \quad \text{for} \quad 0 \leq x \leq x_1 \quad \dots \quad (2.5)$$

$$\text{and} \quad EI \frac{d^4 y}{dx^4} = -ky \quad \text{for} \quad x_1 \leq x \leq L \quad \dots \quad (2.6)$$

where x_1 is the length of plastic zone measured from the top of the pile, and L is the total length of the pile (Fig. 2.6 (c)).



FIG(2.6) FOUR STAGES OF THE PILE IN ACTION

Similarly for stage 3 the equations are

$$EI \frac{d^4 y}{dx^4} = -q \quad \text{for} \quad 0 \leq x \leq x_1 \quad \dots (2.7)$$

$$EI \frac{d^4 y}{dx^4} = -ky \quad \text{for} \quad x_1 \leq x \leq x_2 \quad \dots (2.8)$$

$$EI \frac{d^4 y}{dx^4} = q \quad \text{for} \quad x_2 \leq x \leq L \quad \dots (2.9)$$

where x_2 is the length from the top of the pile to the bottom plastic zone. Finally for stage 4 the two equations for the two plastic zones can be written as

$$EI \frac{d^4 y}{dx^4} = -q \quad \text{for} \quad 0 \leq x \leq x_1 \quad \dots (2.10)$$

$$\text{and} \quad EI \frac{d^4 y}{dx^4} = q \quad \text{for} \quad x_1 \leq x \leq L \quad \dots (2.11)$$

The equations from 2.5 to 2.11 can be modified for variation of yield strength of soil with depth, by writing

$$q = q_0 + ax \quad \dots (2.12)$$

where q_0 is the yield strength at the top of the soil surface i.e. at $x = 0$ and 'a' is constant, that depends upon the type of soil. q_0 would be zero for sands and 'a' may be zero for cohesive soil whose strength remains constant with depth.

Stage 1:

$$\frac{d^4 y}{dx^4} + \frac{k}{EI} y = 0 \quad \text{for} \quad 0 \leq x \leq L \quad \dots (2.13)$$

Stage 2:

$$\frac{d^4 y}{dx^4} + \frac{(q_0 + ax)}{EI} = 0 \quad \text{for } 0 \leq x \leq x_1 \quad \dots \quad (2.14)$$

$$\frac{d^4 y}{dx^4} + \frac{ky}{EI} = 0 \quad \text{for } x_1 \leq x \leq L \quad \dots \quad (2.15)$$

Stage 3:

$$\frac{d^4 y}{dx^4} + \frac{(q_0 + ax)}{EI} = 0 \quad \text{for } 0 \leq x \leq x_1 \quad \dots \quad (2.16)$$

$$\frac{d^4 y}{dx^4} + \frac{k}{EI} y = 0 \quad \text{for } x_1 \leq x \leq x_2 \quad \dots \quad (2.17)$$

$$\frac{d^4 y}{dx^4} - \frac{(q_0 + ax)}{EI} = 0 \quad \text{for } x_2 \leq x \leq L \quad \dots \quad (2.18)$$

Stage 4:

$$\frac{d^4 y}{dx^4} + \frac{(q_0 + ax)}{EI} = 0 \quad \text{for } 0 \leq x \leq x_1 \quad \dots \quad (2.19)$$

$$\frac{d^4 y}{dx^4} - \frac{(q_0 + ax)}{EI} = 0 \quad \text{for } x_1 \leq x \leq L \quad \dots \quad (2.20)$$

2.5 NONDIMENSIONALISING THE EQUATIONS:

By using the characteristic length T , as defined in chapter I, and using the Buckingham Π theorem the non-dimensional parameters may be listed as follows:

$$\text{Depth coefficient} \quad z = \frac{x}{T} \quad \dots \quad (2.21)$$

$$\text{Maximum depth coefficient} \quad z_{\max} = \frac{L}{T} \quad \dots \quad (2.22)$$

$$\text{Soil modulus function (elastic)} \quad r_0 = \frac{kT^4}{EI} \quad \dots \quad (2.23)$$

$$\text{Soil modulus function (plastic)} \quad m_0 = \frac{qT^4}{EI} \quad \dots \quad (2.24)$$

$$\text{Deflection coefficient for load at top } A_y = \frac{EI}{P_t T^3} y \dots (2.25)$$

Deflection coefficient for moment at top

$$B_Y = \frac{EI}{M_t T^2} Y \quad \dots \quad (2.26)$$

$$\text{also } Z_1 = \alpha Z_{\max} = \frac{x_1}{T} \quad \dots \quad (2.27)$$

$$Z_2 = \gamma Z_{\max} = \frac{x_2}{T} \quad \dots \quad (2.28)$$

where α and γ are constants and α is always less than unity. The deflection in the top plastic zone is defined as y_1 , that in the middle elastic zone by y_2 and that in the bottom plastic zone by y_3 . The nondimensional equations can be developed as follows.

Stage 1:

$$\frac{d^4 Ay_1}{dz^4} + r_0 Ay_1 = 0 \quad \text{for } 0 \leq z \leq z_m \quad \dots \quad (2.29)$$

Stage 2:

$$\frac{d^4 Ay_1}{dz^4} + [m_0 + dz] = 0 \quad \text{for } 0 \leq z \leq z_1 \quad \dots \quad (2.30)$$

$$\frac{d^4 Ay_2}{dz^4} + r_0 Ay_2 = 0 \quad \text{for } z_1 \leq z \leq z_m \quad \dots \quad (2.31)$$

$$\text{where } m_0 = \frac{q_0 T}{P_t} \quad \text{and } d = \frac{a T^2}{P_t}$$

Stage 3:

$$\frac{d^4 Ay_1}{dz^4} + [m_0 + dz] = 0 \quad \text{for } 0 \leq z \leq z_1 \quad \dots \quad (2.32)$$

$$\frac{d^4 Ay_2}{dz^4} + r_0 Ay_2 = 0 \quad \text{for } z_1 \leq z \leq z_2 \quad \dots \quad (2.33)$$

$$\frac{d^4 Ay_3}{dz^4} - (m_0 + dz) = 0 \quad \text{for } z_2 \leq z \leq z_m \quad \dots \quad (2.34)$$

Stage 4:

$$\frac{d^4 A y_1}{dz^4} + (m_0 + dz) = 0 \quad \text{for} \quad 0 \leq z \leq z_1 \quad \dots (2.35)$$

$$\frac{d^4 A y_1}{dz^4} - (m_0 + dz) = 0 \quad \text{for} \quad z_1 \leq z \leq z_m \quad \dots (2.36)$$

Equations (2.29) to (2.36) are the final forms of the basic differential equations.

2.6 SOLUTION:

The basic equations from (2.29) to (2.36) can be solved for different boundary condition corresponding to different physical conditions of the pile in action. The expression for deflection, slope, B.M., S.F. soil-pressure and their non-dimensional forms are given in Table 2.1.

To solve the equations, a set of boundary conditions are needed. In this case, the necessary conditions, for the determination of the Constants, in general are the shear and moment at the top of the pile, continuity conditions for deflection (y), slope (y'), BM (y''), SF(y''') and soil pressure (y^{iv}) and the moment and shear at the bottom of the pile.

In the investigation the method of solution adopted is indirect. Instead of assuming the load or moment at top, a soil-pressure distribution is assumed and for that case the shear or moment at the top is calculated, which is the shear or moment applied on the pile.

TABLE 2.1
NON DIMENSIONAL COEFFICIENTS

Character	Expression	Nondimensional coefficients	
		Load at top	Moment at top
Deflection	y	$A_y = \frac{EI}{P_t T^3} y$	$B_y = \frac{EI}{M_t T^2} y$
Slope	$\frac{dy}{dx}$	$A_s = \frac{EI}{P_t T^2} \frac{dy}{dx}$	$B_s = \frac{EI}{M_t T} \frac{dy}{dx}$
Bending moment	$-\frac{d^2 y}{dx^2}$	$A_m = \frac{EI}{P_t T} \frac{d^2 y}{dx^2}$	$B_m = \frac{EI}{M_t} \frac{d^2 y}{dx^2}$
Shear force	$-\frac{d^3 y}{dx^3}$	$A_v = -\frac{EI}{P_t} \frac{d^3 y}{dx^3}$	$B_v = -\frac{EIT}{M_t} \frac{d^3 y}{dx^3}$
Soil pressure	$\frac{d^4 y}{dx^4}$	$A_p = \frac{EIT}{P_t} \frac{d^4 y}{dx^4}$	$B_p = \frac{EIT^2}{M_t} \frac{d^4 y}{dx^4}$

Stage 1:

Solution of the equation (2.29) is simple and straight-forward. Defining $\beta = \sqrt[4]{r_0/4}$ the solution is given by;

$$\begin{aligned}
 Ay_1 = & A_1 \sin \beta Z \sinh \beta Z + A_2 \sin \beta Z \cosh \beta Z \\
 & + A_3 \cos \beta Z \sinh \beta Z + A_4 \cos \beta Z \cosh \beta Z
 \end{aligned}
 \quad \dots (2.37)$$

The constants A_1 to A_4 are determined by the boundary conditions.

Stage 2:

Equation (2.30) can be solved by integrating four times and the solution is given as:

$$Ay_1 = -\frac{m_0 Z^4}{24} - \frac{aZ^5}{120} + \frac{A_1 Z^3}{6} + \frac{A_2 Z^2}{2} + A_3 Z + A_4 \quad \dots (2.38)$$

The equation (2.31) for the lower elastic zone can be solved for y_2 as in Stage 1 (2.37) and the constants are denoted by B_1 to B_4 . The constant terms can be determined with the help of boundary conditions and the continuity condition. It is seen that nine equations are available viz. eqn. nos. (2.30)&(2.31) for nine unknown constants. In this analysis ' α_1 ' is varied and is known. For various values of ' α_1 ' the corresponding shear at top is determined, which gives the magnitude of ' P_t ' in nondimensional form.

Stage 3:

The general solution of equations (2.32) and (2.33) are the same as (2.38) and (2.37) respectively. The equation (2.34) is solved by integrating it four times and the solution is presented as;

$$Ay_3 = \frac{m_0 Z^4}{24} + \frac{aZ^5}{120} + \frac{C_1 Z^3}{6} + \frac{C_2 Z^2}{2} + C_3 Z + C_4 \quad \dots (2.39)$$

In this case there are fourteen unknown constants which are A_1 to A_4 , B_1 to B_4 , C_1 to C_4 and also ' α_1 ' and ' γ '.

In the actual analysis, the value of ' α_1 ' is assumed and different values of ' γ ' are tried, and the final solution is checked for the bottom boundary condition which is, moment at the bottom of the pile is

zero. If this condition is satisfied the value assumed for α_1 is correct. The other constants are found by top boundary and continuity conditions.

Stage 4:

The general solutions for the equations (2.35) and (2.36) are given by (2.38) and (2.39) respectively. Among the nine unknown constants, the value of α_1 is assumed in this case and eight unknown constants are determined by substituting the boundary and continuity condition.

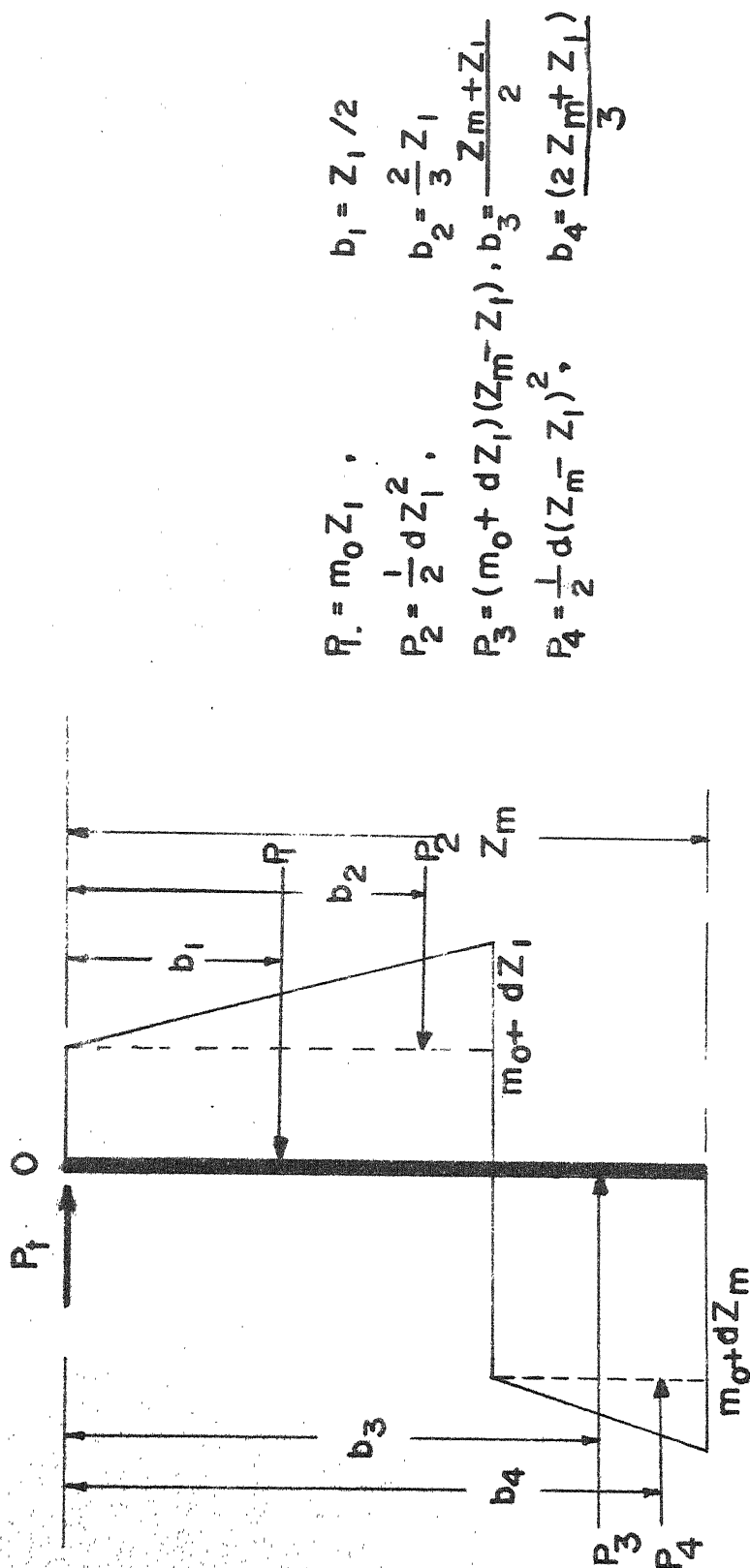
The solution for stage 4 can be arrived at by a different approach. The soil pressure distribution for this stage, with the consideration of increasing ultimate strength with depth is shown in fig. 2.7.

$$\begin{aligned} P_1 &= m_0 Z_1, & b_1 &= Z_1/2 \\ P_2 &= \frac{1}{2} dZ_1^2, & b_2 &= \frac{2}{3} Z_1 \\ P_3 &= (m_0 + dZ_1)(Z_m - Z_1), & b_3 &= \frac{Z_m + Z_1}{2} \\ P_4 &= \frac{1}{2} d(Z_m - Z_1)^2, & b_4 &= \frac{1}{3} (2 Z_m + Z_1) \end{aligned}$$

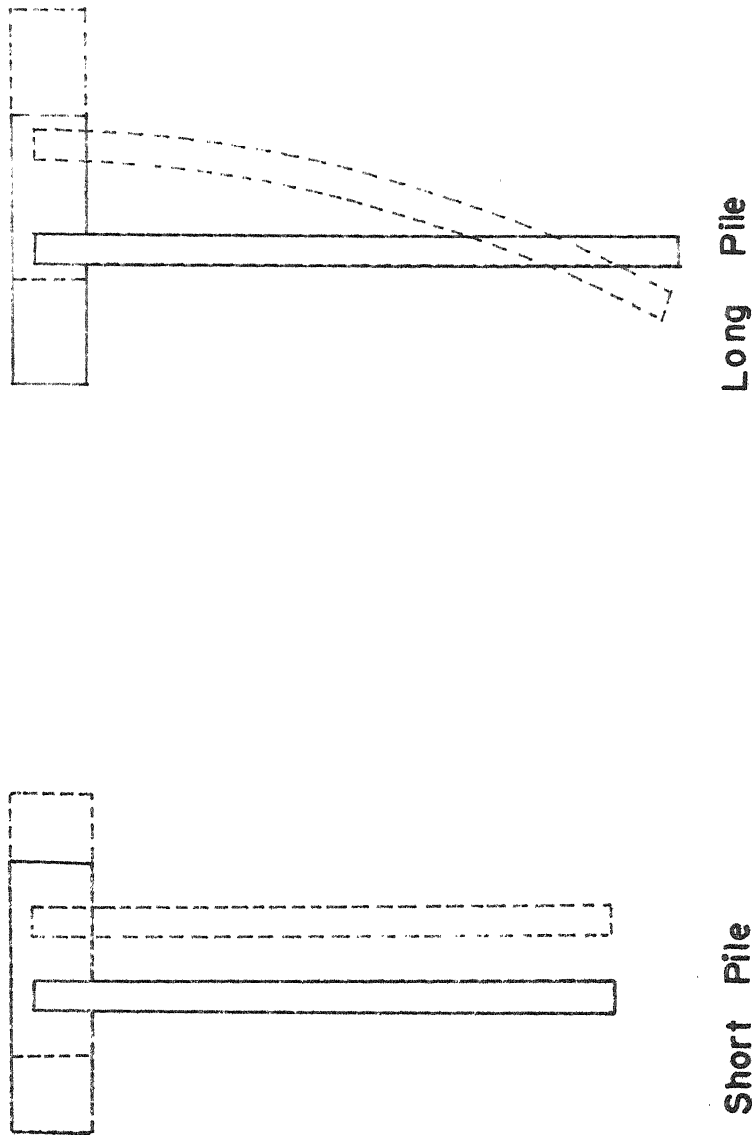
Taking moment of all the resultant forces P_1, P_2, P_3, P_4 about the top of the pile (i.e about 'O') and equating to zero for limiting equilibrium, can be written as;

$$P_1 b_1 + P_2 b_2 - P_3 b_3 - P_4 b_4 = 0 \quad \dots (2.40)$$

substituting all the expressions for P's and b's denoting Z_1 by $\alpha_1 Z_m$ and on simplification, the final form is given as;



FIG(2.7) PRESSURE DISTRIBUTION FOR ULTIMATE LOAD
(Free free Pile, Load at Top)



FIG(2-8) DEFLECTED SHAPE OF FIXED -FREE PILE

$$2 \, dZ_m \alpha_1^3 + 3 \, m_0 \alpha_1^2 - \left(\frac{3}{2} m_0 + dZ_m\right) = 0 \quad \dots \quad (2.41)$$

On substituting 'd' = 0 in (2.41) for uniform soil behavior with depth, the value of α_1 is a constant and is $\sqrt{\frac{1}{2}}$.

CHAPTER III

FREE-FREE AND FIXED-FREE PILE

3.1 INTRODUCTION:

In this chapter actual solution for the different cases for different working condition of the pile and the corresponding boundary condition are discussed.

The pile, when acted upon by lateral loads may undergo several cases depending upon the type of construction of the pile. Considering the general functions of a laterally loaded pile, they may be broadly classified in two types

Type I : free-free pile

Type II : fixed-free pile

A pile which is free to move both at the top and also at the bottom is classified as Type I. This can again be subdivided into two cases.

Case I: Load at top (P_t only)

Case II: Moment at the top (M_t only)

A pile which is fixed at top and free to deflect at the bottom is characterised as fixed-free pile and denoted as type II.

3.2 FREE-FREE PILE:

The boundary and continuity conditions for the free-free pile is given in table 3.1. In the table moment is denoted by 'M' and shear is denoted by 'N'.

TABLE 3.1

TYPE I - FREE-FREE PILE

Stage No.	Type of Load	Governing equation No.	No. of unknowns	No. of available eqns.	Boundary condition at top	Continuity condition at $Z=Z_1$	Continuity condition at $Z=Z_2$	Boundary condition at bottom $Z=Z_m$	Assumed parameters
1	Load	2.29	4	4	$M=0$ $N=P_t$	-	-	$M=0$ $N=0$	-
1	Moment	2.29	4	4	$M=M_t$ $N=0$	-	-	$M=0$ $N=0$	-
2	Load	2.30 2.31	9	9	$M=0$ $N=P_t$	$Y_1=Y_2$ $Y_1'=Y_2'$	-	$M=0$ $N=0$	α_1
	Moment	2.30 2.31	9	9	$M=M_t$ $N=0$	$Y_1''=Y_2''$ $Y_1'''=Y_2'''$ $Y_1^{iv}=Y_2^{iv}$	-	$M=0$ $N=0$	α_1
3	Load	2.32 2.33 2.34	14	14	$M=0$ $N=P_t$	$Y_2=Y_3$ -do- $Y_2'=Y_3'$ $Y_2''=Y_3''$	$M=0$ $N=0$	$M=0$ $N=0$	α_1, δ
	Moment	2.32 2.33 2.34	14	14	$M=M_t$ $N=0$	$Y_2'''=Y_3'''$ $Y_2^{iv}=Y_3^{iv}$ $Y_2=Y_3$	$M=0$ $N=0$	$M=0$ $N=0$	α_1, δ
4	Load	2.35 2.36	9	9	$M=0$ $N=P_t$	-do- -	-	$M=0$ $N=0$	α_1
	Moment	2.35 2.36	9	9	$M=M_t$ $M=0$	-do- -	-	$M=0$ $N=0$	α_1

Regarding continuity conditions, the deflection, slope bending moment, shear force and soil pressure are calculated at the interface of plastic and elastic zones with the help the equations, for plastic and elastic zones separately and they are made equal to satisfy the continuity conditions. In the table the term 'EI' is omitted as it is assumed, EI remains the same for whole length of the pile, which is true for all particular cases.

3.3 FIXED-FREE PILE:

Table 3.2 shows the boundary and continuity conditions for pile type II i.e. fixed-free pile.

From equations (2.29) to (2.36), with the help of conditions from table (3.1) and (3.2) a set of simultaneous equations can be formed for different cases. The set of simultaneous equations are solved by matrix inversion method with the help of IBM 7044 digital computer and all the values of the constants are arrived at.

In this case the variables involved are ' α ', ' γ ', ' r_0 ', ' Z_{max} ', ' m_0 ' and ' d '. Solutions for different combinations of the variables are worked out and the results are presented in the form of graphs.

When $Z_{max} \leq 2$ the pile is called a short pile and when $Z_{max} > 5$ it is called as a long pile. Solution for stage 1 for piles of type I and type II have been dealt with in details by Madhavan (24) so this portion is omitted here.

TABLE 3.2
TYPE II - FIXED-FREE PILE

Stage	Eqn. Nos.	No. of Unkn- own	No. of Eqns.	Boundary condition at $Z=0$	Continuity condition at $Z=Z_1$	Continuity condition at $Z=Z_2$	Bottom condition	Par. assum.
1	2.29	4	4	Slope=0 Deflection =0	-	-	$M = 0$ $N = 0$	-
2	2.30 2.31	9	9	Slope=0 Deflection =0	$Y_1=Y_2$ $Y_1'=Y_2'$ $Y_1''=Y_2''$ $Y_1'''=Y_2'''$ $Y_1^{iv}=Y_2^{iv}$	-	$M = 0$ $N = 0$	α_1
3	2.32 2.33 2.34	14	14	Slope=0 Deflection =0	-do-	$Y_2=Y_3$ $Y_2'=Y_3'$ $Y_2''=Y_3''$ $Y_2'''=Y_3'''$ $Y_2^{iv}=Y_3^{iv}$	$M = 0$ $N = 0$	α_1 γ
4	2.35 2.36	9	9	Slope=0 Deflection =0	-do-	-	$M = 0$ $N = 0$	α_1

Graphs are drawn separately for short and long piles. Equation (2.41) is solved for various combination of d , Z_m and m_0 , to find α_1 and the results are shown in graphs.

3.4 DISCUSSION OF RESULTS:

A. FREE-FREE PILE: LOAD AT TOP, TYPE - I, CASE- I.

Figure (3.1) shows the plot of shear at top versus deflection at pile-top for $Z_m=1$, to $Z_m=4$ and for the values of $m_0=0.2$ and 0.5 . This plot may be called as the load-deflection curve for the pile. It is seen, the load capacity for a given deflection increases with increasing pile length.

With higher value of ' m_0 '; the load capacity is increased. But, with the increase of Z_m , the effect of ' m_0 ' decreases i.e. for a given deflection, the ratio of the loads for $m_0=0.2$ and $m_0=0.5$ respectively approaches unity for higher values of Z_m . But in case of shortpile, the effect of ' m_0 ' is significant. This fact is seen from fig.(3.2. a) and fig. (3.2 b). From fig. (3.3 a) it is seen, ' m_0 ' has significant effect on load-deflection characteristic, for $d = 0$ for long pile. But for $d=1$, the effect is negligible.

The effect of ' r_0 ' is to increase the load-capacity of the pile, which is seen from fig. (3.2 a) and (3.2 b) for shortpiles. Whereas for long piles, the effect of ' r_0 ' is small for $d = 1$.

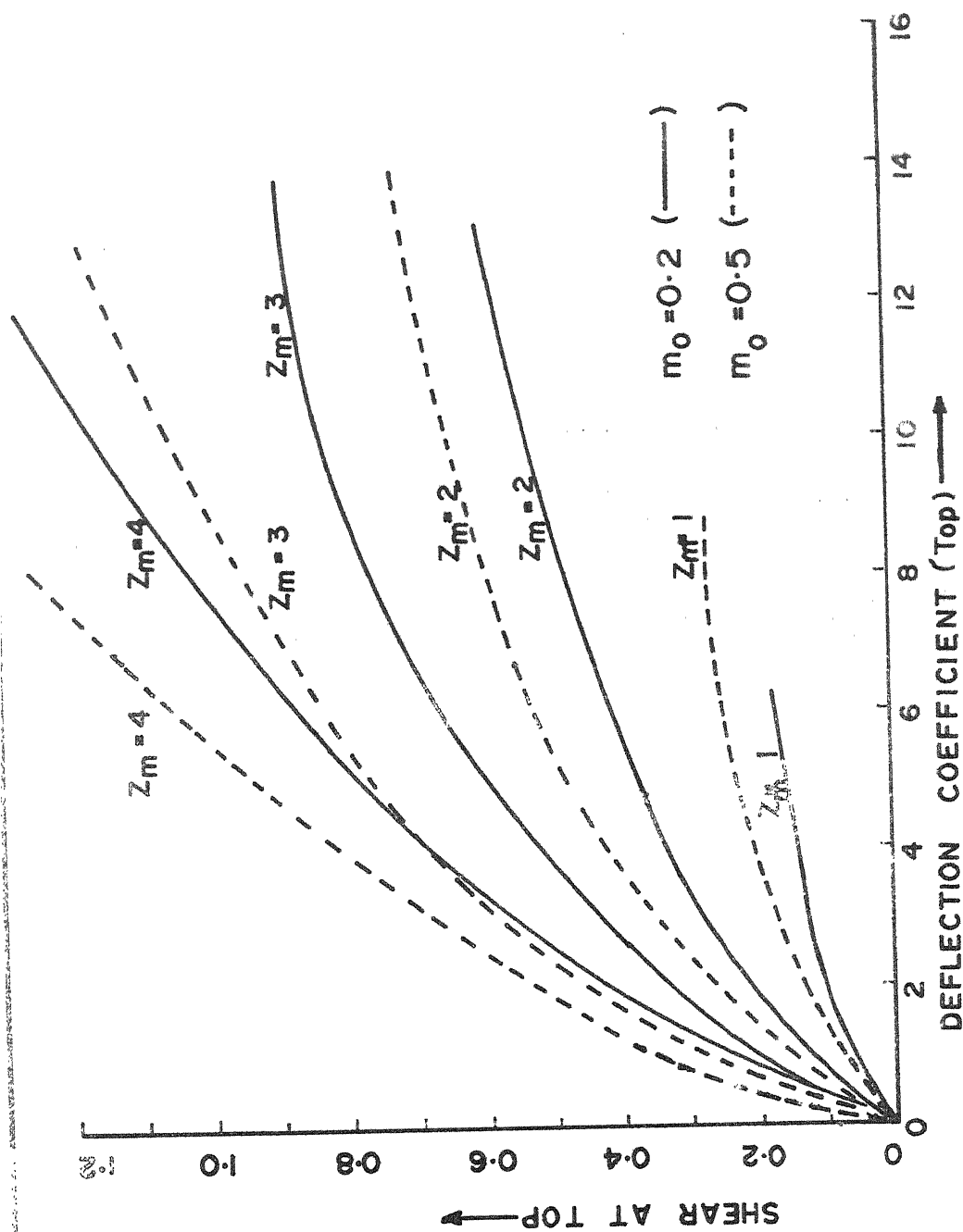
Fig. (3.4 a) shows the plot of top-deflection vs. α_1 . It is seen, that the deflection at the top, increases with the increase of α_1 . Deflection at top reaches very high value for $\alpha_1 = \frac{1}{\sqrt{2}}$, when the pile behavior transforms

from stage 3 to stage 4. This is also seen from the analysis for ultimate load capacity of the pile, in stage 4, (Fig.3.22). The rate of increase in top-deflection is slightly affected by ' m_0 '. Fig. (3.4 b) shows the plot of α_1 vs γ . It is seen, for $\alpha_1=0.384$, the pile behaves, as stated in stage 2. Also for $\alpha_1=0.707$, the pile behaves as in stage 4. So, the pile behaves, as in stage 3 for the range of $\alpha_1=0.384$ to $\alpha_1=0.707$. Bottom plastic zone starts from $\alpha_1=0.707$, the elastic zone is completely eliminated. All these conclusions are valid for uniform soil property with depth (i.e. $d=0$).

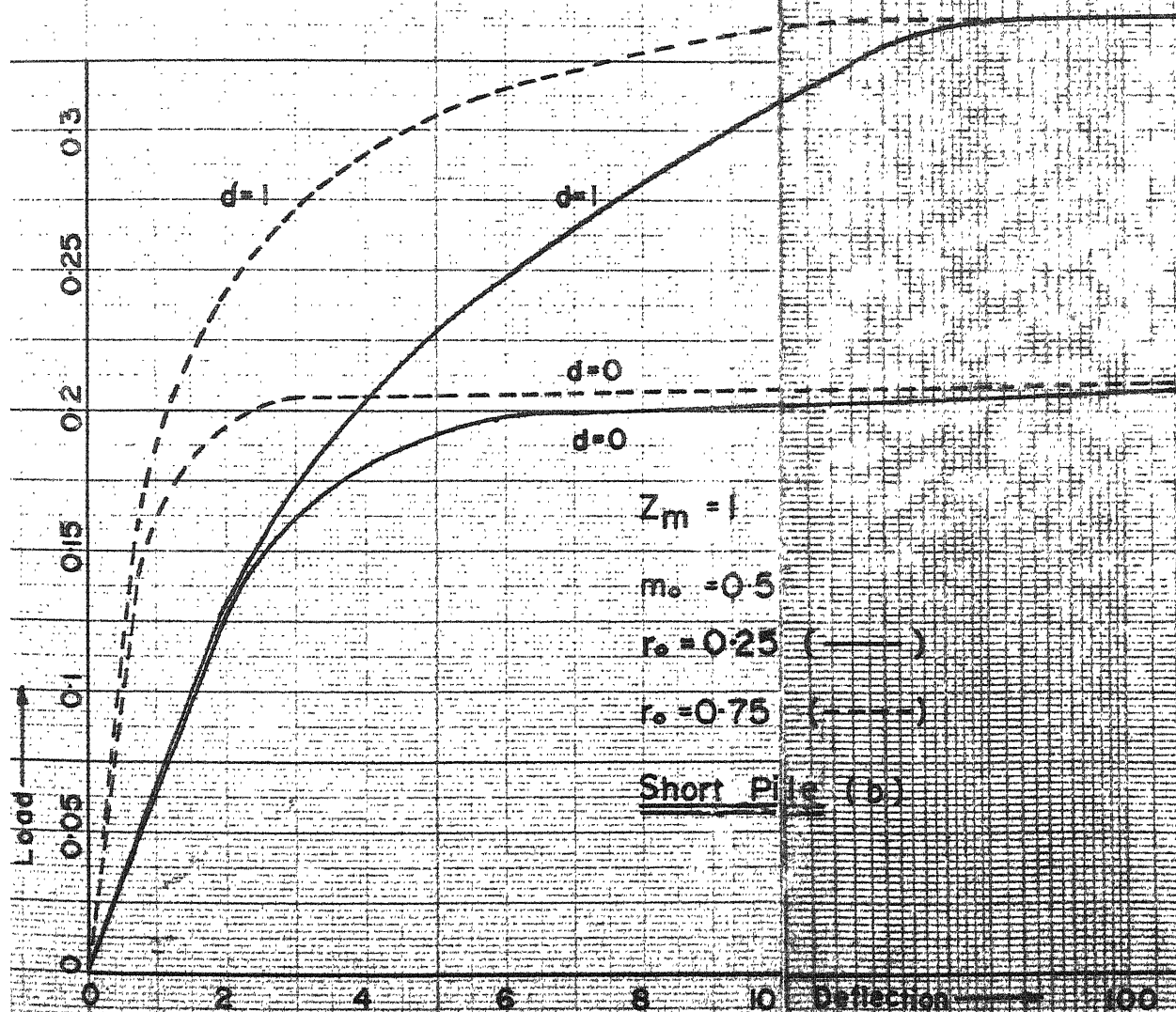
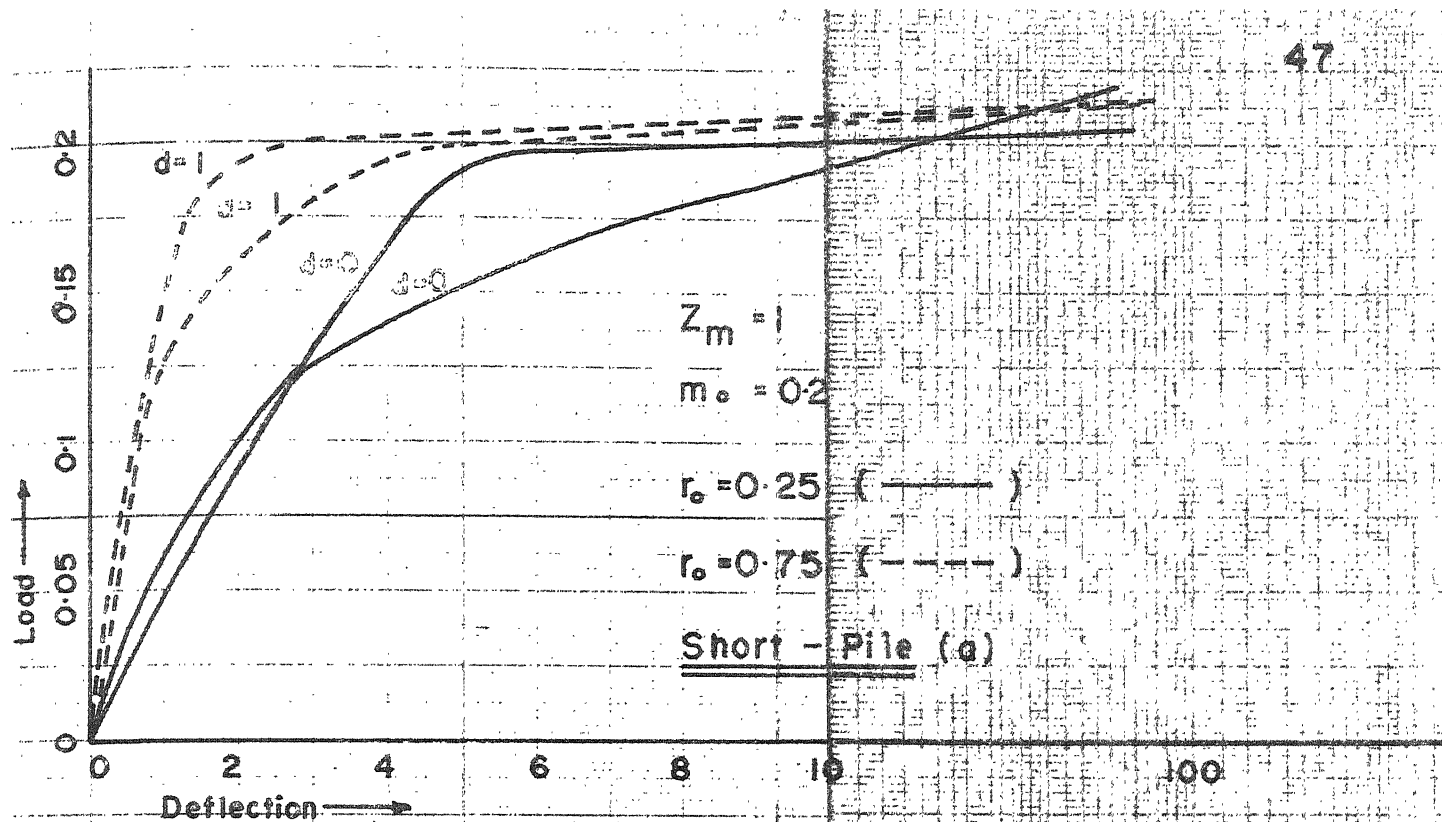
From fig.(3.5), it is evident that the deflection along the length of the pile is lower for higher value of r_0 . For increased value of m_0 , shear distribution along the pile is increased.

The variation of deflection, moment, shear and soil pressure co-efficients, along the length of the pile is shown in fig. (3.6) for different values of α_1 and for short pile. Fig. (3.7) show the same characters for a long pile. It is evident that the short pile is one, which behaves like a rigid pile, and the long pile is one, wherein the behavior is as that of a flexible pile.

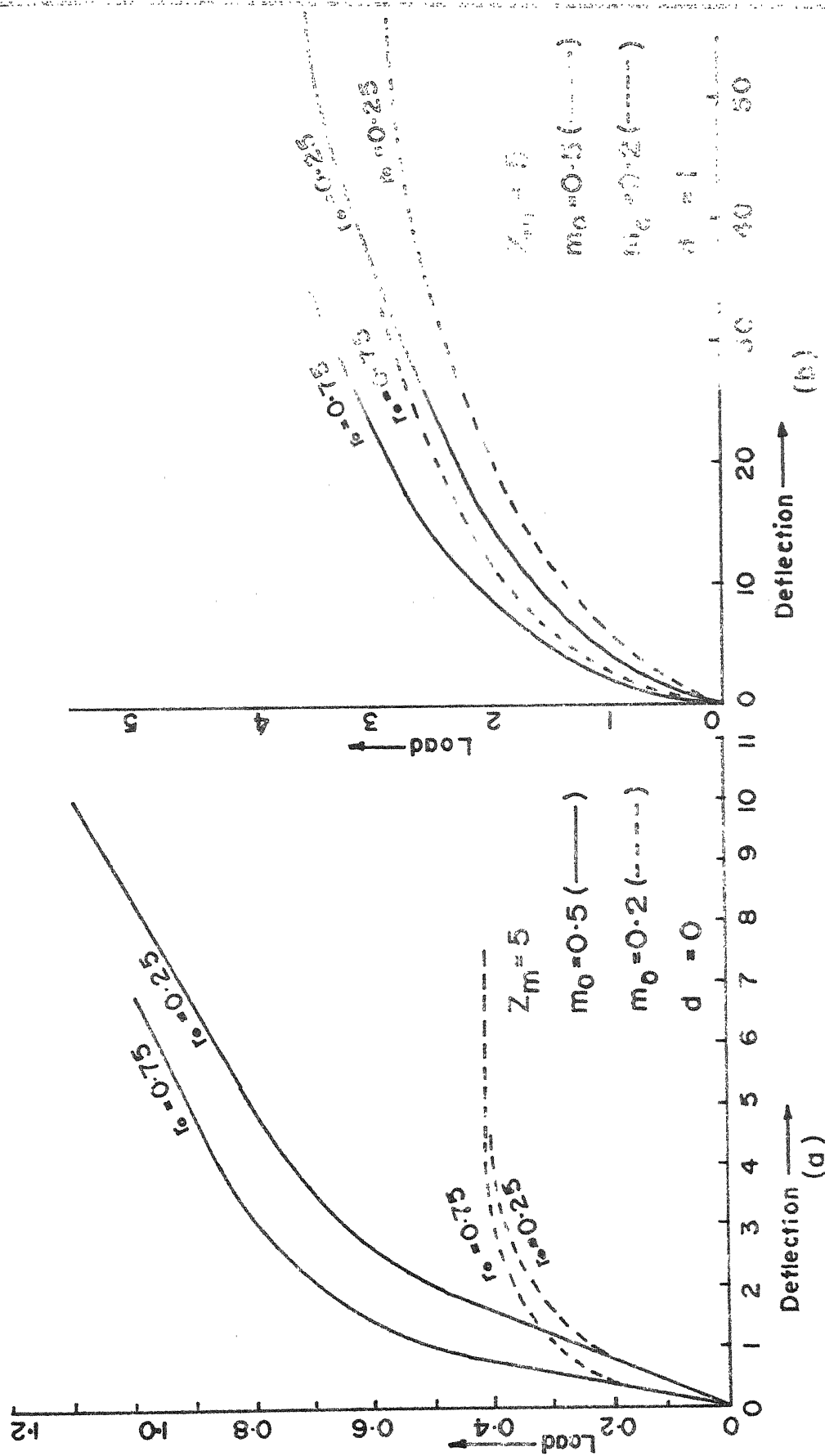
As α_1 increases, the deflection, bending moment, shear force and soil-pressure increases along the depth, which are shown in fig. (3.6) and (3.7) for short and long piles respectively.



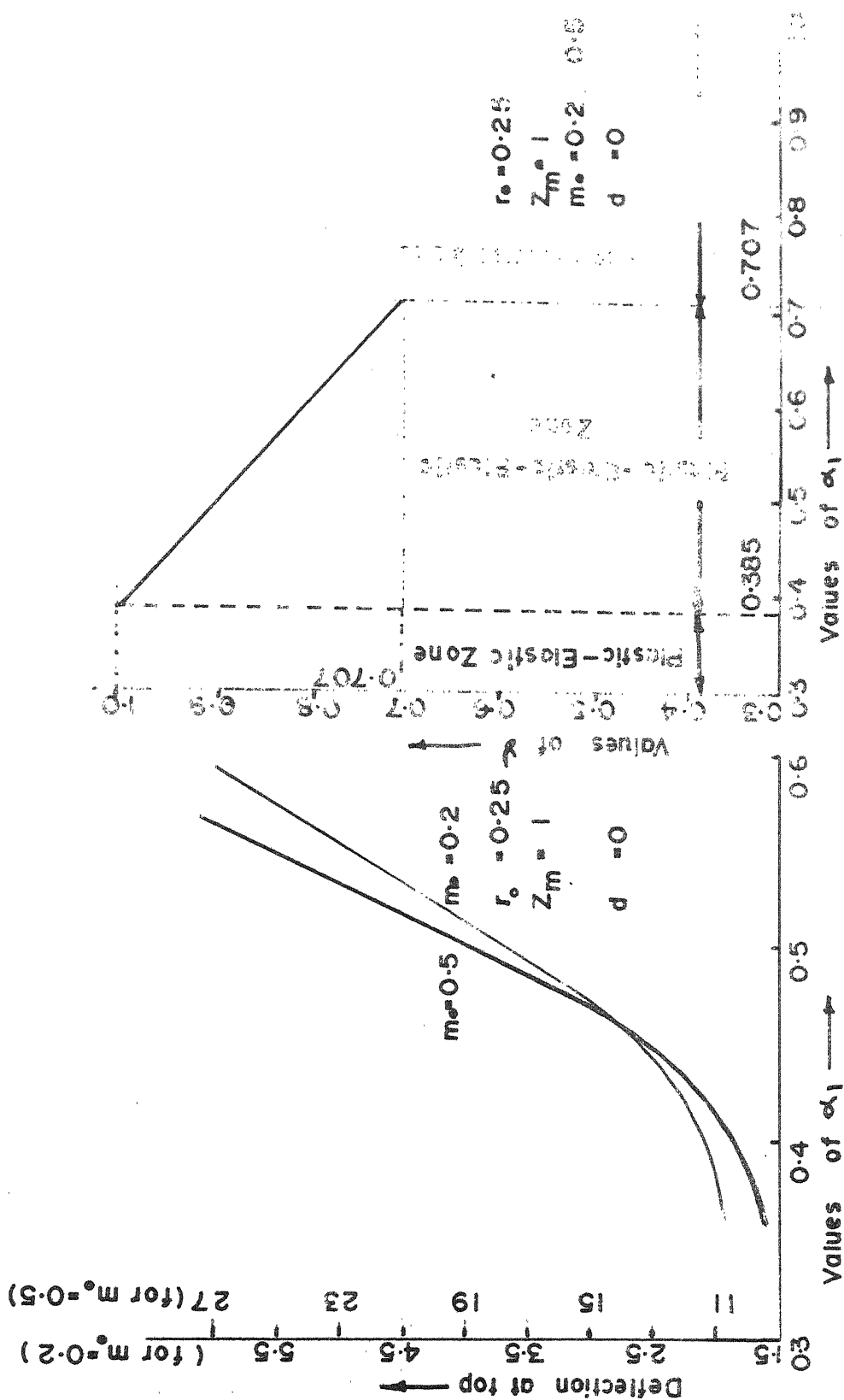
FIG(3.1) LOAD-DEFLECTION CURVE FOR VARIOUS Z_m



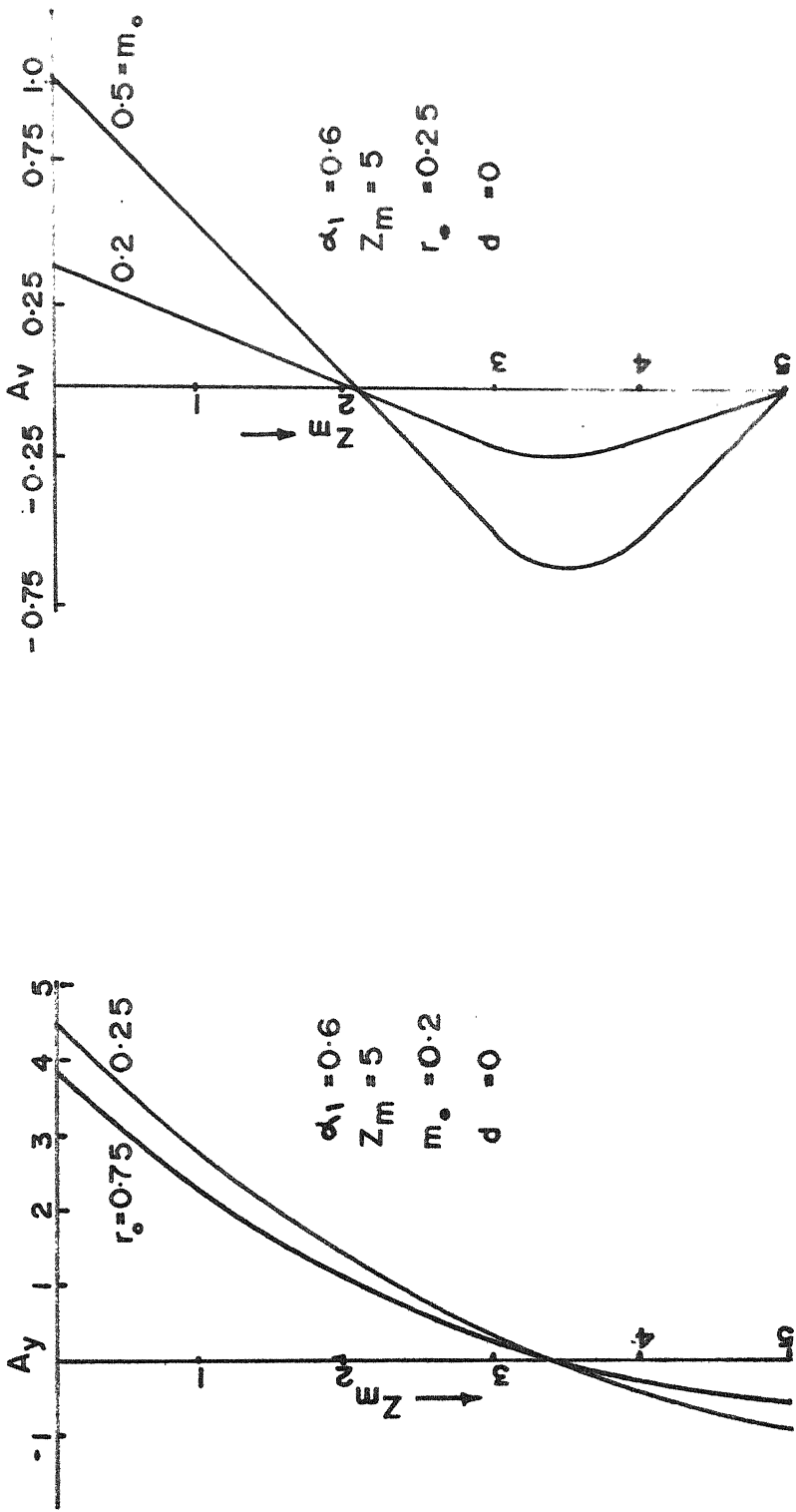
FIG(3-2) LOAD DEFLECTION CURVE FOR SHORT PILE



FIG(3.3) LOAD DEFLECTION CURVE FOR LONG PILE



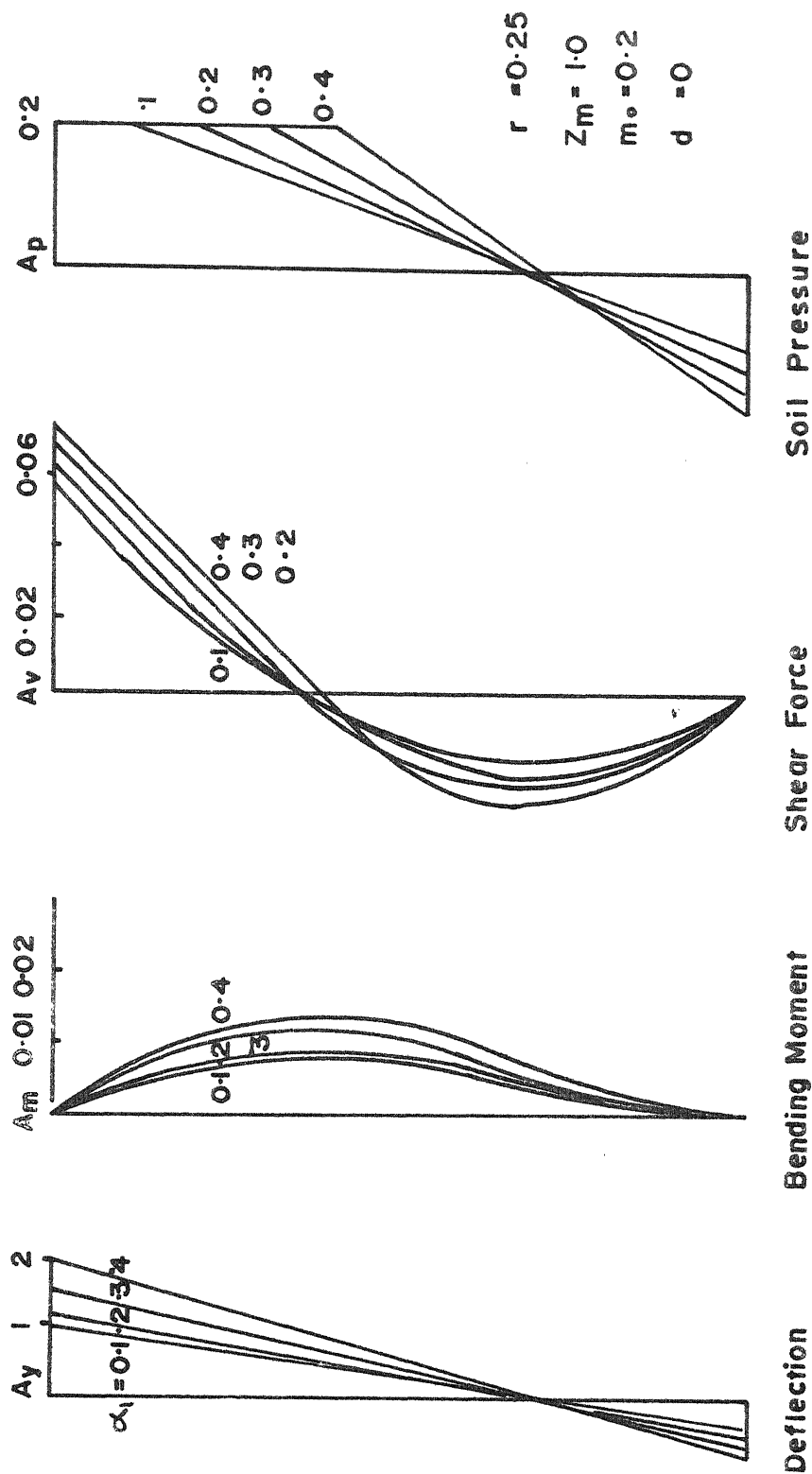
FIG(3.4a) RELATION BETWEEN α_1 AND TOP DEFLECTION
 FIG(3.4b) RELATION BETWEEN α_1 AND γ



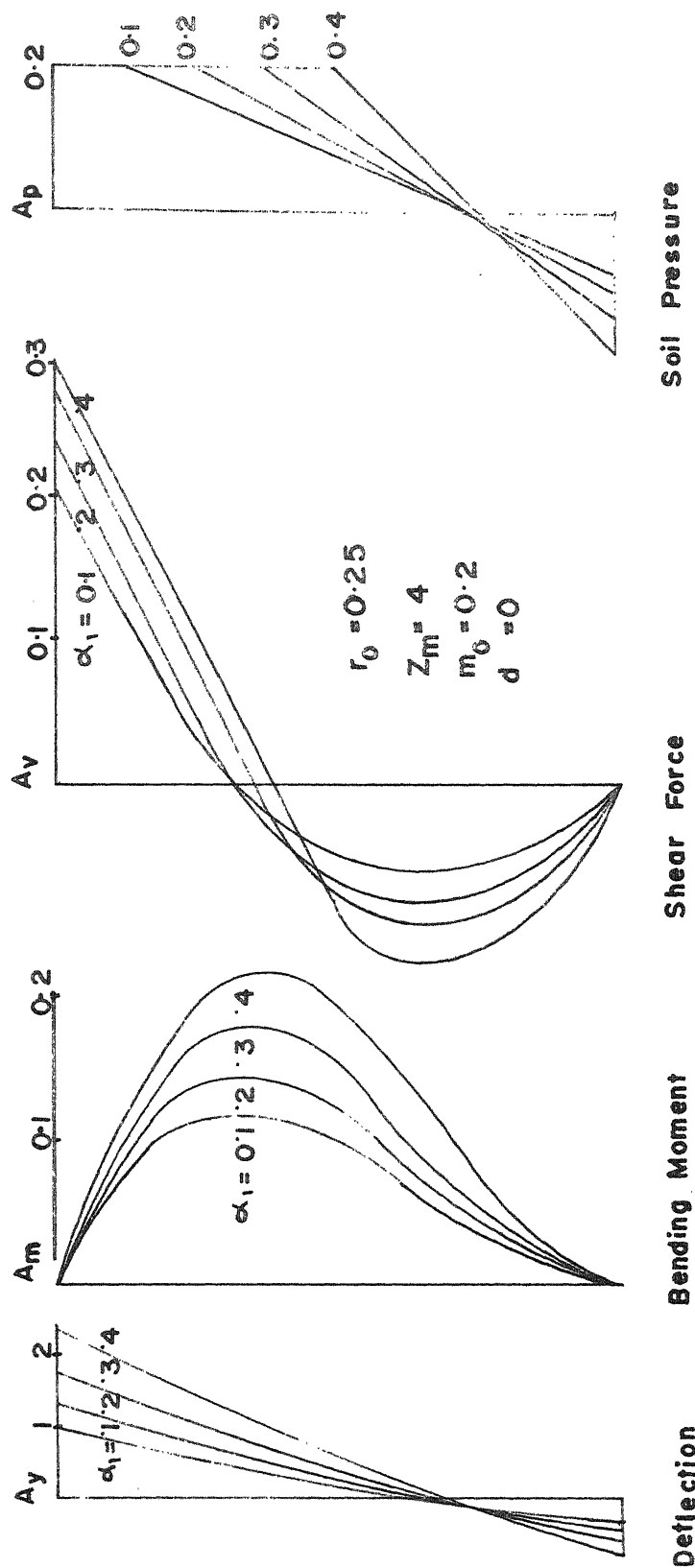
(a)

(b)

FIG(3.5) EFFECT OF r_o AND m_o ON PILE DEFLECTION AND SHEAR DISTRIBUTION



FIG(3-6) VARIATION OF DEFLECTION, B.M., S.F AND SOIL PRESSURE WITH α_1
SHORT PILE



FIG(3.7) VARIATION OF DEFLECTION, B.M. S.F AND SOIL PRESSURE
WITH α_1
LONG PILE

The main advantage of the elasto-plastic analysis of pile is shown by the fact, that it carries greater load. In general, the load capacity is increased by about 10%, when the soil behavior changes from stage 2 to stage 3. and the increase in overall load capacity from stage 1 to stage 3, is about 30%.

B. FREE-FREE PILE: MOMENT AT TOP; TYPE-I, CASE II:

Moment applied at top versus top deflections are plotted in fig. (3.8 a) for $Z_m=3$ to $Z_m=5$. A graphical comparison of the curves for $m_0=0.2$ and $m_0=0.5$ are also shown. It indicates the magnification of deflection and moment for decreased value of ' m_0 '. It is seen that, in the initial stages the moment-deflection relation is linear which shows, the soil behaves elastically (stage 1). When moment is increased a certain limit, stage 2 is reached and finally for higher moment, stage 3 is operating.

Similar informations are seen from fig. (3.8 b); wherein, the increased value of ' r_0 ' induces higher amount of pile deflection for the same value of ' M_t '. It is also seen from the plot, the moment capacity increases with greater pile length.

For $d = 1$, the moment capacity is increasingly magnified for the same pile. This is seen from fig. (3.9).

The effect of ' m_0 ' on short pile is shown in fig. (3.10 a). In this case, with higher value of m_0 , the

moment capacity is increased. For an increase of ' m_0 ' from 0.2 to 0.5, the ultimate moment capacity increases from 0.5 to 1.25. On an average, the increase of m_0 by 0.1, can increase the moment capacity by 2.5 times.

As presented in fig. (3.10 b), the effect of r_0 on long pile is insignificant, so far as moment-deflection is concerned.

From fig. (3.11 a), it is evident that, the effect of increasing ' r_0 ' is to reduce the deflection along the length. The short pile behaves as a rigid pile. Also the bottom being free to move, the depth of zero deflection of the pile, is reached exactly at the mid-depth of the pile.

Fig. (3.11 b) shows, that the moment capacity of the pile, increases with the increasing value of m_0 and also the distribution, of moment, along the depth is increased proportionately with ' m_0 '. It is also evident from the figure, that the moment capacity increases in the same proportion, with m_0 .

Variation of deflection, moment, shear force and soil pressure along depth for short pile is presented in fig. (3.12). Symmetry in deflection at top and bottom is clearly seen. This shows that, the pile behaves as, it is hinged at the mid-depth. The shear force distribution is linear for the plastic zones at top and bottom. The soil-pressure distribution is also symmetric about the mid-depth.

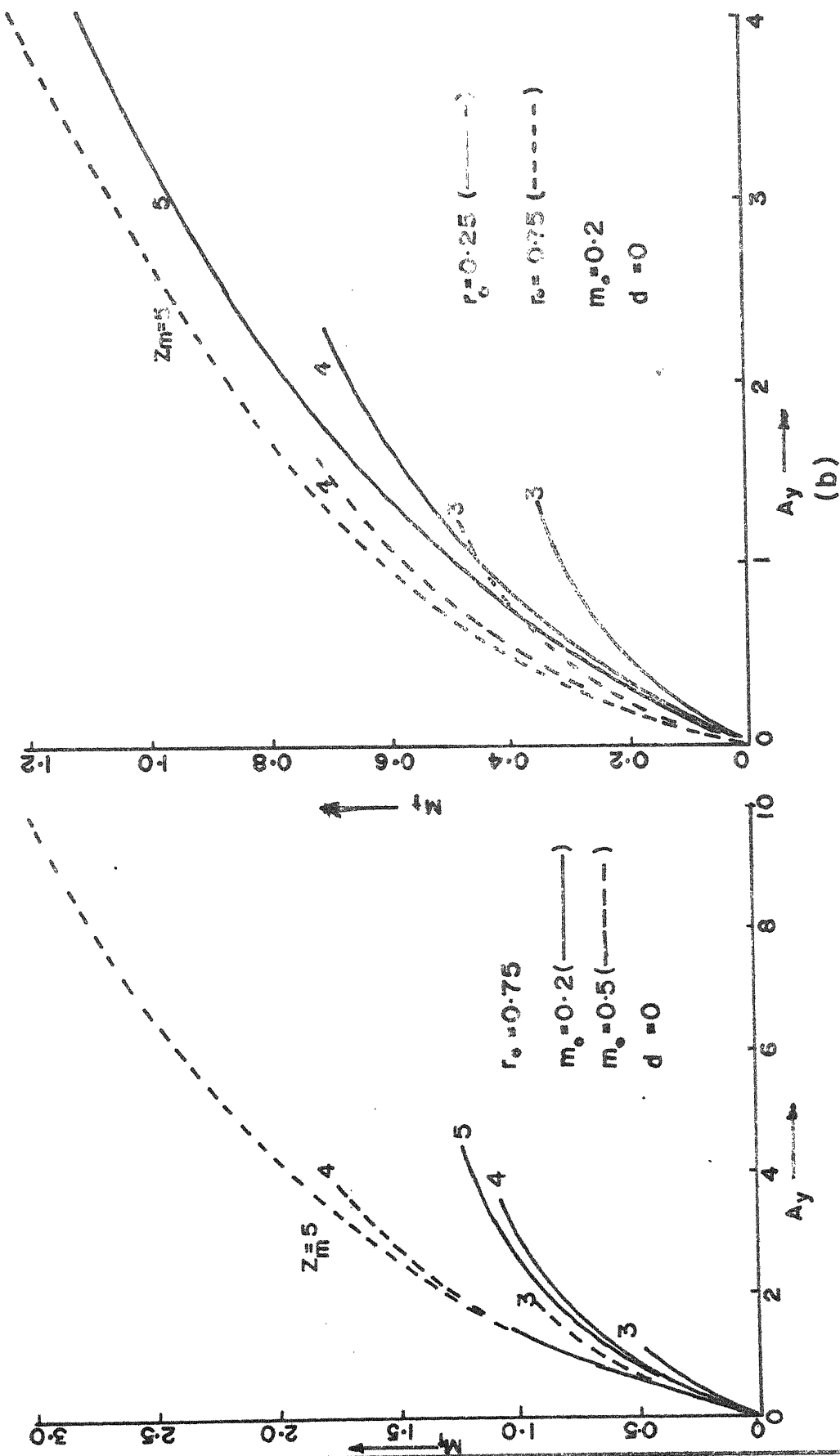
All these properties are valid for $d=0$ i.e. soil property is invariant with depth and for stage 3.

Variation of deflection, moment, shear and soil pressure distribution along the depth for a short pile, in stage 2 and for $d=1$ is shown in fig. (3.13). Variation of the above said properties for different α_1 , are also shown in the figure. With $d=1$, the moment capacity of the pile is increased.

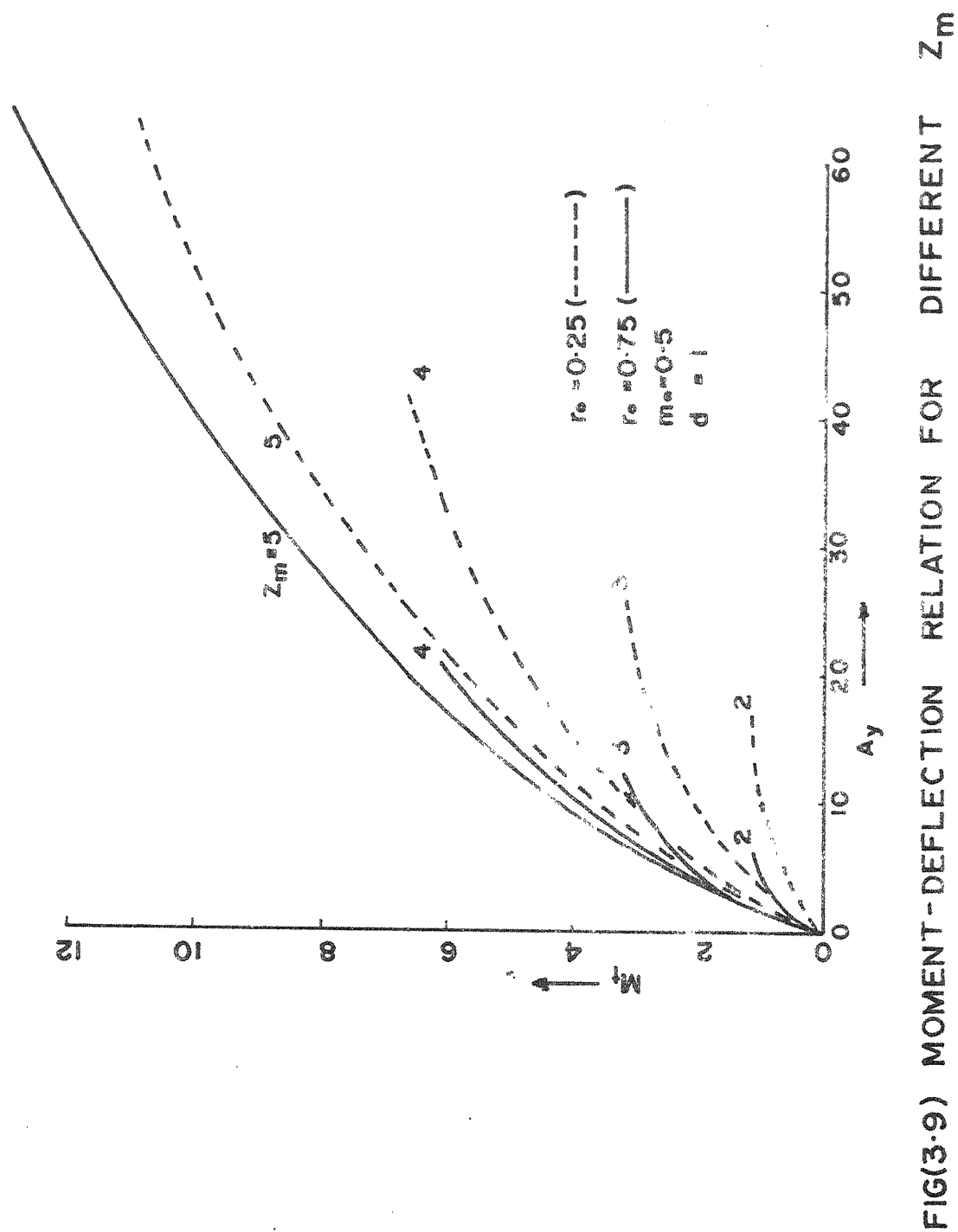
Typical plot for variation of deflection, BM, SF and soil pressure is shown for a long pile and the soil property changing with depth, in fig. (3.14). Deflection at the bottom being very small, the bottom plastic zone does not develop in this case.

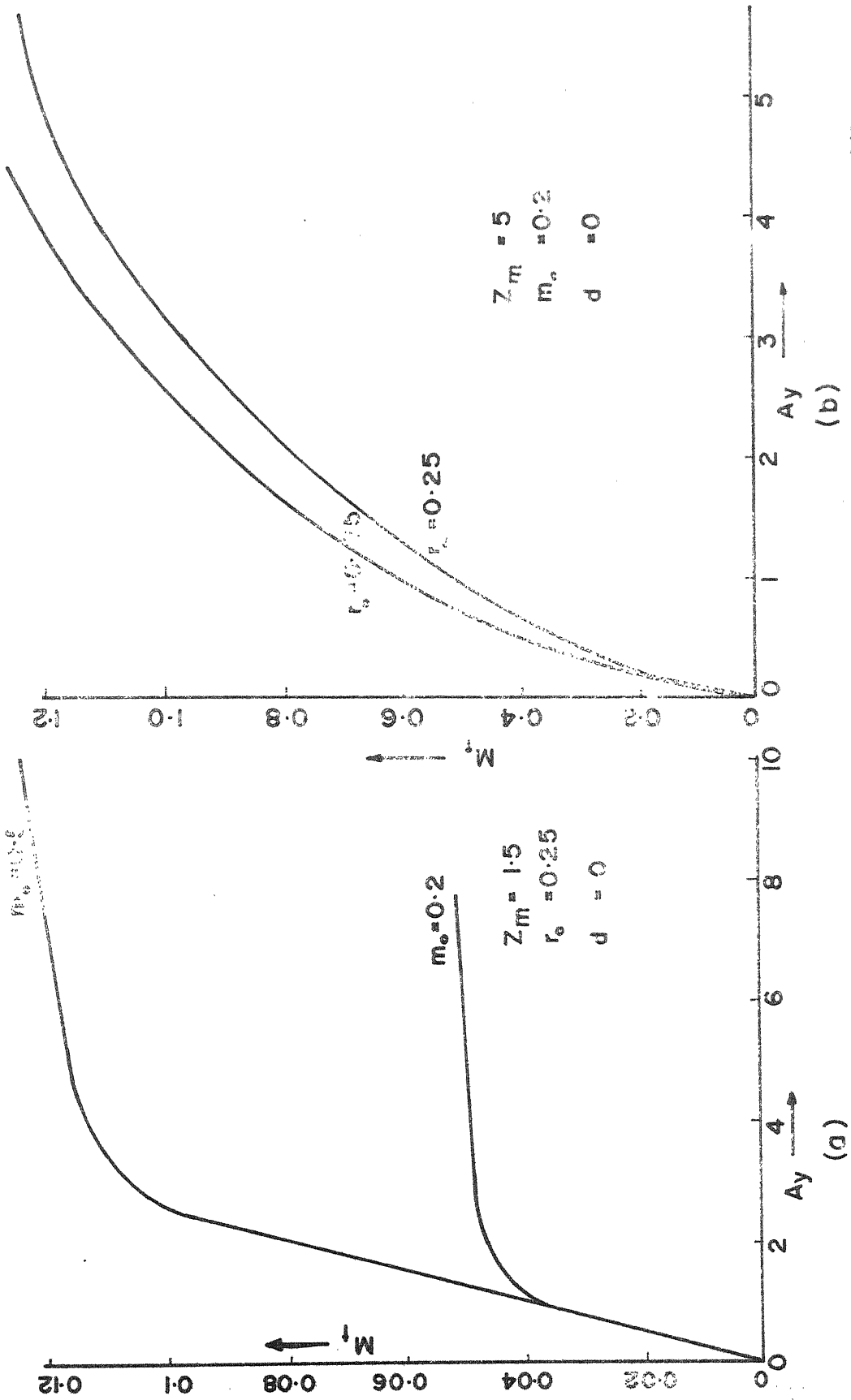
For uniform soil behavior with depth, and for short pile, stage 2 is not reached in the case of free-free pile with moment applied at top. As there is no lateral load at top, the soil pressures on both the sides of the pile is equal and this give rise to a moment, which is equal to the moment at top. For this reason, the deflection is symmetric about the mid-depth of the pile and a plastic zone is formed at the bottom, corresponding to a plastic zone at top. From the same reasoning, it can be shown that, the ultimate capacity of the pile is reached, for $\alpha_1=0.5$, which is apparent from fig. (3.12).

As in the previous case, the increase in pile capacity is about 10%.

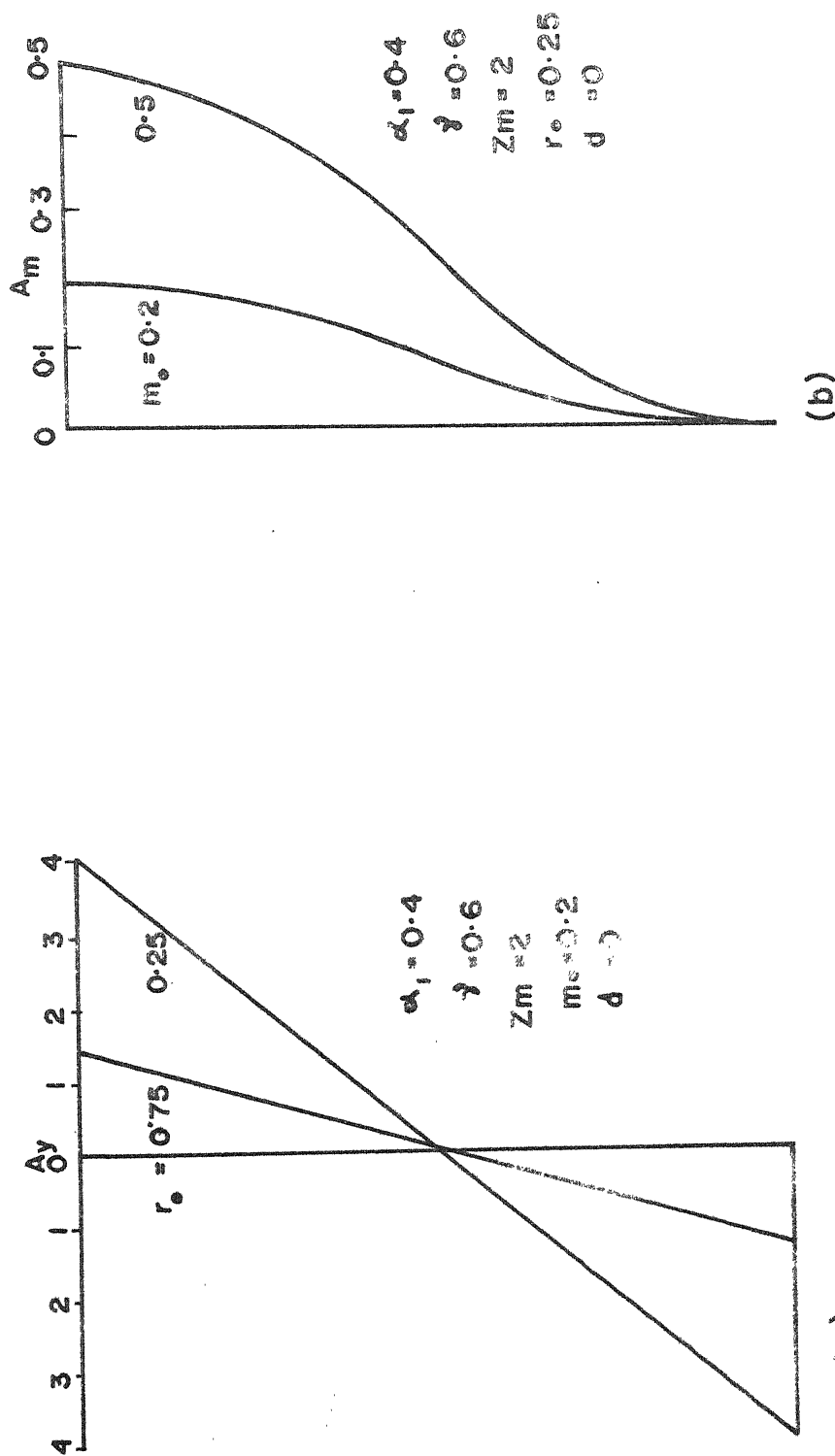


FIG(3.8) MOMENT-DEFLECTION RELATION FOR DIFFERENT Z_m

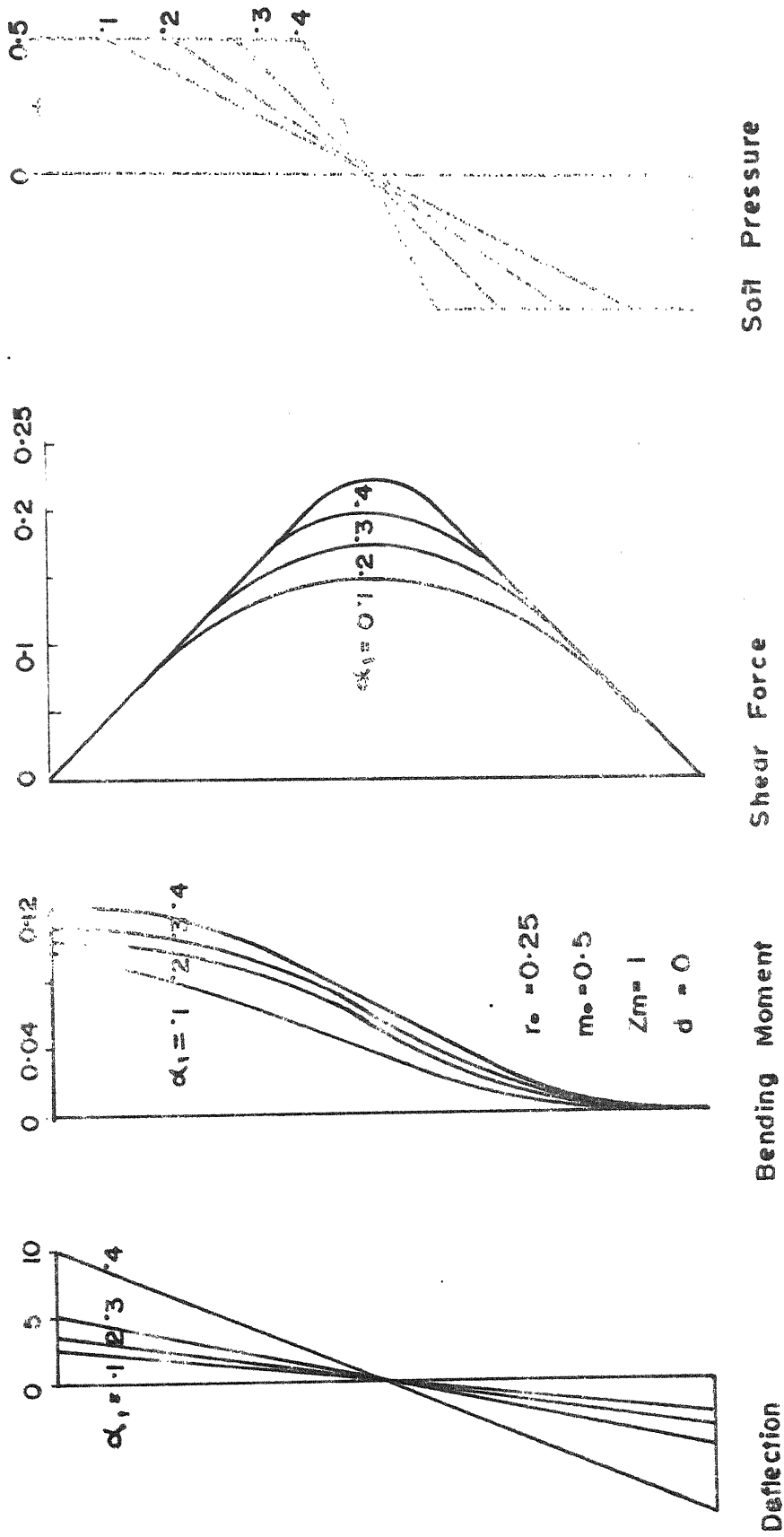




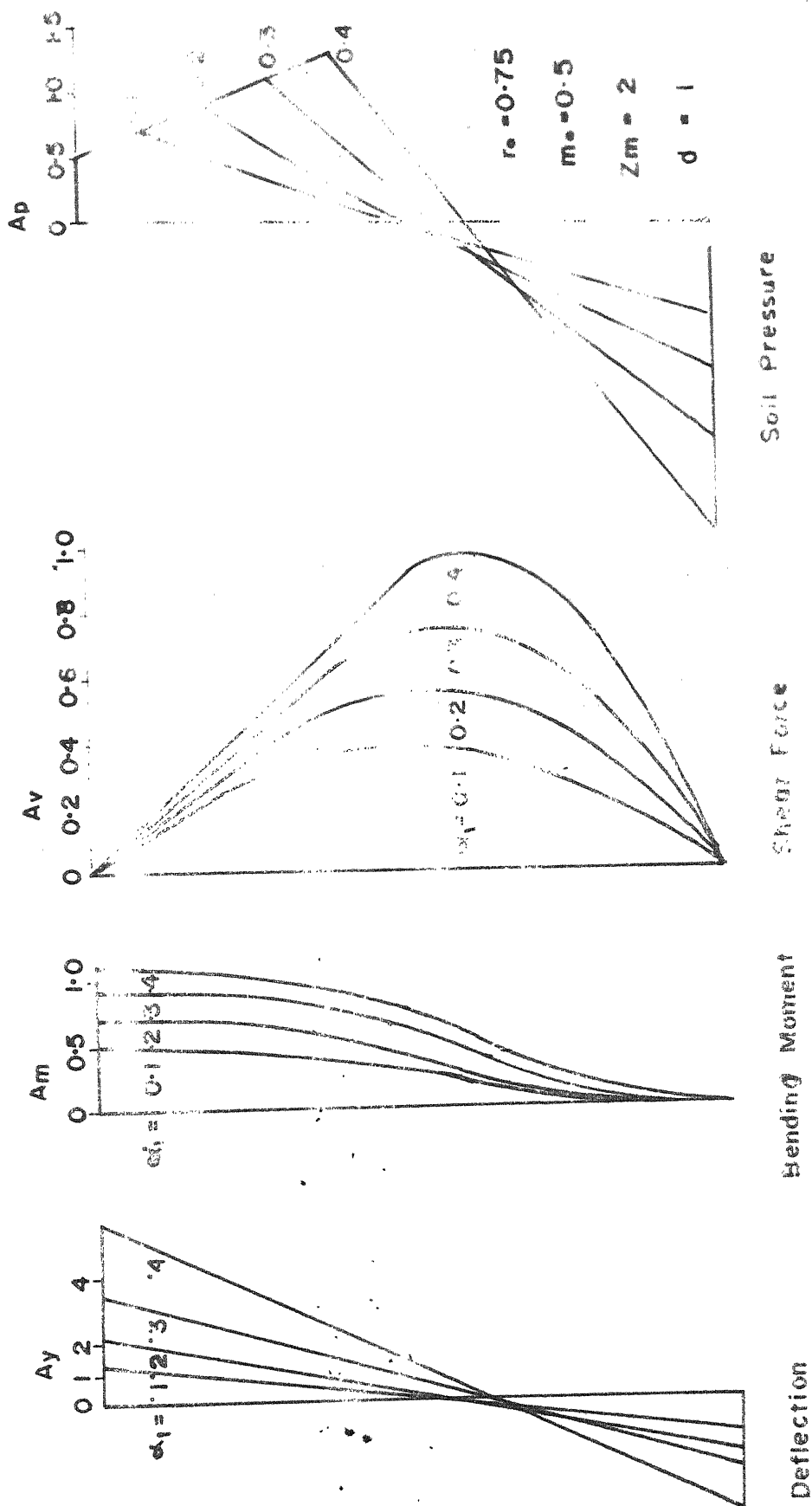
FIG(3.10) MOMENT- DEFLECTION RELATION FOR DIFFERENT m_o AND r_o



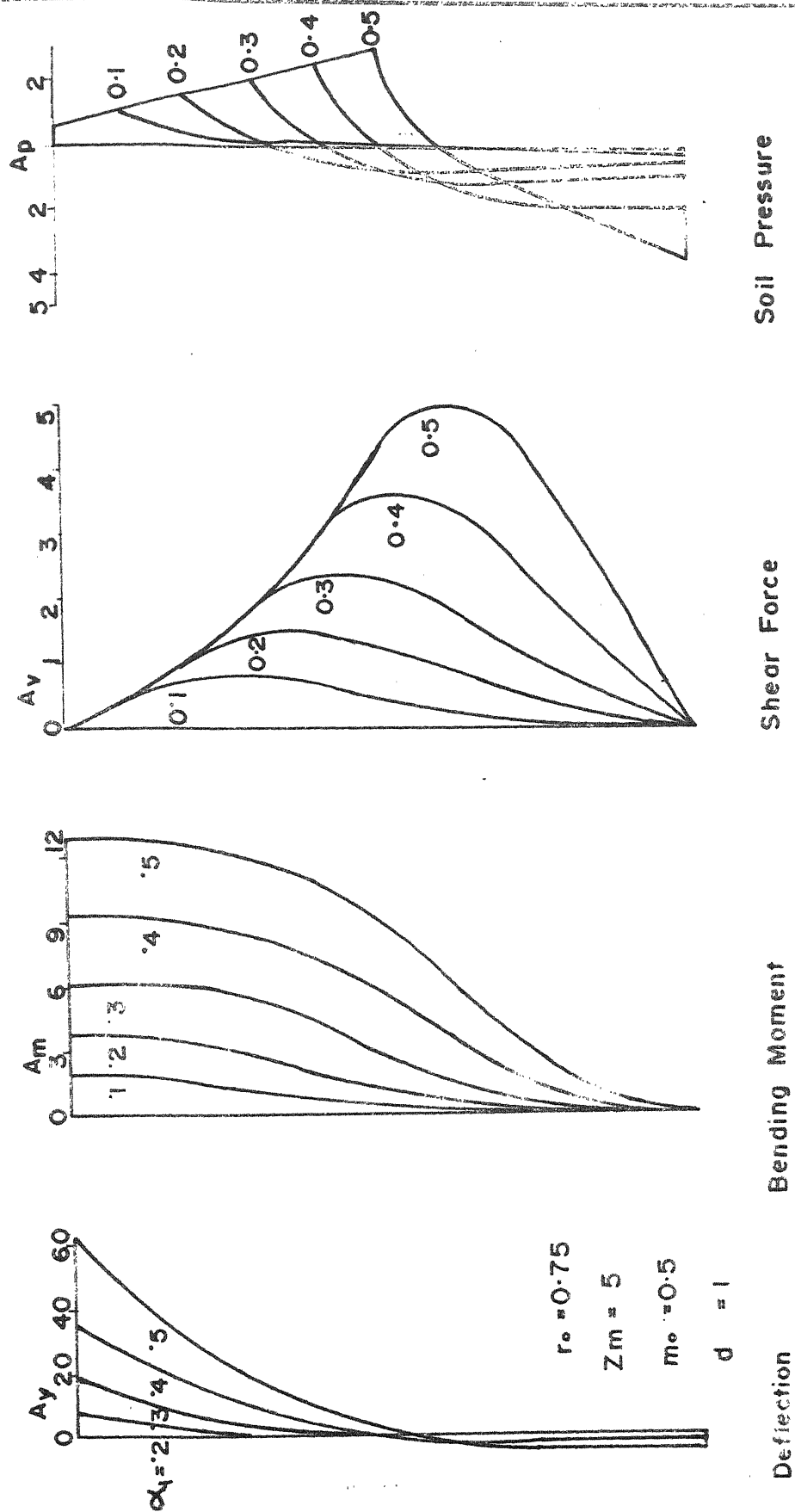
FIG(3-11) EFFECT OF r_0 AND m_0 ON DEFLECTION AND BENDING MOMENT



FIG(3.12) VARIATION OF DEFLECTION, B.M., S.F. AND SOIL PRESSURE
WITH α_1
SHORT PILE



FIG(3.13) VARIATION OF DEFLECTION, B.M., S.F. AND SOIL PRESSURE
WITH α_1 (for $d=1$)
SHORT PILE



FIG(3-14) VARIATION OF DEFLECTION, B.M., S.F. AND SOIL PRESSURE WITH α_1 LONG PILE

C. FIXED-FREE PILE TYPE: II:

As stated earlier, the method of solution applied in this case, has no control over the moment or shear applied at the top. In the actual solution, a soil pressure distribution is assumed, and the corresponding moment and shear at the top is computed. In the results only the effect of shear at top is shown and discussed.

In fig. (3.15) the effect of ' r_0 ' on load-deflection character is shown. For short pile, the effect of ' r_0 ' is significant. For higher values of ' r_0 ', the load-capacity of the pile is increased. The effect of ' r_0 ', on load-deflection character for long piles is insignificant, as in the previous cases.

Effect of ' m_0 ' on load-deflection property, for a short pile is practically negligible for the initial portions i.e. for stage 1 and stage 2. The response of ' m_0 ' gradually becomes significant with increasing load. But for long pile, the effect of ' m_0 ' is small and is fairly uniform. The curves for load versus deflection at top are shown for $m_0=0.2$ and 0.5 , and for short and long piles separately in fig. (3.16).

In fig. (3.17) load-deflection curves for $d=0$ and $d=1$ are shown for short and long piles separately. It is evident that, with $d=1$, the pile capacity increases to a large extent for both short and long piles.

Effect of ' r_0 ' on deflection, BM, SF and soil pressure along the length of long pile is shown in fig.(3.18), with increasing ' r_0 ' the deflection decreases.

Fig. (3.19) shows the typical behavior of a fixed free, short pile. In this case, the pile being rigid and also fixed at top, the pile moves bodily when acted upon by lateral load. Shear force distribution is linear. The soil pressure distribution is uniform and of the same nature for the whole length of the pile.

Typical deflection, BM, SF and soil pressure distribution along the length of a long pile is shown in fig. (3.20) for stage 2.

Because long pile does not behave as rigid pile, stage 3 of soil pressure distribution is possible in this case and this is shown in fig. (3.21).

As stated earlier, that a short pile behaves as a rigid pile, and it moves bodily, under lateral load. The soil pressure distribution for $d = 0$, have a particular effect. In this case, the proposed stages of pile-soil interaction is not valid. Soil behaves uniformly, for the whole length of the pile. Deflection being uniform, the soil pressure is uniform ($= -ky$ or m_0) and have the same sense. So, the soil behaves elastically or plastically for the whole length of the pile. The ultimate load in this case is given by:

$$P_u = m_o Z_m$$

where,

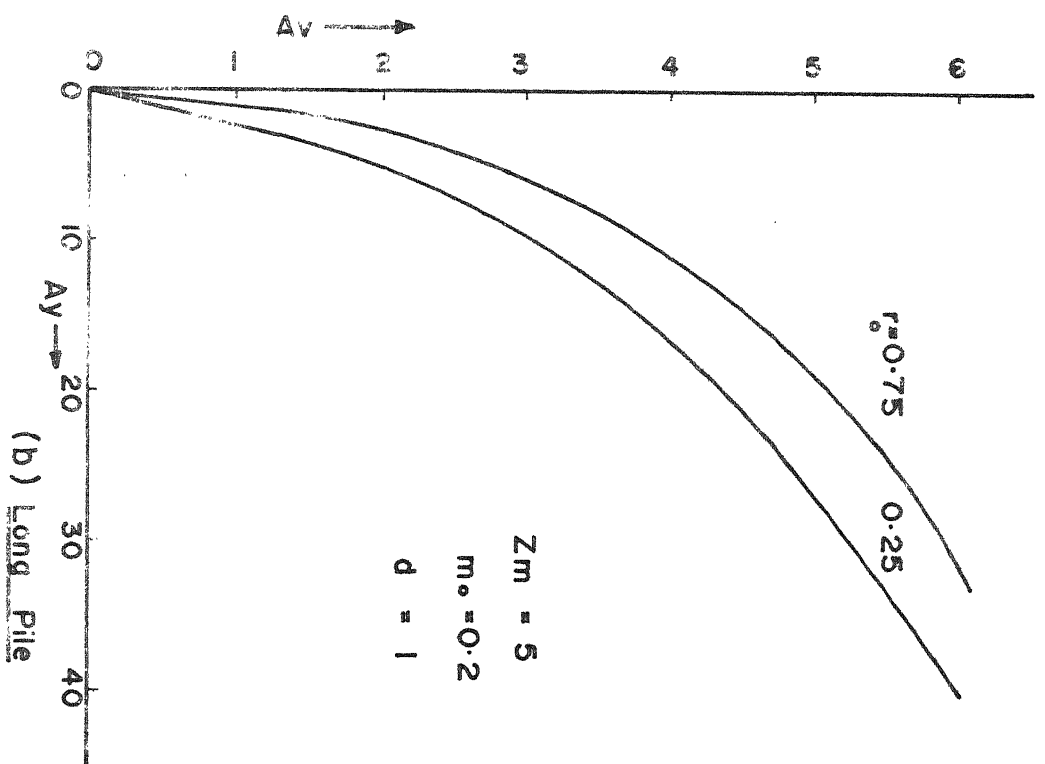
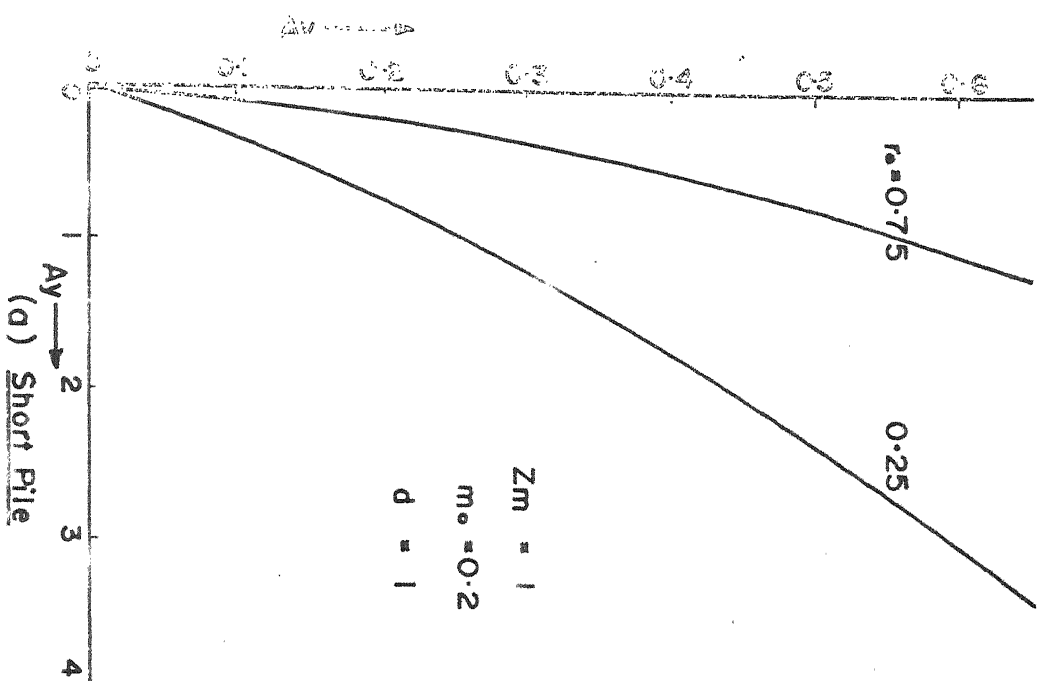
P_u = ultimate load capacity of the pile,

For long pile stage 1, stage 2, and stage 3 are possible and the proposed model is valid in the case of fixed-free, long pile.

D. ULTIMATE LOAD FOR FREE-FREE PILE, LOAD AT TOP:

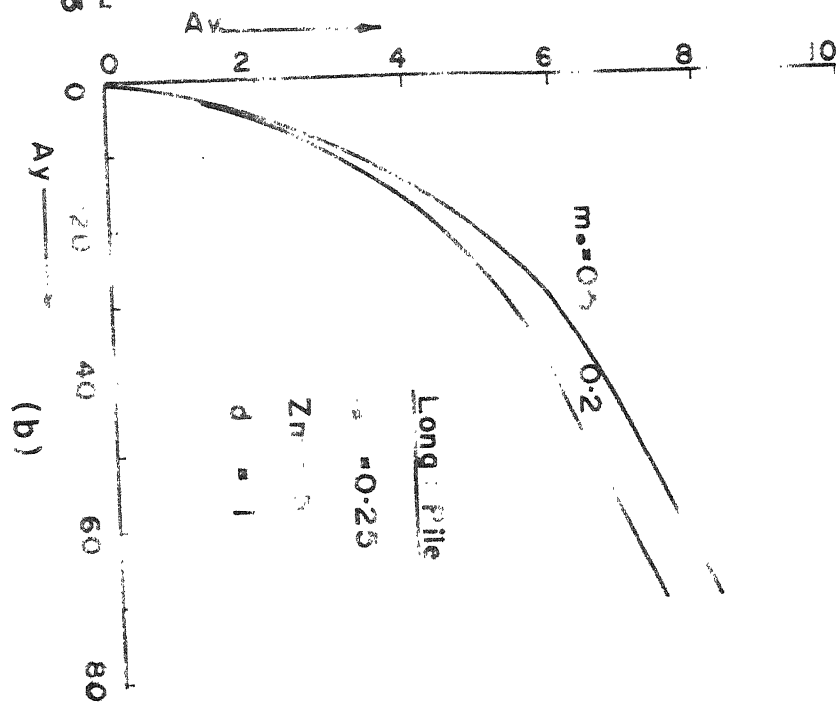
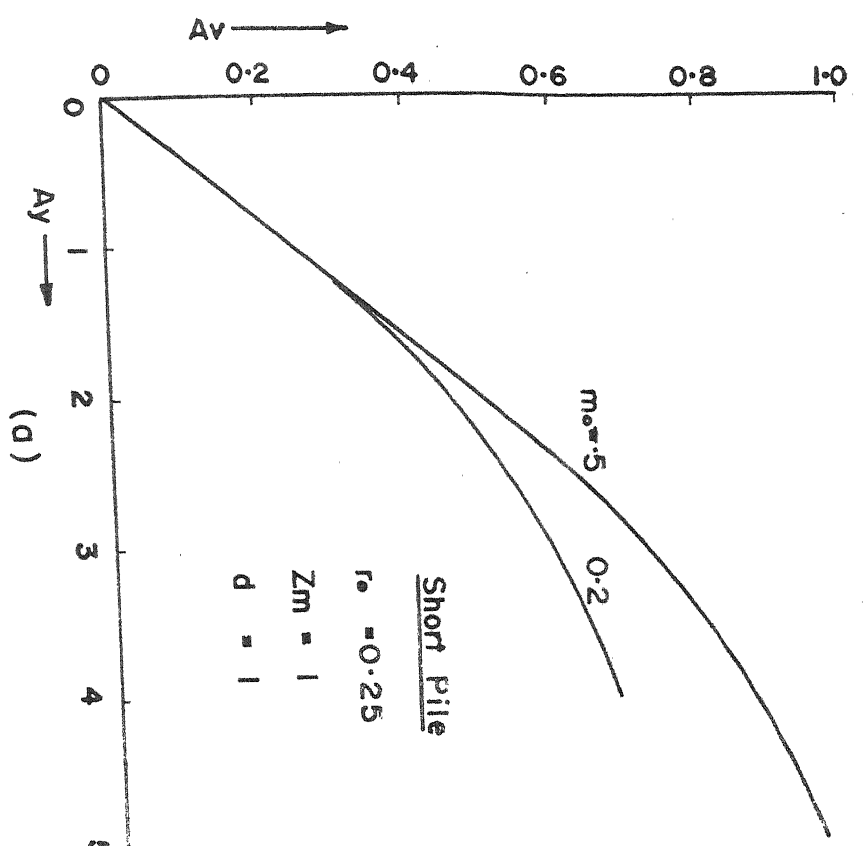
Values of α_1 for different values of ' m_o ' and for various values of ' d ' are plotted in fig. (3.22 a). From the plot, it is evident that, for higher values of ' d ', the values α_1 are increased. This is explained by the fact that, for higher value of ' d ', the effect of overburden is increased. On the other hand, for higher value of ' m_o ' the value of ' α_1 ' is decreased for a given value of ' d '.

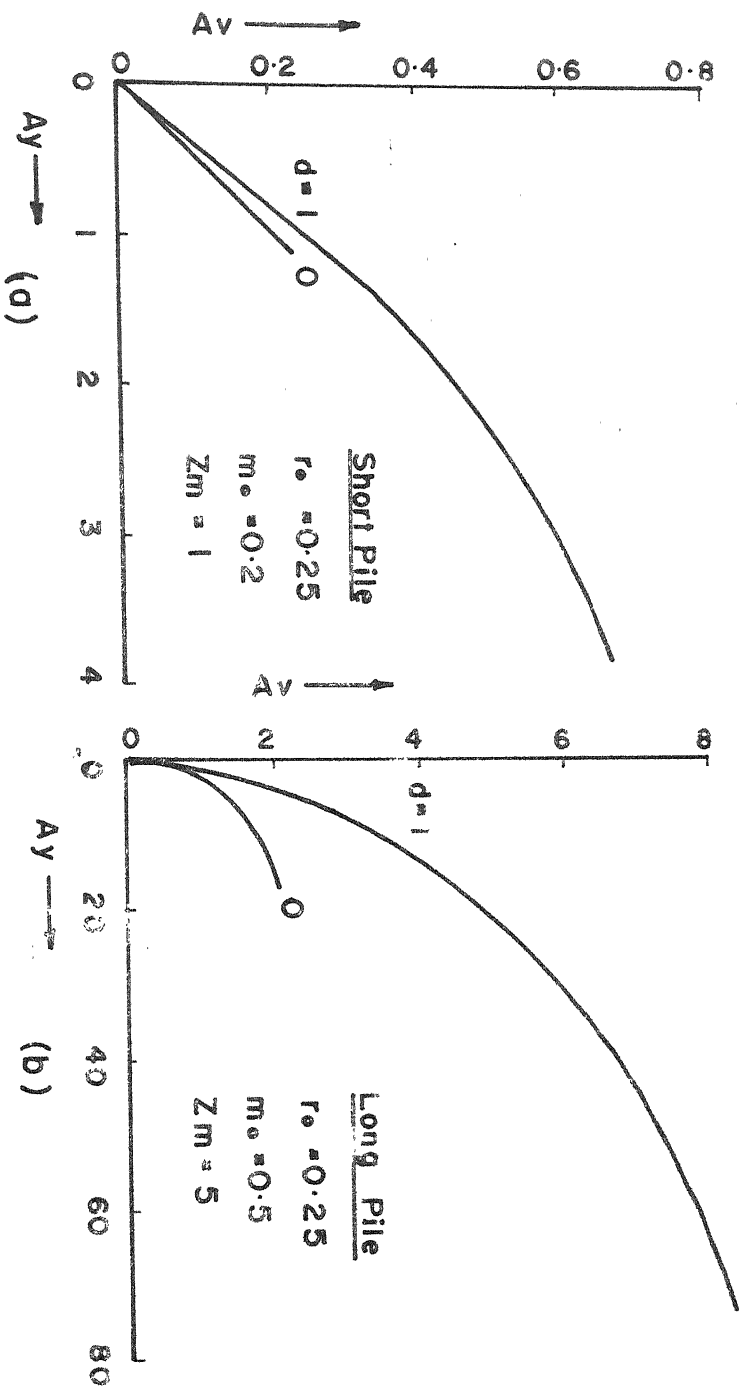
In fig. (3.22 b), values of α_1 are plotted against the value of ' d ' for different Z_m . As stated in section 2.6, for $d=0$, the value of α_1 is $\frac{1}{\sqrt{2}}$, for any value of Z_m . It is seen from the plot, the value of α_1 starts from $\alpha_1=0.707$ and it asymptotically reaches the value of $\alpha_1=0.79$ with increasing Z_m . Theoretically for infinite pile length (i.e. $Z_m = \infty$), the value of α_1 reaches 1. (See appendix B).



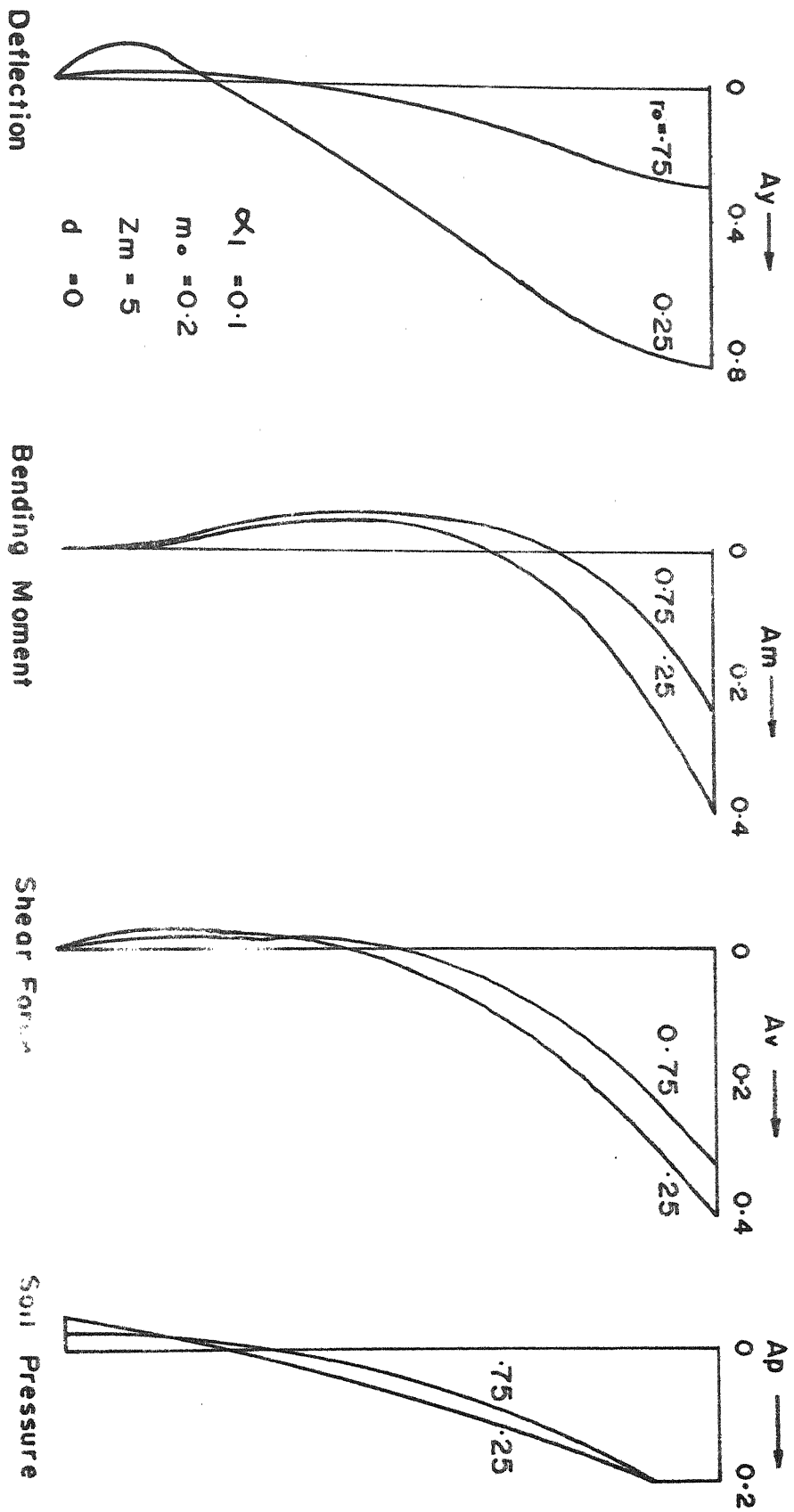
FIG(3.15) EFFECT OF r_o ON LOAD-DEFLECTION RELATIONSHIP

FIG(3.16) EFFECT OF m_o ON LOAD-DEFLECTION RELATIONSHIP

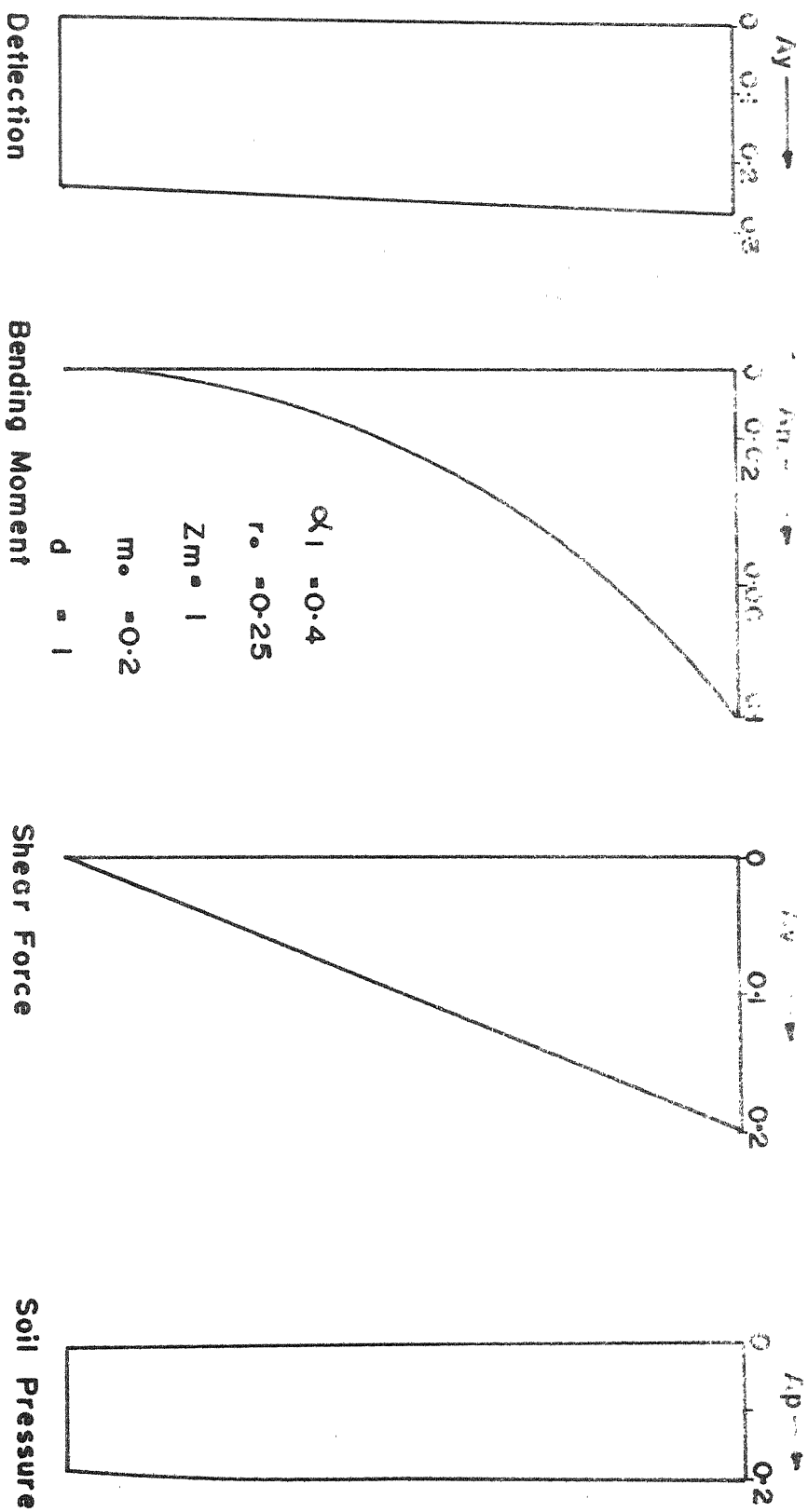




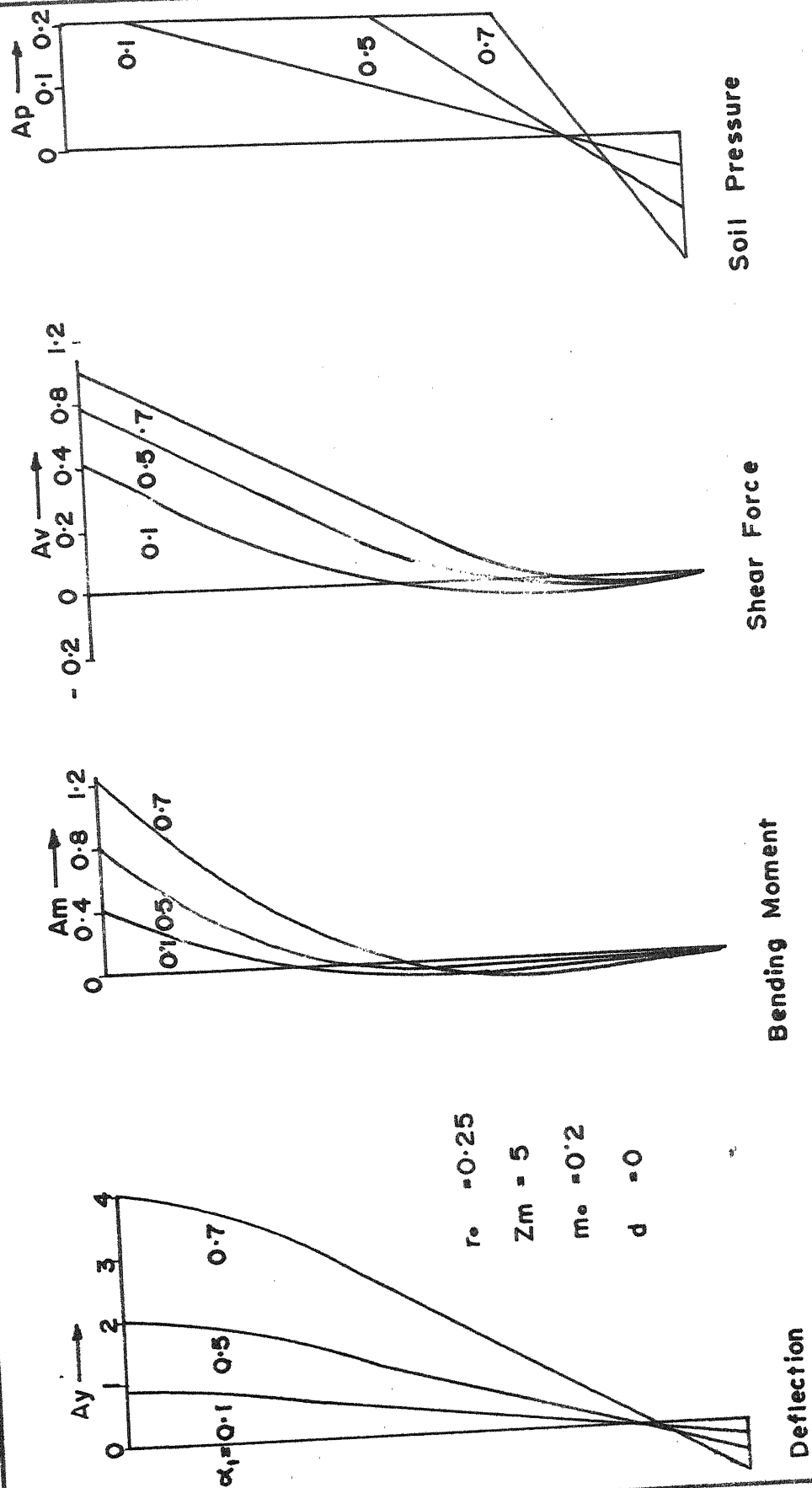
FIG(3.17) EFFECT OF d ON LOAD-DEFLECTION RELATIONSHIP



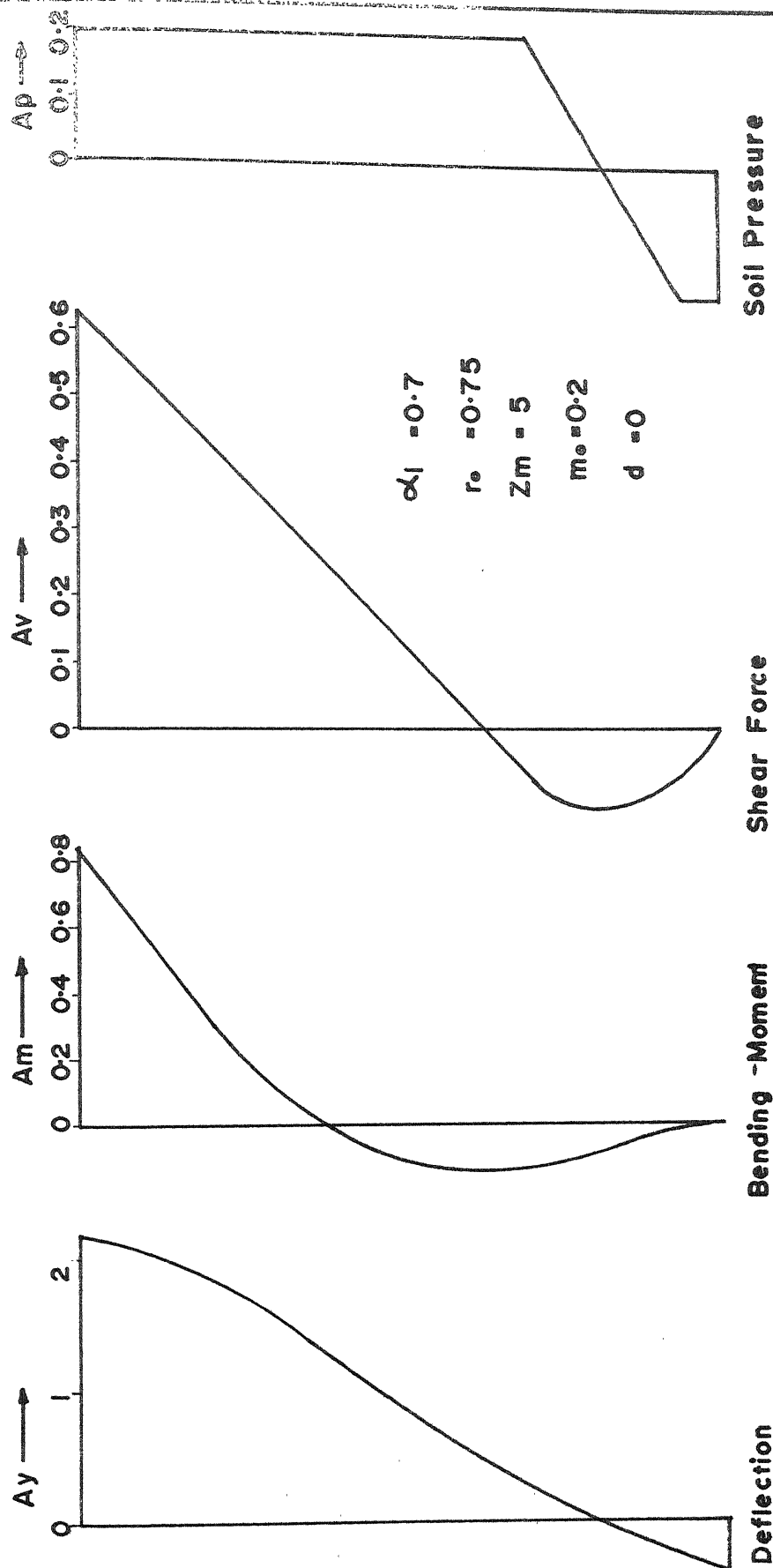
FIG(3.18) EFFECT OF r_0 ON DEFLECTION, B.M., S.F. AND SOIL PRESSURE



FIG(3.19) DEFLECTION, B.M, S.F. AND SOIL PRESSURE DISTRIBUTION
Short Pile

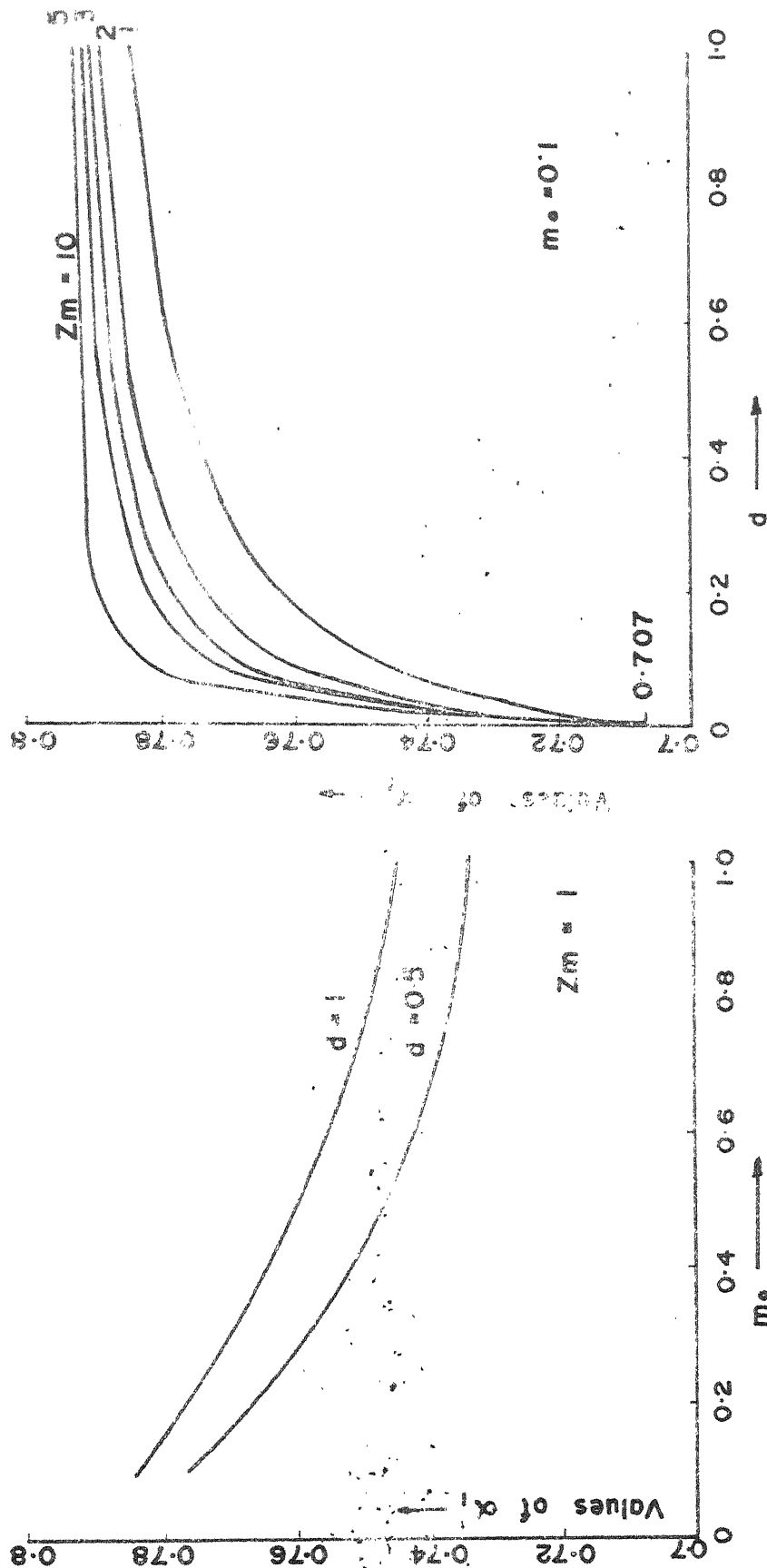


FIG(3.20) DEFLECTION, B.M., S.F. AND SOIL PRESSURE DISTRIBUTION
Long Pile (Stage - 2)



FIG(3.21) DEFLECTION, B.M., S.F. AND SOIL PRESSURE DISTRIBUTION

Long Pile (Stage - 3)



FIG(3.22) ULTIMATE LOAD - FREE - FREE PILE (Load at top)

CHAPTER IV

OVERHANG PILES

4.1 INTRODUCTION:

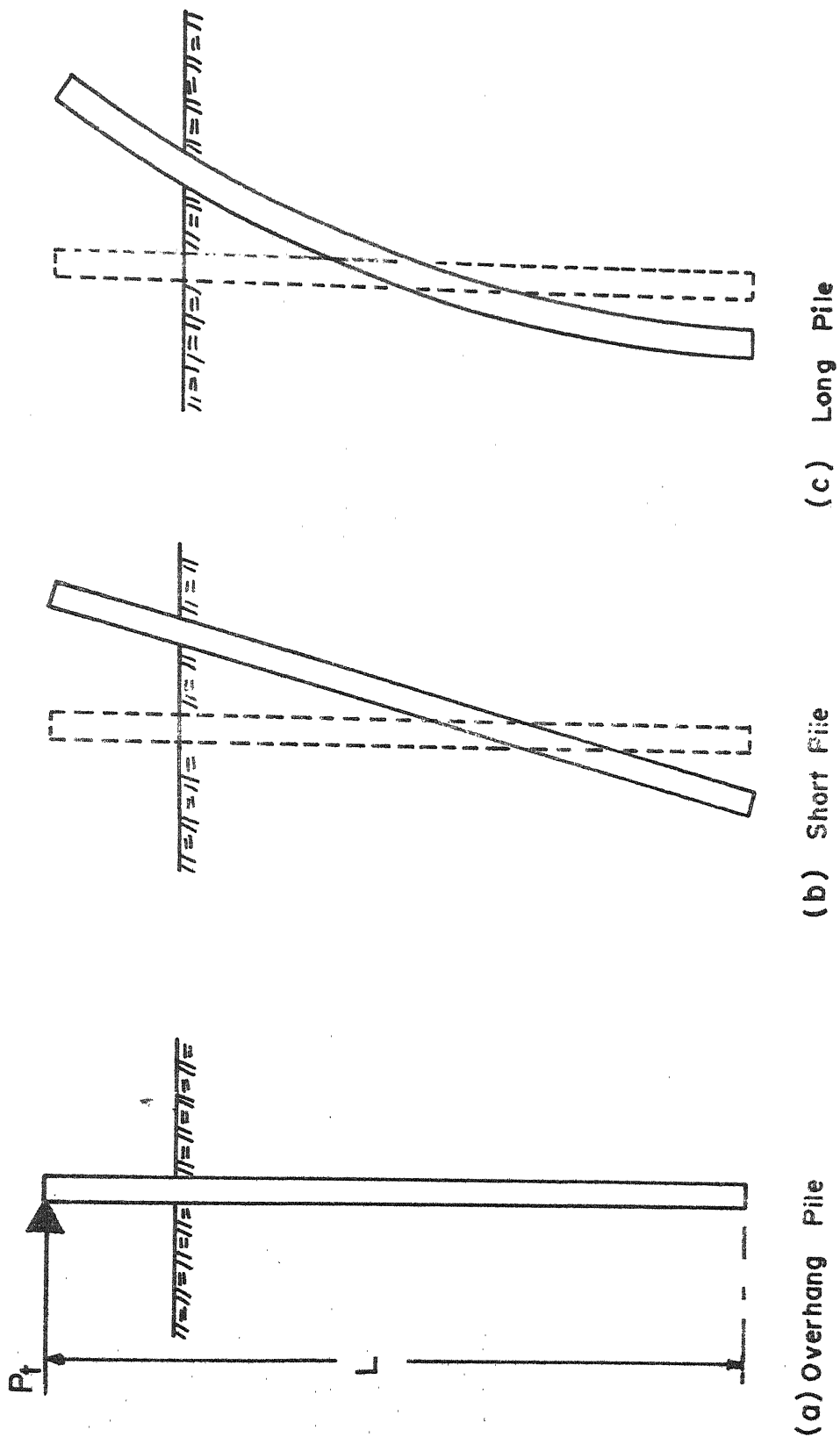
In general, the laterally loaded piles which are used in off-shore structures, have some portion of the pile projecting above the soil. This type of piles have certain characteristics which are different from the types discussed previously. This type of piles are named as "overhang piles." The effect of overhang is to induce a certain amount of moment and shear force at a section of the pile at the top of the soil. In this section, a direct approach to the problem is dealt with, and the solutions are obtained in nondimensional forms. The deflection pattern of overhang piles is same as discussed in section 2.1.

4.2 PILE BEHAVIOR:

The deflection at the top is maximum, it gradually reduces and reaches zero at some point, the deflection increases and reaches a high negative value at the bottom of the pile (Fig. 4.1).

4.3 SOIL BEHAVIOR:

As discussed in section 2.2, all the four stages of soil-pressure distribution are possible in the case of overhang piles (Fig. 4.2). The model proposed in section 2.3



FIG(4-1) DEFLECTED SHAPE OF OVERHANG PILE

is also applicable to this case. The characteristics of the pile may be represented by the fact that the soil reaction is zero upto a depth x_1 , starting from the top of the pile. Corresponding to this fact, there is no spring and friction block in the model for a depth upto x_1 . The corresponding model is shown in fig. 4.3 .

The soil and the pile behavior in the present case is the same as free-free or fixed-free pile cases.

4.4 FORMULATION OF THE PROBLEM:

In this case, the basic differential equations are same as the previous cases. Using the notations defined earlier, the equations can be written in the following manner for different stages;

Stage 1:

$$\text{For overhang portion: } EI \frac{d^4 y_1}{dx^4} = 0 \text{ for } 0 \leq x \leq x_1 \dots (4.1)$$

$$\text{For elastic zone : } EI \frac{d^4 y_2}{dx^4} + ky = 0 \text{ for } x_1 \leq x \leq L \dots (4.2)$$

Stage 2:

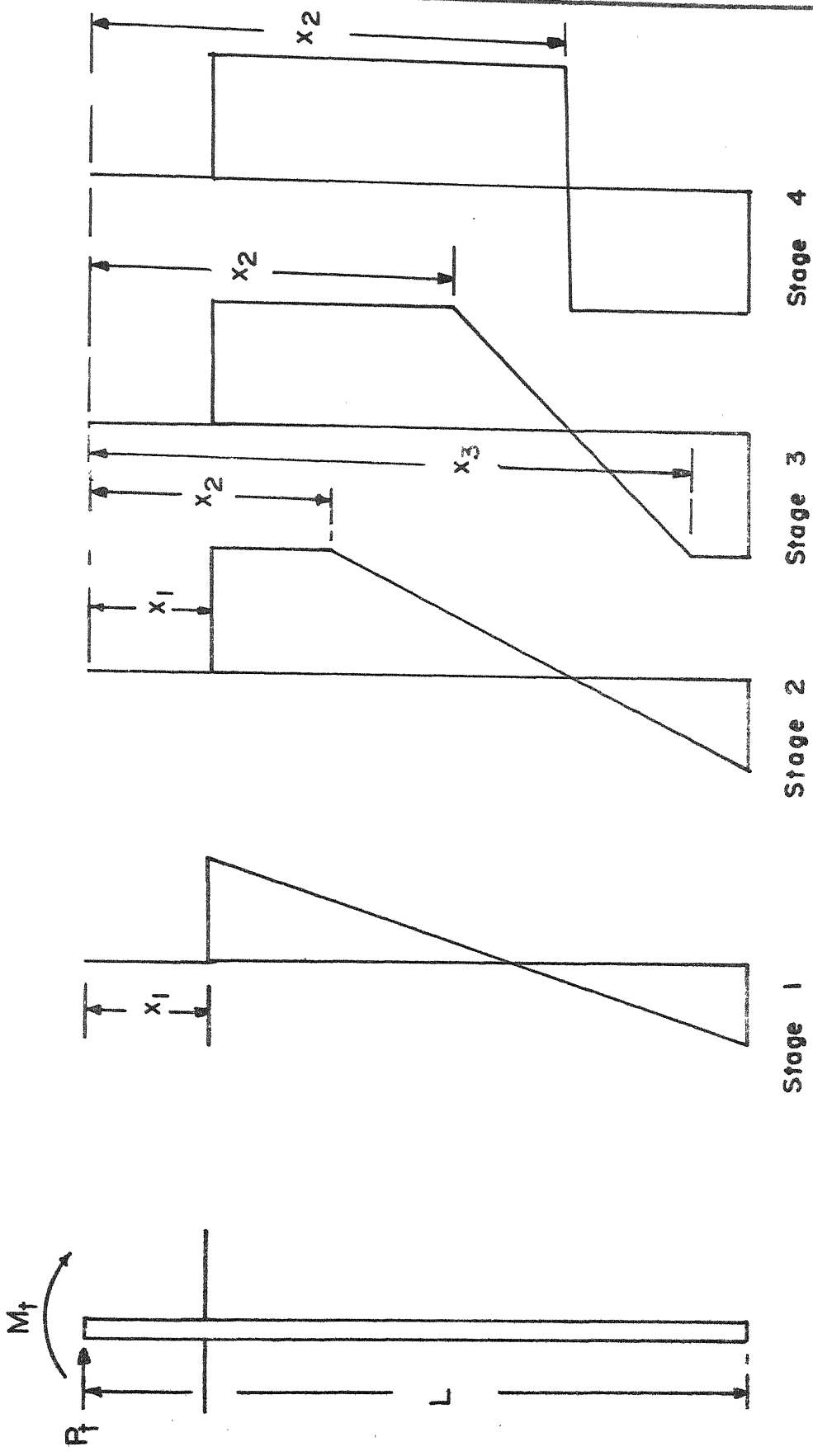
$$\text{For overhang portion: } EI \frac{d^4 y_1}{dx^4} = 0 \text{ for } 0 \leq x \leq x_1 \dots (4.3)$$

$$\text{For top plastic zone: } EI \frac{d^4 y_2}{dx^4} + q = 0 \text{ for } x_1 \leq x \leq x_2$$

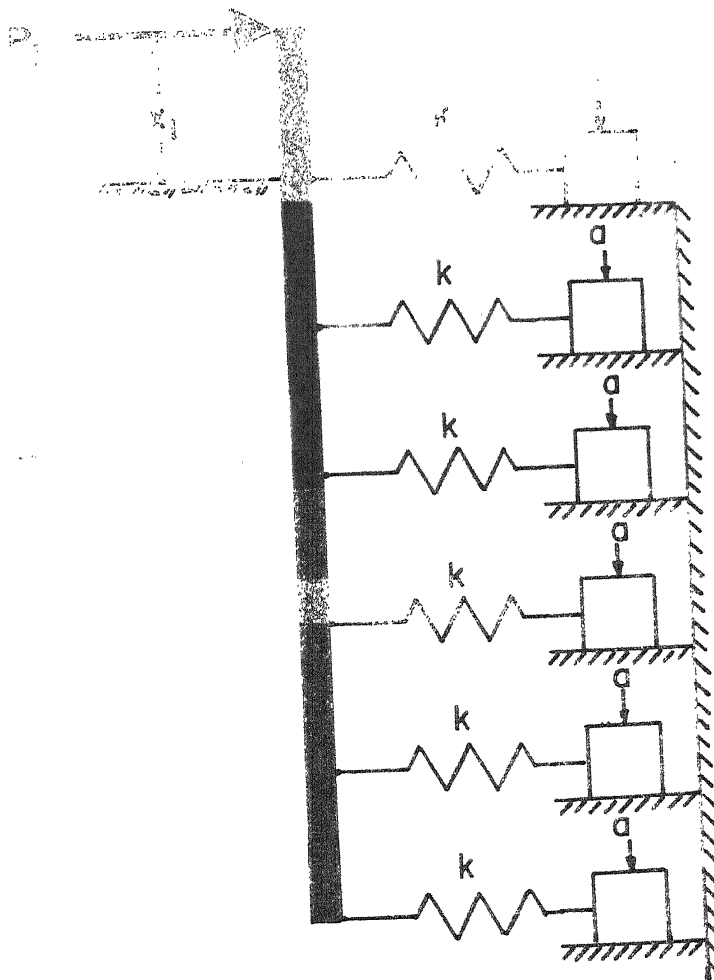
$$\dots (4.4)$$

$$\text{For bottom elastic zone: } EI \frac{d^4 y_3}{dx^4} + ky = 0 \text{ for } x_2 \leq x \leq L$$

$$\dots (4.5)$$



FIG(4.2) FOUR STAGES OF OVERHANG PILE



FIG(4-3) MODEL FOR OVERHANG PILE

Stage 3:

$$\text{For overhang portion : } EI \frac{d^4 y_1}{dx^4} = 0 \quad \text{for } 0 \leq x \leq x_1 \quad \dots (4.6)$$

$$\text{For top plastic zone: } EI \frac{d^4 y_2}{dx^4} + q = 0 \quad \text{for } x_1 \leq x \leq x_2 \quad \dots (4.7)$$

$$\text{For middle elastic zone: } EI \frac{d^4 y_3}{dx^4} + ky = 0 \quad \text{for } x_2 \leq x \leq x_3 \quad \dots (4.8)$$

$$\text{For bottom plastic zone: } EI \frac{d^4 y_4}{dx^4} - q = 0 \quad \text{for } x_3 \leq x \leq L \quad \dots (4.9)$$

Stage 4:

$$\text{For overhang portion: } EI \frac{d^4 y_1}{dx^4} = 0 \quad \text{for } 0 \leq x \leq x_1 \quad \dots (4.10)$$

$$\text{For top plastic zone: } EI \frac{d^4 y_2}{dx^4} + q = 0 \quad \text{for } x_1 \leq x \leq x_2 \quad \dots (4.11)$$

$$\text{For bottom plastic zone: } EI \frac{d^4 y_3}{dx^4} - q = 0 \quad \text{for } x_2 \leq x \leq L \quad \dots (4.12)$$

Using the nondimensional terms defined earlier and the process of algebraic operations, the final form of the equations are expressed as:

Stage 1:

$$\frac{d^4 A y_1}{dz^4} = 0 \quad \text{for } 0 \leq z \leq z_1 \quad \dots (4.13)$$

$$\frac{d^4 A y_2}{dz^4} + r_o A y_2 = 0 \quad \text{for } z_1 \leq z \leq z_m \quad \dots (4.14)$$

Stage 2:

$$\frac{d^4 A y_1}{dz^4} = 0 \quad \text{for } 0 \leq z \leq z_1 \quad \dots (4.15)$$

$$\frac{d^4 A y_2}{dz^4} + [m_0 + a(z - z_1)] = 0 \quad \text{for } z_1 \leq z \leq z_2 \quad \dots (4.16)$$

$$\frac{d^4 A y_3}{dz^4} + r_0 A y_3 = 0 \quad \text{for } z_2 \leq z \leq z_m \quad \dots (4.17)$$

Stage 3:

$$\frac{d^4 A y_1}{dz^4} = 0 \quad \text{for } 0 \leq z \leq z_1 \quad \dots (4.18)$$

$$\frac{d^4 A y_2}{dz^4} + [m_0 + a(z - z_1)] = 0 \quad \text{for } z_1 \leq z \leq z_2 \quad \dots (4.19)$$

$$\frac{d^4 A y_3}{dz^4} + r_0 A y_3 = 0 \quad \text{for } z_2 \leq z \leq z_3 \quad \dots (4.20)$$

$$\frac{d^4 A y_4}{dz^4} - [m_0 + a(z - z_1)] = 0 \quad \text{for } z_3 \leq z \leq z_m \quad \dots (4.21)$$

Stage 4:

$$\frac{d^4 A y_1}{dz^4} = 0 \quad \text{for } 0 \leq z \leq z_1 \quad \dots (4.22)$$

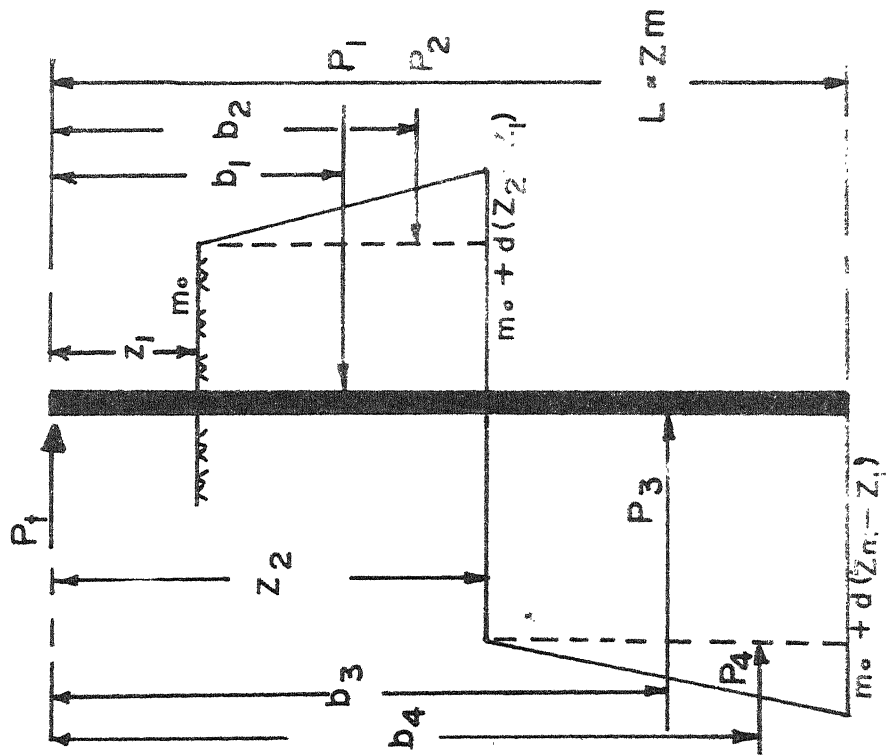
$$\frac{d^4 A y_2}{dz^4} + [m_0 + a(z - z_1)] = 0 \quad \text{for } z_1 \leq z \leq z_2 \quad \dots (4.23)$$

$$\frac{d^4 A y_3}{dz^4} - [m_0 + a(z - z_1)] = 0 \quad \text{for } z_2 \leq z \leq z_m \quad \dots (4.24)$$

The set of equations from (4.13) to (4.24) completely defines all the possible stages of an overhang pile, acted upon by lateral load.

4.5 SOLUTION:

The equations can be solved exactly in the same manner as the free-free or fixed-free pile. The solution



FIG(4.4) PRESSURE DISTRIBUTION FOR ULTIMATE LOAD , OVERHANG PILE

$$b_1 = \frac{\alpha_1 + \alpha_2}{2} Zm$$

$$P_1 = m_0(\alpha_2 - \alpha_1) Zm,$$

$$b_2 = \frac{\alpha_1 + 2\alpha_2}{3} Zm$$

$$P_2 = \frac{d}{2}(\alpha_2 - \alpha_1)^2 Zm,$$

$$P_3 = \left[m_0 + d Zm(\alpha_2 - \alpha_1) \right] (1 - \alpha_2) Zm, \quad b_3 = \frac{1 + \alpha_2}{2} Zm$$

$$b_4 = \frac{2 + \alpha_2}{3} Zm$$

$$P_4 = \frac{d}{2}(1 - \alpha_2)^2 Zm,$$

The method of solution adopted for stage 1 to stage 3 is the same as before. The variables used are $\alpha_1, \alpha_2, \alpha_3, r_0, z_m, m_0$ and d . Different combination of these variables are chosen for both short and long piles and numerical solutions are obtained for the set of simultaneous equations by the method of matrix inversion in the digital computer IMB 7044. Values of deflection, B.M., S.F. and soil pressure are worked out in nondimensional form and are shown in graphs.

SOLUTION FOR STAGE 4:

The solution for stage 4 in the overhung case is carried out in the same manner as that in chapter 3. The soil pressure distribution for this case is shown in fig. 4.4 with the consideration of increasing ultimate strength with depth.

Taking moment of all the forces about the top end of the pile 'O' and equating to zero for limiting equilibrium, can be written as;

$$P_1 b_1 + P_2 b_2 - P_3 b_3 - P_4 b_4 = 0 \quad \dots \quad (4.26)$$

Substituting the expressions for P's and b's from fig. 4.4 and on simplification, the final expression is given by;

$$\frac{4}{3} dz_m \alpha_2^3 + 2 m_0 \alpha_2^2 + \left[\frac{dz_m}{3} \alpha_1^3 - m_0 \alpha_1^2 + dz_m \alpha_1 - \frac{2dz_m}{3} - m_0 \right] = 0 \quad \dots \quad (4.27)$$

Substituting $d=0$ for invariant soil properties with depth, the equation (4.27) simplifies to a form as given below;

$$2\alpha_2^2 - \alpha_1^2 - 1 = 0 \quad \dots (4.28)$$

Solutions for both the cubic and quadratic equation (4.27) and (4.28) respectively for various combination of α_1 , α_2 , Z_m , m_0 , d are worked out and presented in figures.

4.6 DISCUSSION OF RESULTS:

Typical plot of load at top versus deflection at top for overhang piles are plotted for short and long piles separately in fig. (4.5). In fig. (4.5 a), load-deflection curves for varying length of overhang are shown. It is evident from the plots, that, for increasing length of overhang, the load capacity of the pile is decreased. The same information for long piles are shown in fig. (4.5 b). The effect of ' r_0 ' as seen from the plot, is to reduce deflection for the same load. This behavior is valid for both short and long piles. But in both the cases, the ultimate load remains the same for a given length of overhang.

The response of ' m_0 ' is to increase the load-capacity for both long and short piles, as seen from fig. (4.6 a) and (4.6 b). In both the cases, when m_0 is increased from 0.2 to 0.5, the load capacity is increased by 2.5 times. From the figures it is seen that the load capacity increases linearly with the increase in ' m_0 ', which is also evident from the formulation.

The contribution of 'd' on load deflection characteristics are plotted in fig. (4.7) for both short and long piles. As in the case of free-free pile, load at top, the effect of 'd' is to increase the load capacity of the pile to a great extent. This is true for both short and long piles.

The effect of ' r_0 ' along the length of a long or short pile, is to decrease the deflection for increased value of ' r_0 '. This is shown in fig. (4.8 a). The increased value of ' m_0 ', enables a pile to take higher shear, as seen in fig. (4.8 b).

The relation between α_2 and α_3 , for different values of α_1 are plotted in fig. (4.9). From the figure it is seen that, for $\alpha_1=0.1$, the bottom plastic zone (stage 3) starts from the value of $\alpha_2=0.375$. Similarly for $\alpha_1=0.2, 0.3$ and 0.4 , the corresponding values of α_2 are $0.4, 0.44$ and 0.49 , when the bottom plastic zone starts. ' r_0 ' and ' m_0 ' have very insignificant effects on the nature of α_2 .

In fig. (4.10) the variation of deflection, BM, SF and soil pressure along the length of a short pile for different values of α_2 are shown. For a given length of overhang, the load capacity is increased with the increase in α_2 .

Similar plot for long pile is shown in fig.(4.11).

The nature of deflection along the length for different loads for a long pile, is similar to that seen

by Gleser (51) in **actual tests**. The movement of the pile subjected to a given lateral load is an inverse function of the rigidity of the pile. In general the increase in load capacity of the overhang pile, increases by about 10 to 12.5%, when the pile-soil interaction pattern changes from stage 2 to stage 3. This shows, the elasto-plastic analysis results greater load capacity when compared with elastic analysis.

ULTIMATE LOAD FOR OVERHANG PILE:

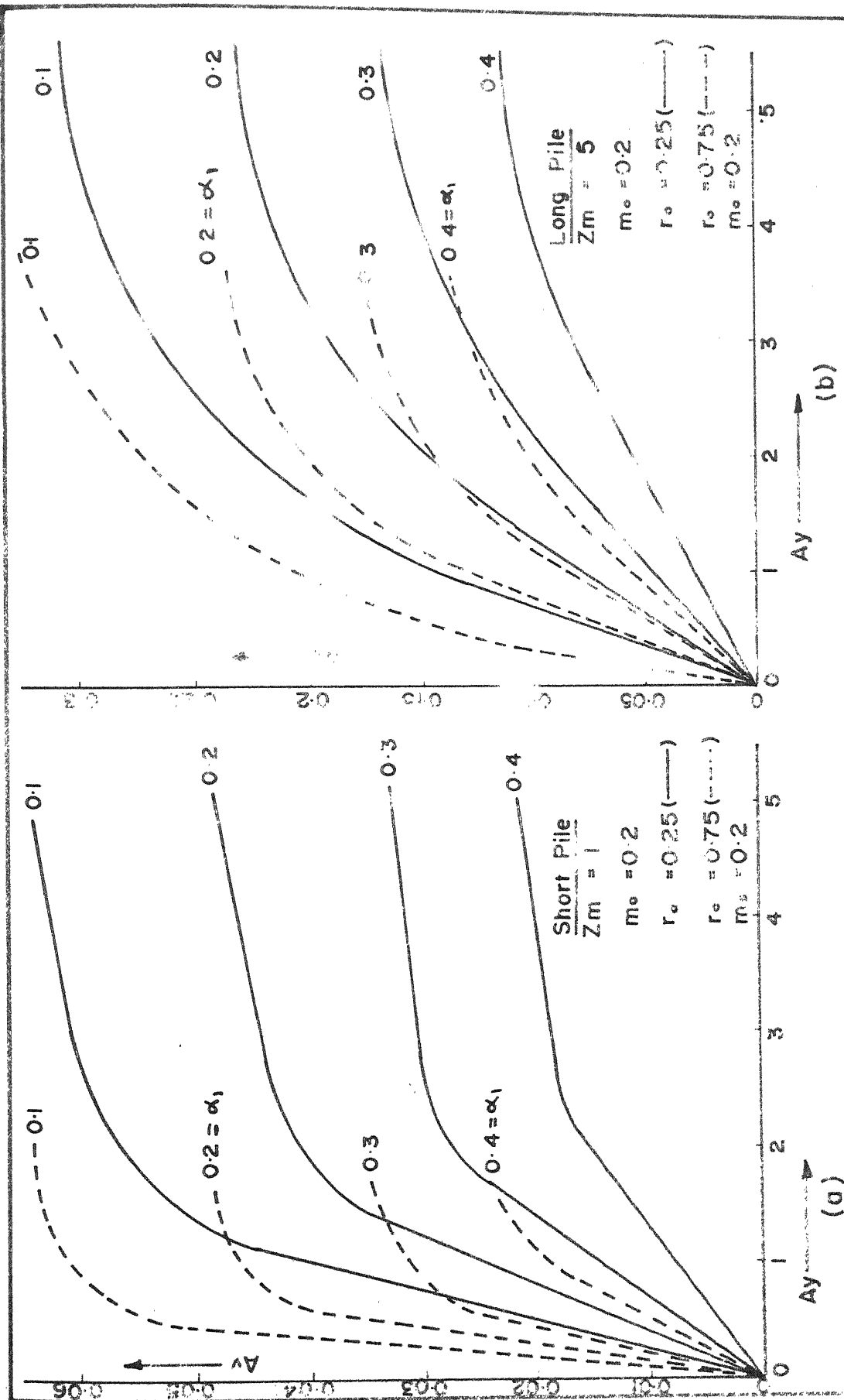
Values of α_2 are plotted against the values of 'd', for $\alpha_1=0.1$, 0.5 and for $m_0=0.2$, and 0.5 in fig. (4.12). For $d=0$, the values of α_2 are given below:

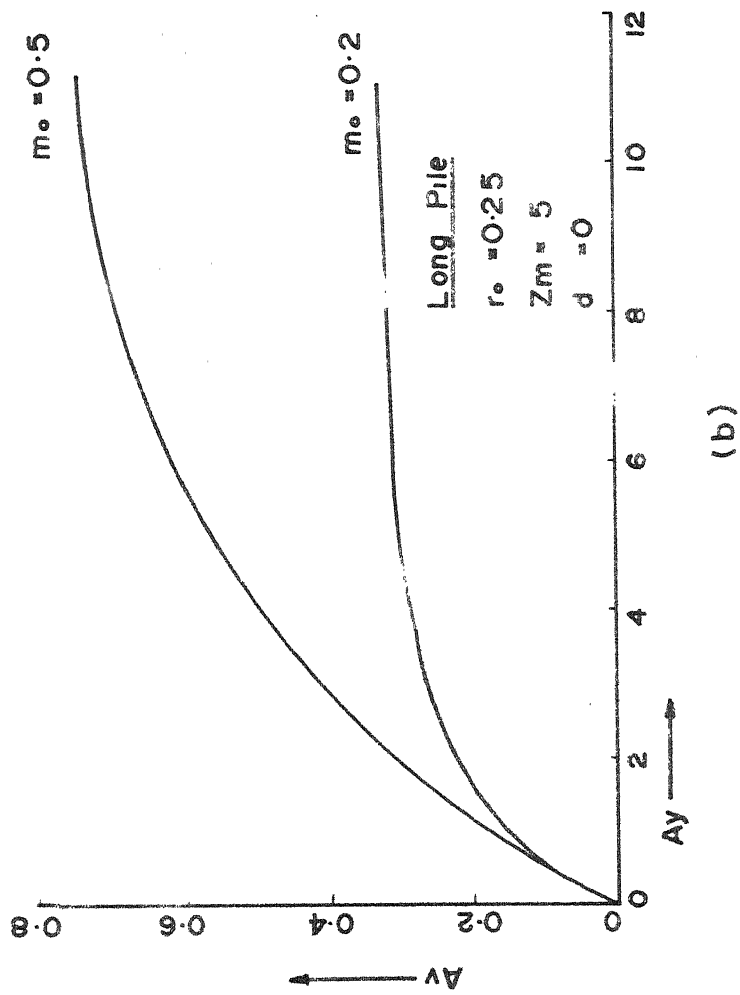
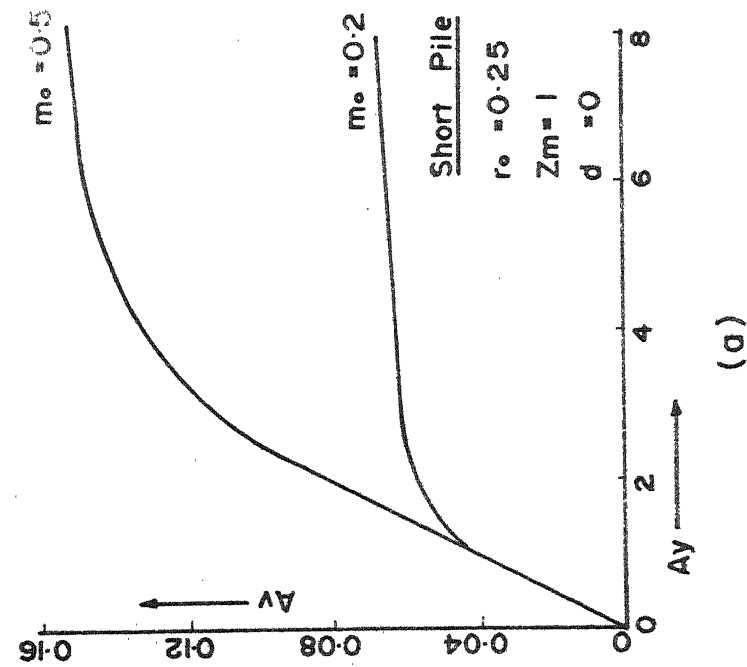
$$\alpha_2 = 0.71 \quad \text{for } \alpha_1 = 0.1$$

$$\alpha_2 = 0.79 \quad \text{for } \alpha_1 = 0.5$$

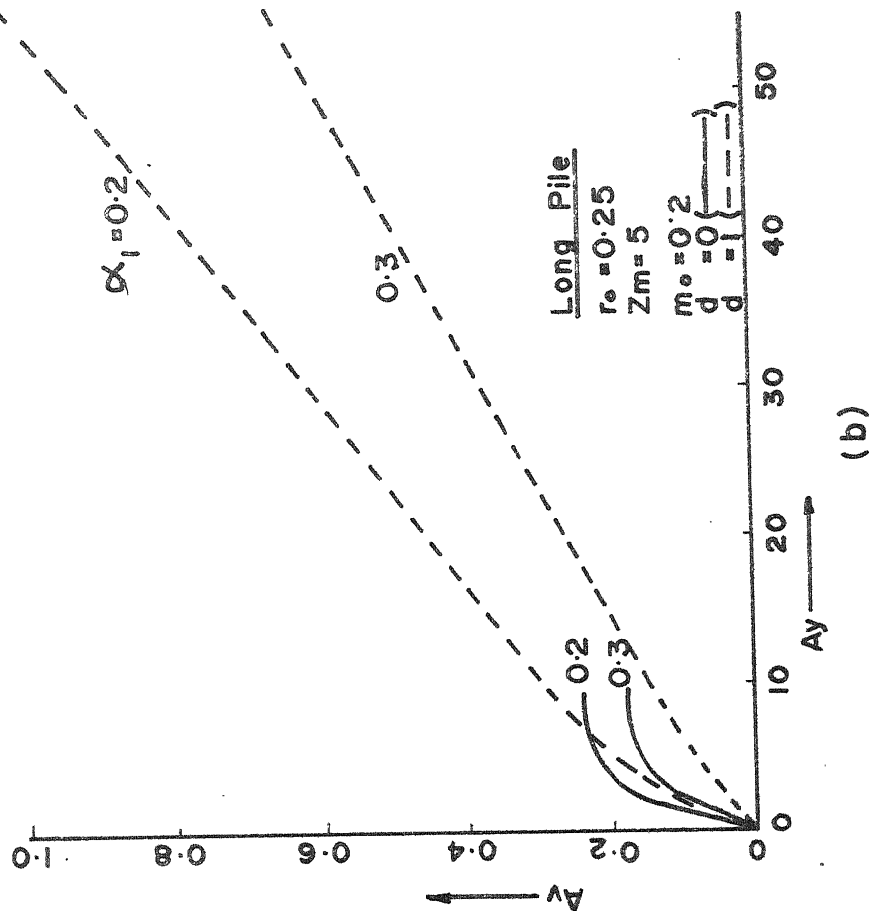
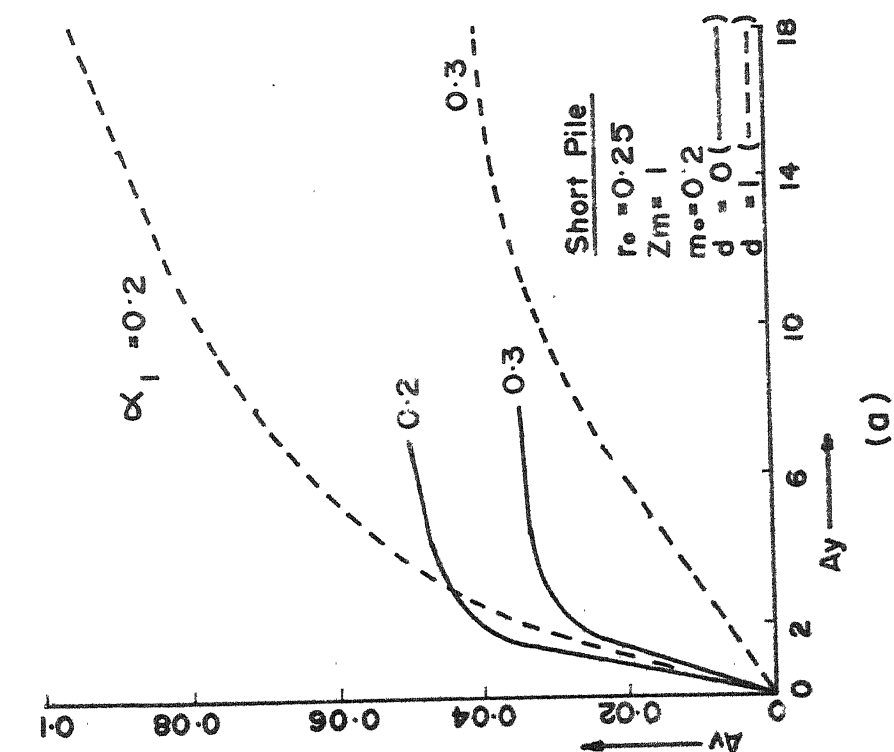
These values of α_2 for the corresponding values of α_1 are also obtained in table (B-1). For increased value of 'm₀' the value of α_2 increase and for decreasing value of α_1 the value of α_2 increases.

Similar nature for long pile is seen in fig.(4.12 b).

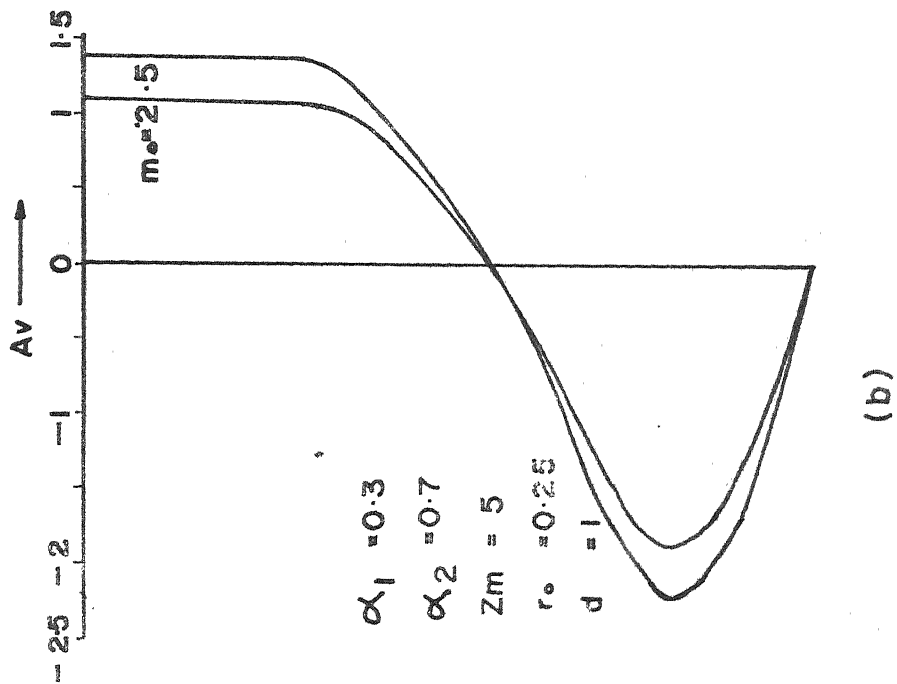
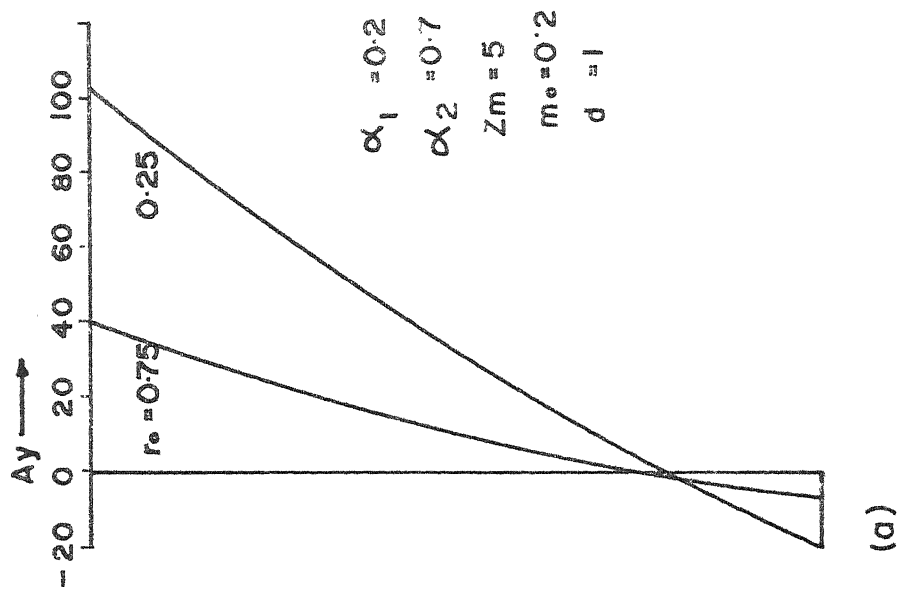
FIG(4.5) EFFECT OF r_0 ON LOAD-DEFLECTION RELATION



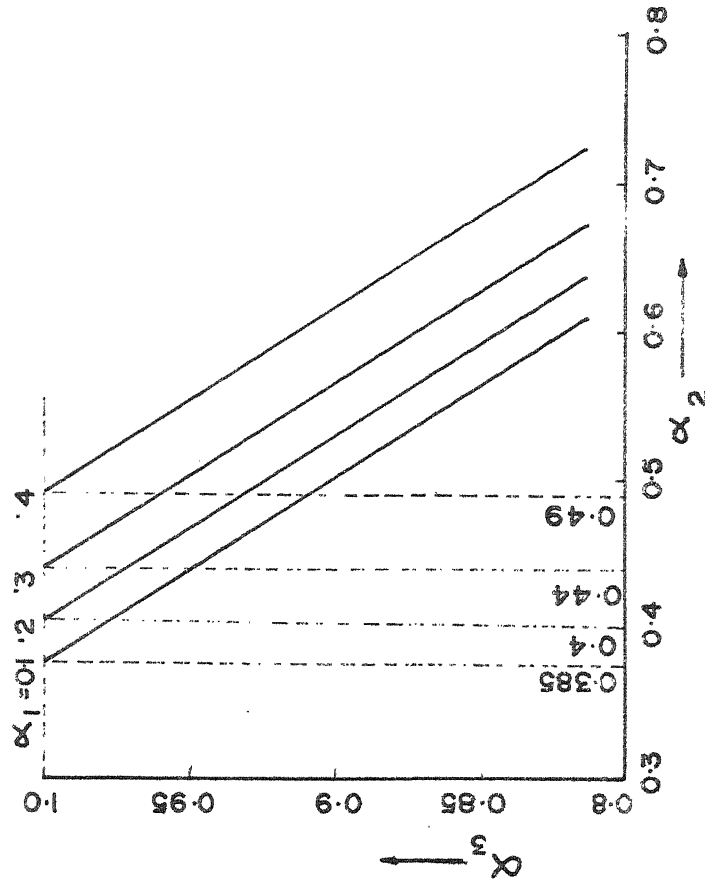
FIG(4.6) EFFECT OF m_o ON LOAD-DEFLECTION RELATION



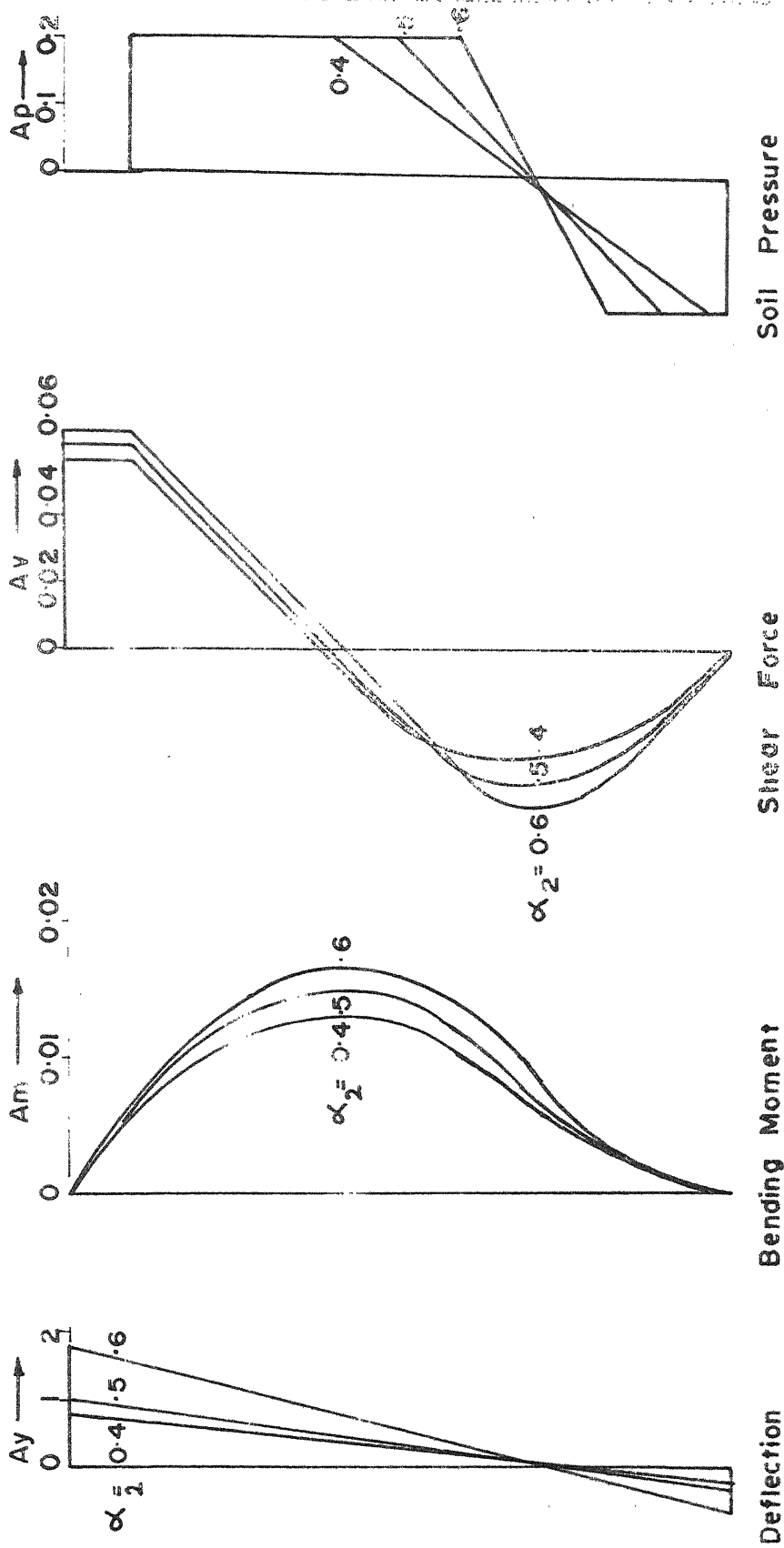
FIG(4.7) EFFECT OF d ON LOAD - DEFLECTION RELATION



FIG(4.8) EFFECT OF r_0 & m_0 ON DEFLECTION AND SHEAR DISTRIBUTION



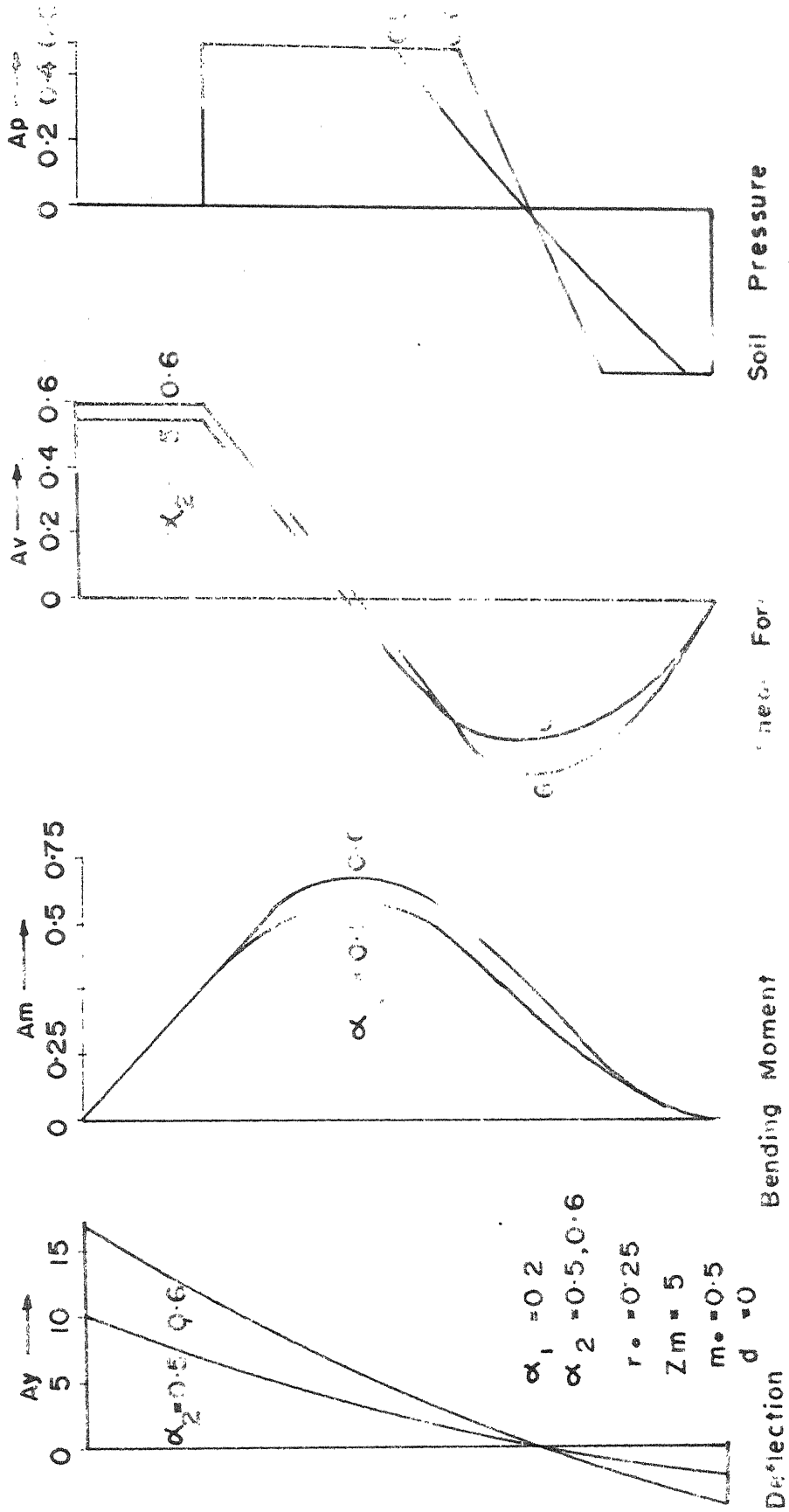
FIG(4.9) VARIATION OF α_3 WITH α_2 FOR DIFFERENT α_1



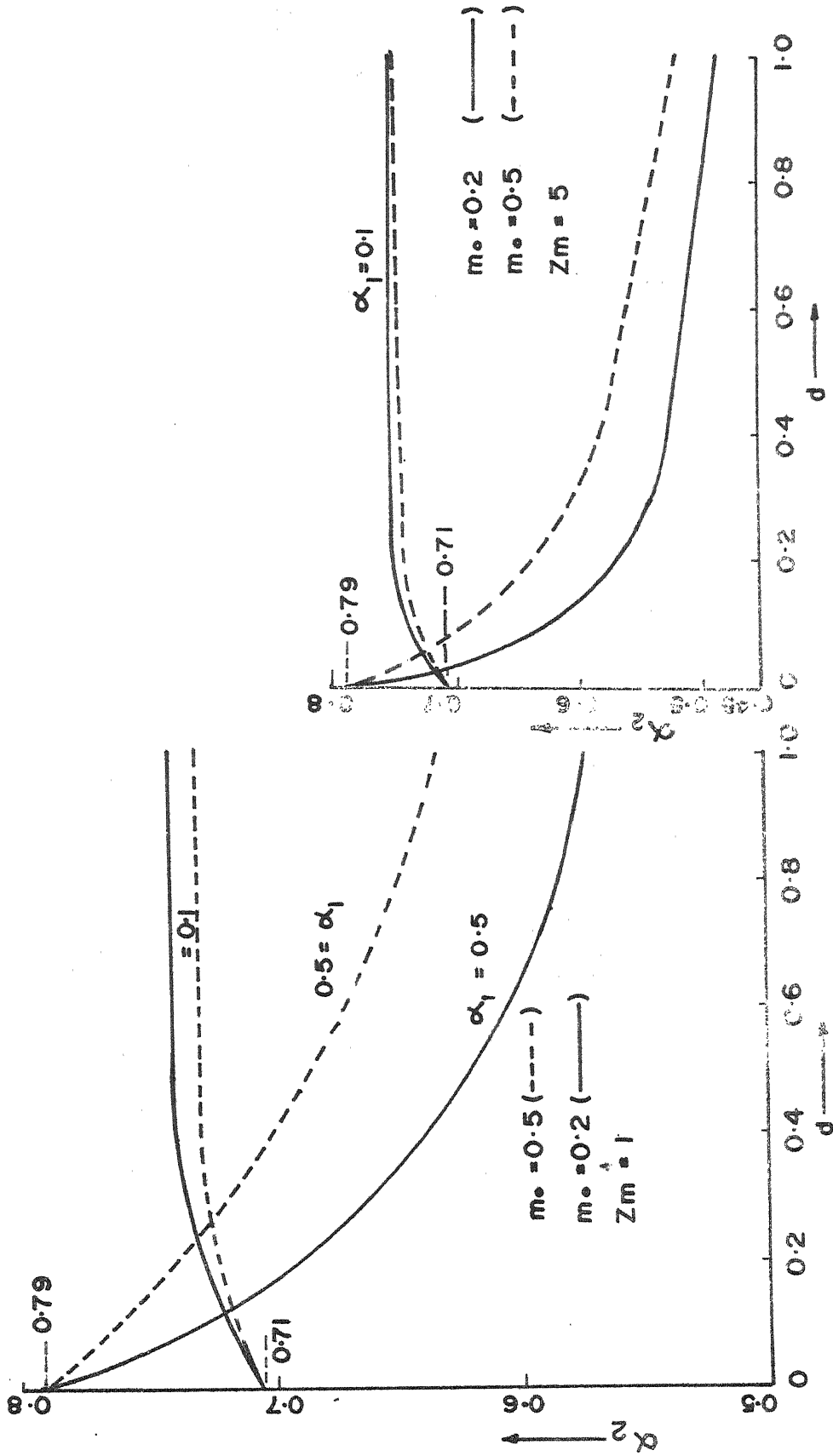
FIG(4-10) VARIATION OF DEFLECTION, B.M., S.F. AND SOIL PRESSURE

WITH α_2

Short Pile



FIG(4-11) VARIATION OF DEFLECTION, B.M., S.F AND SOIL PRESSURE WITH α_2
 Long Pile



(b) Long Pile

(a) Short Pile

FIG(4.12) ULTIMATE LOAD — OVERHANG PILE

CHAPTER V

EXPERIMENTAL VERIFICATION

5.1 INTRODUCTION:

The prime objective of this experimental study is to investigate the static effects on a single model pile embedded in sand. Attempts have been made to compare the pile deflections and moments induced by static loading predicted by the present theory with those observed experimentally.

One characteristic has been common to all the experimental testing conducted to date, namely, static loading and strain or moment measurements. The most common test apparatus employs some device for measuring strains at fixed locations on the pile. Strains are converted to stresses and the distribution of bending moment in the pile as a function of depth is then determined. By integrating the function twice and applying proper boundary conditions, the deflection of the pile at different depths can be determined. Similarly differentiating the function twice the soil pressure distribution can be found out.

In this part only bending moment at few points along the depth and the deflection at the top of the pile are determined for various lateral loads. Accordingly, the test program has been divided in two parts.

5.2 SOIL BEHAVIOR:

The foundation medium chosen is medium fine dry sand. The physical properties of the soil are:

Specific gravity : $G = 2.663$

Void ratio : $e = 0.886$

Bulk density : $\gamma_s = 88 \text{ pcf.}$

Sand passing B.S.S. Sieve No: 14.

To determine the strength parameter (i.e. angle of internal friction ϕ) of the sand direct shear (shear-box) test was run for various normal loads. Shear-box test may not truly represent the behavior of the soil that is acted upon by a laterally loaded pile. However the results of the shear-box test have been assumed to be representative of the soil. It is also assumed in the test that the shear strength of the sand is small at the surface. The shear strength is only due to overburden pressure and the variation assumed is linear.

Shear-box tests are run for various normal loads namely 0.05, 0.1, 0.15, 0.2 and 0.25 TSF. The stress curves are shown in figure 5.1 also the plot between normal and shear stresses is shown in the same figure. The value of ϕ is found to be 28.6° .

The value of constant for variation of shear strength with depth 'd' is determined by the following procedure:

Normal stress due to overburden at a depth $x = \gamma_s x$

For this value of normal stress, the corresponding value of shear-stress is found from the plot of normal stress vs. shear stress from fig. 5.1. The value of shear stress obtained is τ (say). Then the value of 'a' is given by:

$$a = \frac{\tau}{x} \quad \dots \dots (5.1)$$

From actual tests and for the value of $\gamma_s = 88$ pcf, the value of 'a' obtained is 0.03.

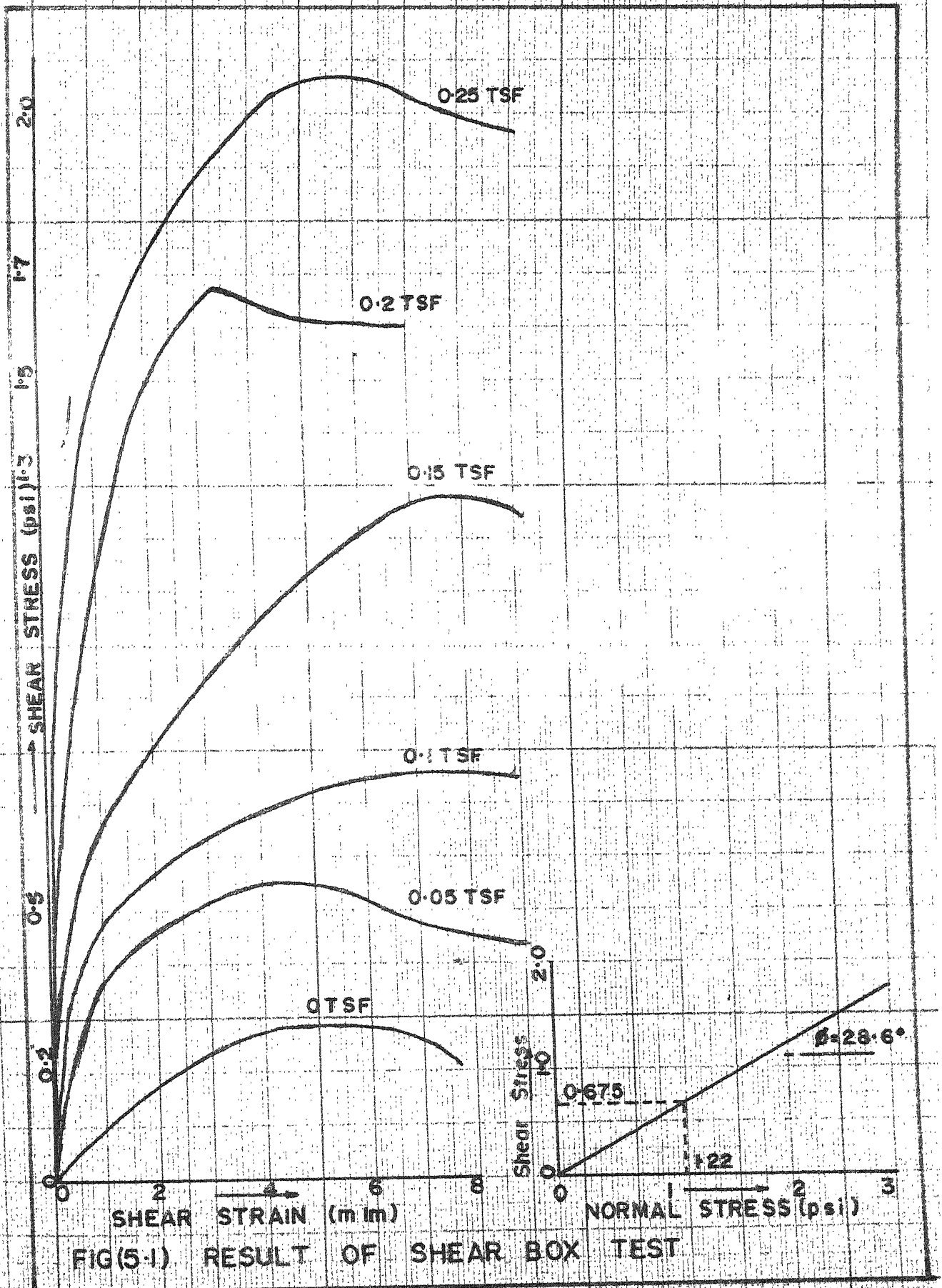
5.3 EXPERIMENTAL SET-UP:

For the purpose of description, the apparatus may be considered as composed of five component parts; the tank, pile, load application device, foundation medium and electronic equipment.

TANK, LOADING DEVICE AND FOUNDATION MEDIUM:

Figure 5.2 shows the tank assembly and also the arrangements for static loading. A circular tank, 3 ft. in diameter and 3 ft. 6 inch. high made of 1/16 inch thick mild-steel plate is chosen for holding the foundation material.

The tank is filled upto the top level with the sand, as described in section 5.2. Filling is done in layers of 8 inches each and each layer tamped with a round bottom $\frac{1}{2}$ inch diameter steel rod for 25 times.



FIG(5-1) RESULT OF SHEAR BOX TEST

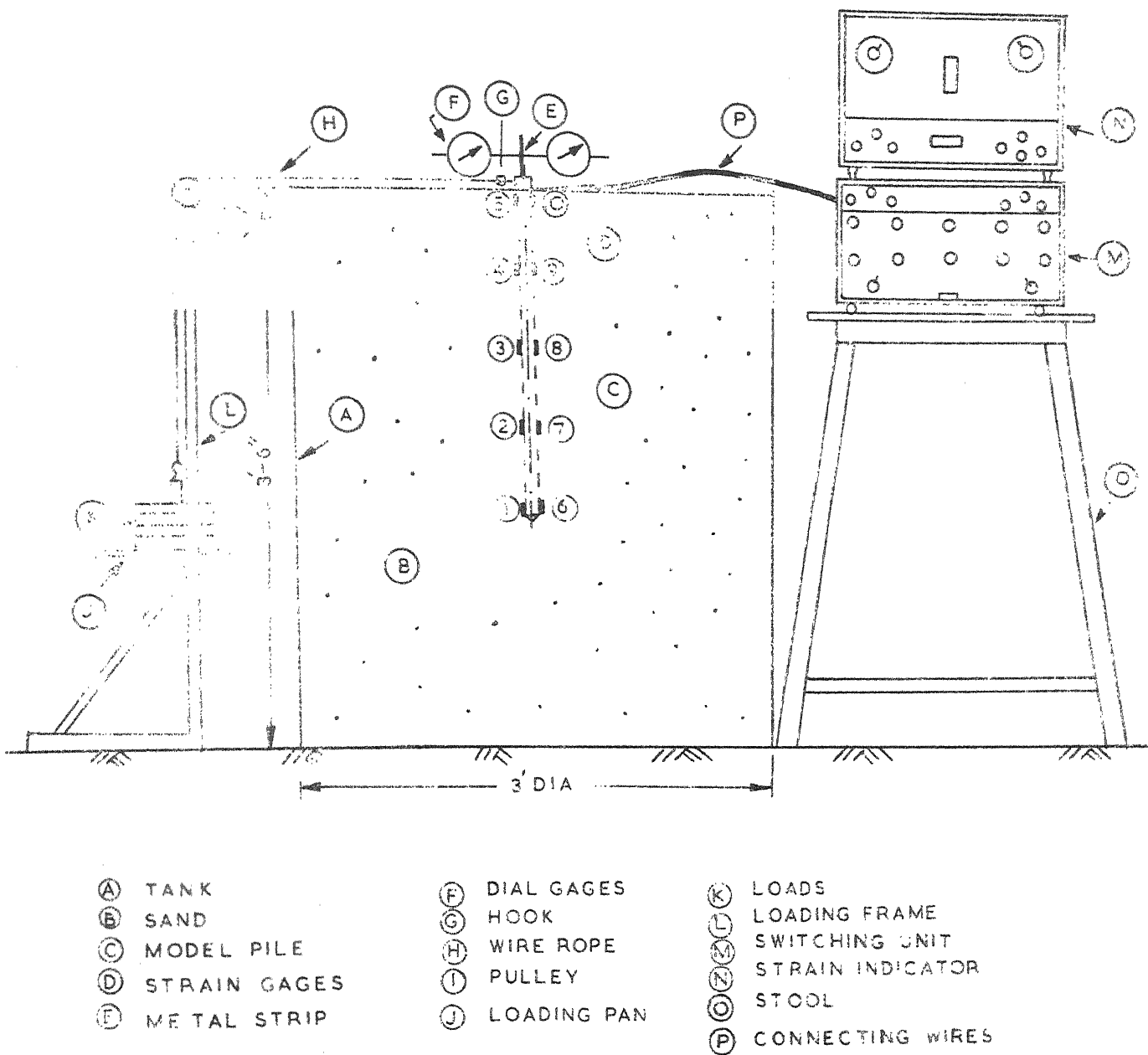


FIG. 5-2 TANK ASSEMBLY AND EXPERIMENTAL SET-UP

The loading device is very simple. The pile head is connected to a nut to which a steel hook is welded. A flexible steel rope is connected to the hook and passes over a frictionless pulley. A loading pan is connected to the other end of the rope. Loads are applied on the pan in stages.

PILE ASSEMBLY:

The tests are run for two separate cases. The tests in which the load vs top deflection for various pile-lengths are determined, simple steel piles of lengths 6, 12, 18, 24 and 30 inches are used.

Pile material : mild-steel round

Diameter = $\frac{1}{2}$ inch.

E = 30×10^6 psi

I = 0.118 cm^4

Bottom of the piles are rounded.

In the other test, in which bending moment at various depths are measured, the pile is made of aluminium. Several features of the model pile are worthy of special note. Aluminium with its lower modulus of elasticity is used in order to allow greater lateral deflections and bending strains at lower applied loads. The specifications for the model pile are as follows:

Aluminium pile = square pile.

Cross-section = 1 cm x 1 cm.

Unit weight = 0.232 kg/metre

Length of the pile = 2'-0"

EI = 24800 lb.in²

Five strain-gage locations are chosen and are shown in figure (5.3 a). Ten strain-gages are placed on opposite faces and are aligned with respect to pile bending axis. Each gage is placed so as to measure the maximum bending strain of the pile. The strain-gage specifications are:

Make: Mahavir Optical and Scientific Works, Roorkee, India.

Type : ET - 5

Gage-factor: 2.02

Resistance : 125 ohms.

To prevent short-circuit and also to avoid the disturbance in the soil, No. 28 gage enamelled copper wire is used for connection. The strain gages placed on the pile are wrapped with cellotape to prevent any disturbance during testing. Switching and balancing unit of BLH make, model no. 225 has been used. The strain indicator used is made of BLH, model 120 (The gages are connected for four-arm bridge).

The combination of switching unit and the strain indicator is capable of recording highly amplified strain variations.

5.4 CALIBRATION OF TEST PILE:

The strainage locations, as stated in the previous section, are used to measure strain due to a calculated amount of bending moment. For this purpose, the pile is placed horizontally on roller supports placed at 20 inch apart like a simply supported beam, and the vertical concentrated load is applied at the centre through a knife edge support. Figure (5.3 b).

The bending moment at any section, x , along the simply supported pile is given by:

$$M_x = \frac{Px}{2} \quad \dots (5.2)$$

In the actual experiment, different loads are applied, the deflections are measured by dial gages and the total strain induced in different gages are noted. Bending moment at different points are calculated from the equation (5.2). The final calibration factor arrived at is 11.5 microinch/inch per ft.lb. Temperature effects are considered while calibrating the pile (Table 5.1).

5.5 DATA COLLECTION:

Only static tests are conducted on the model pile. At zero load, the initial readings of all the strainages are noted. The load increment chosen is 2.5 lbs. After the application of the load on the pan, some time is allowed for the pile to come to a rest position. (When the top and the bottom plastic zones extend to take up the lateral load)

TABLE 5.1
CALIBRATION OF THE TEST PILE FOR MOMENT

Gage Location	x inch	Initial strain	Final Strain	$\Delta \epsilon$	M_i initial	M_f final	ΔM	$\Delta \epsilon / \Delta M$
		P=4.22	P=5.22					
2	4	110	155	45	8.44	12.22	4	11.25
3	10	245	355	110	21.10	31.10	10	11.00
4	16	120	170	50	8.44	12.22	4	12.5
7	4	105	155	50	8.44	12.22	4	12.5
8	10	250	360	110	21.10	31.10	10	11.0
9	16	110	155	45	8.44	12.22	4	11.25
		P=12.22	P=14.22					
2	4	290	335	45	24.44	28.44	4	11.25
3	10	675	780	105	61.10	71.10	10	10.5
4	16	315	365	50	24.44	28.44	4	12.5
7	4	300	345	45	24.44	28.44	4	11.25
8	10	690	800	110	61.10	71.10	10	11.0
9	16	300	345	45	24.44	28.10	4	11.25
		P=24.22	P=27.22					
2	4	555	630	75	48.44	54.44	6	12.5
3	10	1295	1455	160	121.10	136.10	15	10.7
4	16	600	675	75	48.44	54.44	6	12.5
7	4	595	660	65	48.44	54.44	6	10.8
8	10	1350	1510	160	121.10	136.10	15	10.7
9	16	590	665	75	48.44	54.44	6	12.5

Average $\frac{\Delta \epsilon}{\Delta M} = 11.497$

Calibration factor = 11.5 microinch/inch/in.lb.

Then the dial gage and the strainage readings are noted. When the soil starts behaving plastically, it is observed that the sand at top starts heaving on the loading side of the pile. This fact is also recognised by Broms (3), figure (5.4). Loads are increased in steps as stated earlier and continued upto that amount when the unloading is done in steps. The results are shown in graphs.

5.6 DISCUSSION OF RESULTS:

Static load versus top deflection results for different pile lengths are shown in fig. (5.5). It is seen that, the load capacity of a pile increase with increasing pile length, which is predicted by the theory. It is also seen from the figure, that increase in length does not improve the lateral resistance appreciably, provided the pile is sufficiently embeded. The increase in load capacity is only 5 lbs. when the pile length is increased from 2 ft. to 2 ft. 6 inches. This fact has been recognised by Wagner (51) in actual tests. The load-deflection curves assume horizontal shape when the soil reaches its ultimate strength and the soil behaves plastically in this zone.

The percentage recovery of pile deflection, on complete removal of the load, to maximum deflection is also plotted against pile length, in fig. (5.5). It is seen that for small pile-length the recovery is very small and

the rate of recovery increases rapidly with increasing pile length. This behavior is explained by the fact that, in case of small pile-length, the soil behaves plastically for the major portion of pile depth (i.e. the soil approaches stage 4 rapidly). Whereas for large pile length. The soil behavior is mainly of stage 2 or stage 3.

The results of shear-box tests are shown in fig.(5.1) and the value of ϕ obtained is 28.6° .

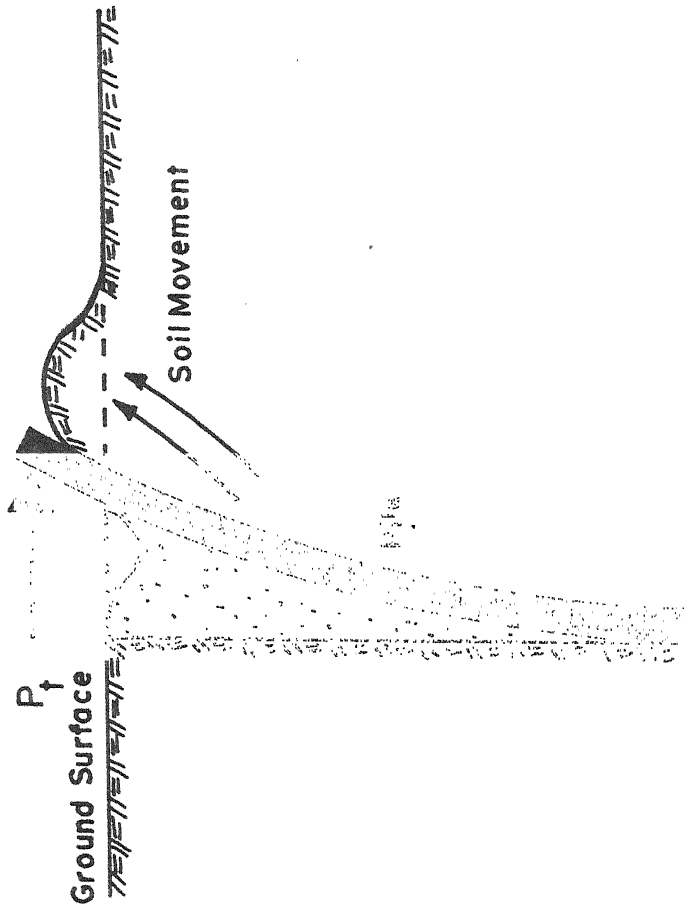
The complete cycle of load-deflection curve is shown in fig. (5.6). The plastic deformation of the pile is seen to be 54.5%. The same pile behavior is also seen by Subrahmanyam (44). In fig. (5.6 b), the load-deflection curve for different dial gage locations are shown for the calibration of the model pile.

Fig. (5.7) shows the bending-moment distribution along the length of the pile for increasing loads. The existence of a small amount of moment at top and bottom is explained by the fact that, the strain gages cannot be fixed at the tip ends of the pile. In actual practice the strain gages are placed at a certain distance from the top and bottom ends, and the small moment is the effect of that variation in length.

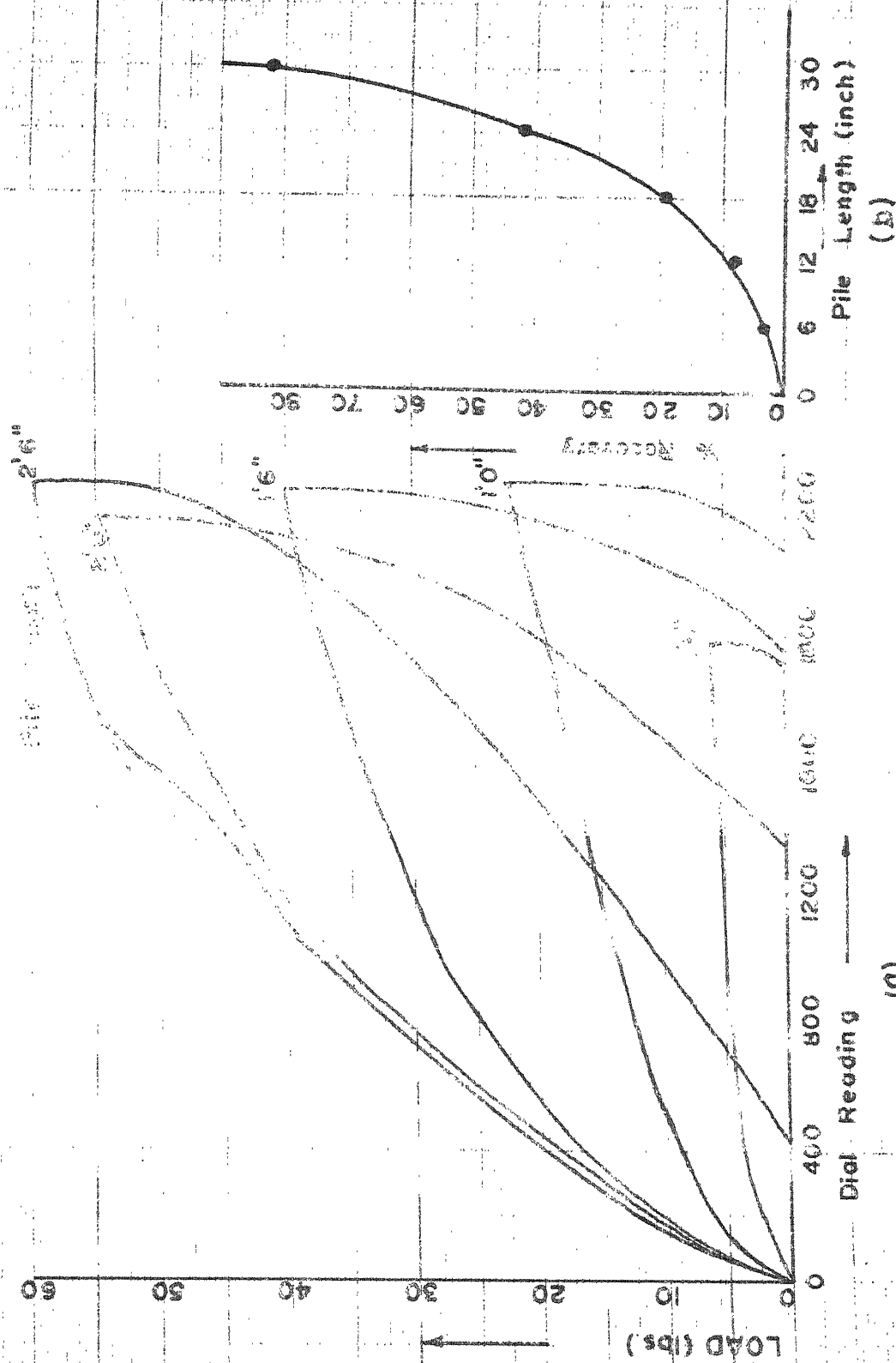
The nature of bending moment distribution is the same as that shown for long free-free pile, load at top. As the value of 'd' is very small, the effect of 'd' on

moment distribution is practically negligible. The point of occurrence of the maximum bending moment is fixed at the same depth for different loads. This behavior is predicted from fig. (3.7). The nature of bending moment distribution is in complete agreement with the theory. Similar pile behavior under static load is also seen in static load test no. 2 by Gaul (13).

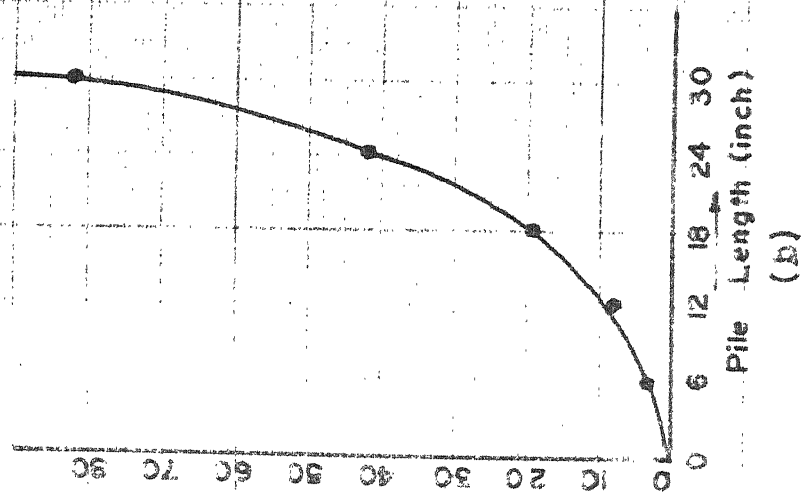
The test suggest that the depth, at which the maximum bending moment occurs is not dependent upon the magnitude of lateral load unless pile deflection becomes large enough to stress the soil beyond its elastic range.



FIG(5.4) SHAPE OF SOIL SURFACE AFTER FAILURE

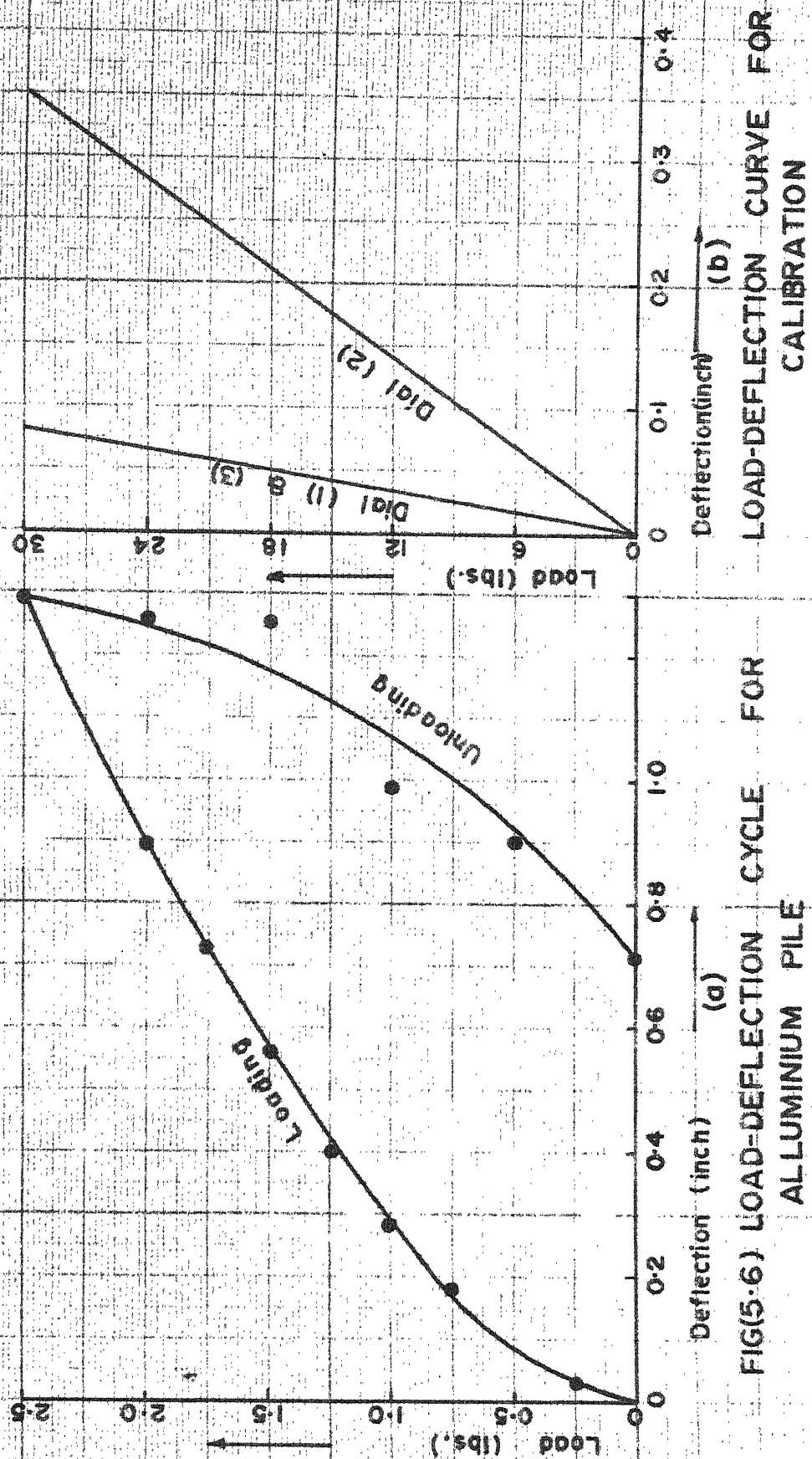


(a)

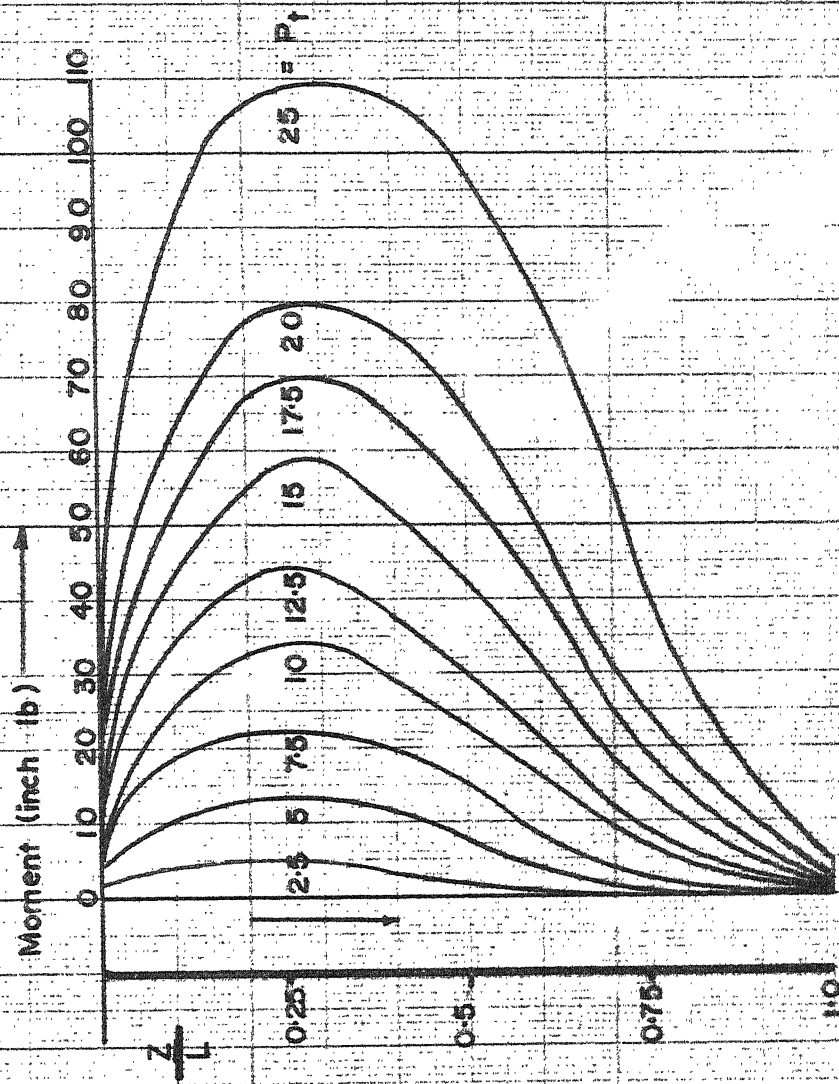


(b)

FIG (5-5) LOAD DEFLECTION RELATION FOR DIFFERENT PILE LENGTHS



FIG(5.6) LOAD-DEFLECTION CYCLE FOR ALUMINUM PILE



FIG(5.7) BENDING MOMENT DISTRIBUTION ALONG THE PILE LENGTH FOR DIFFERENT LOADS

CHAPTER VI

DISCUSSION AND CONCLUSION

The response of a pile to a lateral load is a function of the pile and the soil properties. Between the two, the latter is difficult to consider in design and analysis. A common and much simplified approach has been to ignore the true nonlinear nature of the stress-strain behavior of the soil and to assume it be linearly elastic. This approach leads to the Winkler's model and to the use of the coefficient of horizontal subgrade reaction (k) of the soil. An obvious improvement of this model has been to consider k to increase with depth either linearly or nonlinearly. However, solutions based on this approach do not predict the actual load-deflection response of the pile.

In any design, it is imperative to know the load-deflection response of the pile, so that for an allowable deflection of the top of the pile, the corresponding permissible load can be determined. The main concern of this thesis is the determination of the load-deflection response of the pile. For this purpose, the actual stress-strain behavior of the soil has been idealised by a two-parameter or bilinear relation. The soil is assumed to behave elastically up to a stress level, q_0 , and once the stress equals q_0 , the soil flows plastically. The proposed idealisation is improved by considering the soil-strength to increase with depth.

With this response pattern of the soil, the soil-pile interaction can be seen to consist of four stages. At very small loads, the soil adjacent to the pile will be in the elastic range only. With increasing loads, plastic yield begins at the top and moves down. With farther increase in load, plastic yielding will be initiated at the bottom also and will travel upwards. Accordingly, a model is presented to represent the four stages of pile behavior in elasto-plastic soil. At ultimate load, the pile throws the soil adjacent to it into complete plastic range. These different stages have been expressed mathematically. The governing differential equations, boundary and continuity conditions are nondimensionalised and closed form solutions are obtained. Numerical results are obtained for a range of (i) soil stiffness and strength parameters; (ii) pile lengths and (iii) the constant and linear variation of soil strength with depth.

The load-deflection response of the pile has been predicted to be nonlinear, as is observed in practice. This has been the main contribution of the present investigation. The dependence of the response curve on the soil properties and the pile length is clearly brought out. Higher resistance to deformation is offered by long piles over short piles, by piles in strong soils compared to piles in weak soils, by piles in soil whose strength increases with depth and by pile in stiff soils.

Analysis of piles with overhang in elasto-plastic soils, has also been carried out bringing out the importance of the length of the overhang. The load-deflection characters, predicted by this analysis are similar to those obtained by field tests. The experimental data presented, varifies qualitatively some of the concepts presented in the thesis. The results of the investigation can be made useful to the designer to simplify his task.

Farther work can be carried out on these lines to include variation of the modulus of subgrade reaction with depth and to consider strain hargening of the material.

APPENDIX A

NON-DIMENSIONALISING THE GOVERNING EQUATIONS

The basic differential equations from (2.13) to (2.20), for all the four stages of the pile in action, can be non-dimensionalised in the following procedure. The non-dimensional terms, defined in chapter II, have been used.

As defined in equation (2.21)

$$Z = \frac{x}{T}, \text{ Differentiating with respect to } x,$$

$$\frac{dZ}{dx} = \frac{1}{T} \quad \dots \quad (A-1)$$

$$\frac{dy}{dx} = \frac{dy}{dZ} \cdot \frac{dZ}{dx} = \frac{dy}{dZ} \cdot \frac{1}{T} \quad \dots \quad (A-2)$$

Differentiating (A-2) three times

$$\frac{d^4y}{dx^4} = \frac{d^4y}{dZ^4} \cdot \frac{1}{T^4} \quad \dots \quad (A-3)$$

Also from equation (2.25)

$$y = \frac{P_t T^3}{EI} A_y$$

$$\text{or } \frac{dy}{dx} = \frac{P_t T^3}{EI} \cdot \frac{dA_y}{dx}$$

$$\text{or } \frac{d^4y}{dx^4} = \frac{P_t T^3}{EI} \cdot \frac{d^4A_y}{dx^4} \quad \dots \quad (A-4)$$

Combining (A-3) and (A-4),

$$\frac{d^4y}{dx^4} = \frac{P_t T^3}{EI} \cdot \frac{d^4A_y}{dZ^4} \cdot \frac{1}{T^4} \quad \dots \quad (A-5)$$

Equations (2.13) to (2.20) can be written as follows.

Stage 1:

$$\frac{P_t T^3}{EI} \frac{d^4 A_{y1}}{dz^4} + \frac{1}{T^4} + \frac{k}{EI} \frac{P_t T^3}{EI} A_{y1} = 0 \quad \dots \quad (A-6)$$

or
$$\frac{d^4 A_{y1}}{dz^4} + \frac{kT^4}{EI} A_{y1} = 0$$

denoting
$$\frac{kT^4}{EI} = r_0$$

$$\frac{d^4 A_{y1}}{dz^4} + r_0 A_{y1} = 0 \quad \dots \quad (A-7)$$

Stage 2:

Equation (2.14) can be written as:

$$\frac{P_t T^3}{EI} \frac{d^4 A_{y1}}{dz^4} + \frac{1}{T} + \frac{(q_0 + ax)}{EI} = 0 \quad \dots \quad (A-8)$$

or
$$\frac{d^4 A_{y1}}{dz^4} + \frac{q_0 T}{P_t} + \frac{aT^2}{P_t} = 0 \quad \dots \quad (A-9)$$

denoting
$$\frac{q_0 T}{P_t} = m_0 \text{ and } \frac{aT^2}{P_t} = d,$$

$$\frac{d^4 A_{y1}}{dz^4} + (m_0 + d) = 0 \quad \dots \quad (A-10)$$

For elastic zone in stage 2, the equation (2.15) can be written in the same manner for stage 1 as:

$$\frac{d^4 A_{y2}}{dz^4} + r_0 A_{y2} = 0 \quad \dots \quad (A-11)$$

In this way, all the equations for stage 3 and stage 4 can be non-dimensionalised and the final forms are the same as given in equations (2.29) to (2.36).

APPENDIX B

DIRECT APPROACH TO DETERMINE THE ULTIMATE LOAD CAPACITY

The ultimate load capacity of a pile is reached when the soil reaches the ultimate strength for the whole length of the pile. This stage is described by two plastic soil zones in stage 4 in Chapter II.

FREE-FREE PILE: LOAD AT TOP.

Considering linear increase in ultimate strength of soil with depth, the complete soil pressure distribution is shown in fig. 2.7. The trapezoidal plastic zone is divided into a rectangular and a triangular zone. Total pressure applied by the rectangular zones are denoted by P_1 and P_3 and that applied by triangular portions are represented by P_2 and P_4 respectively. The lever arms are denoted by b_1 , b_2 , b_3 , and b_4 corresponding to the resultant reactions P_1 , P_2 , P_3 , P_4 .

For equilibrium of the pile under the load ' P_t ' and the soil pressure distribution, moment of all the forces about the top of the pile is zero.

$$P_1 b_1 + P_2 b_2 - P_3 b_3 - P_4 b_4 = 0 \quad \dots (B-1)$$

Substituting the expressions for P & b , the expression is given as follows:

$$\frac{m_0 z_1^2}{2} + \frac{a z_1^3}{3} - \frac{m_0 + d z_1}{2} (z_m^2 - z_1^2) - \frac{a}{6} (z_m - z_1)^2 (2 z_m + z_1) \dots (B-2)$$

Substituting $\alpha_1 Z_m$ for Z_1 the final form is given by:

$$2d Z_m \alpha_1^3 + 3 m_0 \alpha_1^2 - \left(\frac{3}{2} m_0 + d Z_m\right) = 0 \quad \dots (B-3)$$

In the case, when the effect of overburden on the strength of soil is neglected, 'd' is made equal to zero in (B-3) and the expression is simplified and α_1 reaches a constant value $\alpha_1 = \frac{1}{\sqrt{2}}$.

This value of α_1 is also reached from the analysis of stage 3. In the actual procedure, the value of ' α_1 ' is gradually increased and the corresponding value of ' γ ' is iterated. It is seen that, with the increase of ' α_1 ', the value of ' γ ' approaches ' α_1 ' and finally for $\alpha_1 = 0.707$, value of ' γ ' equals α_1 . This aspect is discussed and shown in graph in section 3.2 for free-free pile.

OVERHANG PILE:

The soil-pile interaction for an overhang pile is the same as for the free-free pile in stage 4. To determine the ultimate capacity of an overhang pile the same procedure is applied.

Expressions for the total soil pressure and the lever arms for different zones are shown in fig. 4.4. Taking moment of all the resultant forces about the top end of the pile, and equating to zero for limiting equilibrium the expression can be written as:

$$P_1 b_1 + P_2 b_2 - P_3 b_3 - P_4 b_4 = 0 \quad \dots (B-4)$$

Substituting the values for P and b in (B-4) and denoting,

$$Z_1 = \alpha_1 Z_m \quad \text{and} \quad Z_2 = \alpha_2 Z_m$$

the expression (B-4) takes the following form

$$m_0 (\alpha_2^2 - \alpha_1^2) + d (\alpha_2 - \alpha_1)^2 (\alpha_1 + 2\alpha_2) \frac{Z_m}{3} =$$

$$\left[m_0 + d Z_m (\alpha_2 - \alpha_1) \right] (1 - \alpha_2^2) + d (1 - \alpha_2)^2 \frac{2 + \alpha_2}{3} Z_m \quad \dots (B-5)$$

on simplification, the final expression is:

$$\frac{4}{3} d Z_m \alpha_2^3 + 2 m \alpha_2^2 + \left[\frac{d Z_m}{3} \alpha_1^3 - m_0 \alpha_1^2 + d Z_m \alpha_1 - \frac{2 d Z_m}{3} - m_0 \right] = 0 \quad \dots (B-6)$$

Substituting $d=0$ in (B-6)

$$\alpha_2 = \sqrt{\frac{\alpha_1^2 + 1}{2}} \quad \dots \quad (B-7)$$

For different values of α_1 , the corresponding values of α_2 are given in table (B-1).

TABLE B-1
VALUES OF α_2 FOR α_1 ($d=0$)

$\alpha_1 = 0.0$	0.1	0.2	0.3	0.4	0.5	0.6	0.7	0.8	0.9	1.0
$\alpha_2 = 0.707$	0.71	0.72	0.737	0.761	0.79	0.825	0.863	0.905	0.95	1.0

These values are plotted and shown in graph in Chapter IV.

For $\alpha_1 = 0$, the overhanging pile transforms to the free-free pile, load at top on substituting $\alpha_1 = 0$, in (B-7) the value of α_2 is found to be $\frac{1}{\sqrt{2}}$, same as free-free pile.

REFERENCES

1. Aschenbrenner, R., "Three Dimensional Analysis of Pile Foundations," ASCE, Structural Div., Feb., 1967.
2. Bergfelt, A., "The Axial and Lateral Load Bearing Capacity and Failure by Buckling of Piles in Soft Clay," Proc. 4th Int. Conf. SMFE, Vol. 2, London, England, 1957, pp.8-13.
3. Broms, B.B., "Lateral Resistance of Piles in Cohesive Soils," Jr. SMFE, ASCE, March, 64, pp. 27-64.
4. Broms, B.B., "Lateral Resistance of Piles in Cohesionless Soils," Jr. SMFE, May 1964, SM 3, pp. 123-156.
5. Broms, B.B., "Design of Laterally Loaded Piles," Jr. SMFE, May, 1965, pp. 79-100.
6. Chang, Y.L., et. al., Discussion of "Lateral Pile Loading Tests," by Lawrence, B. Feagin, Trans, ASCE, Vol. 102, 1937, pp. 272-278.
7. Chang, Y.L., et. al., Discussion of "Lateral Pile Loading Tests," by Lawrence, B. Feagin, Trans. ASCE, Vol. 102, 1937, pp. 272-278.
8. Davisson, M.T. and Gill, H.L., "Laterally Loaded Piles in a Layered Soil System", Jr. of SMFE, ASCE, SM-3, Vol. 89, May, 1963, pp. 63-94.
9. Davisson, M.T., and Robinson, K.E., "Bending and Buckling of Partially Embedded Piles," Proc. 6th Int. Conf. on SMFE, Vol. II, Toronto, Canada, 1965, (243-246).
10. Debeer, E., "Computation of Beams Resting on Soils", Proc. 2nd. Int. Conf. on SMFE, Vol. I, 1948, Rotterdam, Holland, pp. 119, 121.
11. Focht, T.A. and McClelland, B., "Soil Modulus for Laterally Loaded Piles," Trans. ASCE, 1958, Vol. 123, pp. 1049-1063.
12. Feagin, L.B., "Lateral Pile Loading Tests," Trans. ASCE, Vol. 102, 1937.
13. Gaul, R.D., "Model Study of a Dynamically Loaded Pile," J. SMFD, ASCE, Vol. 84, No. SM 1, Proc. Paper, 1535, Feb, 1958.
14. Hayashi, S. and Miyajima, N., "Dynamic Lateral Load Tests on Steel H-Piles," Proc. Japan National Symposium on Earthquake Engineering, Tokyo, Japan, 1962.

15. Hayashi, "Horizontal Resistance of Steel Piles Under Static and Dynamic Loads," Proc. 3rd, WCFE, 1967.
16. Hetenyi, M., "Beams on Elastic Foundations," University of Michigan Press, Ann. Arbour, Mich. Oxford Univ. Press, London, England, 1946.
17. Hrennikoff, A., "Analysis of Pile Foundations with Batter Piles," Trans. ASCE, Vol. 115, 1950, pp. 351-382.
18. Juhe, Heing, G., "Loads on Vertical Pile Groups," Jr. of Structural Division, ASCE, Vol. 92, No. ST 2, Proc., Paper, 4774, April, 1966, pp. 103-114.
19. Kazarnovskii, V.S. and Fadeer, G.P., "Investigation of the Bearing Capacity of Horizontally Loaded Piles in Slump Type Soils," Soil Mechanics and Foundation Engineering (Translated from Russian), No. 3, May-June, 1969.
20. Klohmn, E.J., and Hughes, G.T., "Buckling of Long Unsupported Timber Piles," Jr. SMFE, ASCE, Vol. 90, No. SM 6, Proc. paper 4141, Nov. 64, pp. 107-123.
21. Kondner, R.L., "Hyperbolic Stress-Strain Response: Cohesive Soils," Jr. ASCE, SM 1, Vol. 89, Feb. 1963, pp. 115-143.
22. Kubo, K., "Experimental Study on the Lateral Resistance of Piles," monthly, reports of TTRI, No. 6 July 1961 (Part I), Vol. 11, No. 12, January, 1962 (Part III), Vol. 11, No. 12, Feb. 1962.
23. Kubo, K., "Experimental Study of the Behavior of Laterally Loaded Piles," Proc. 6th Int. Conf. on SMFE, Vol. 2, Div. 4/11, Sept. 1965, pp. 275.
24. Madhaavan, K., "Studies on Laterally Loaded Piles", M.Tech. Thesis Submitted to the Dept. of Civil Engg., IIT, Kanpur, August, 1969.
25. Matlock, H. and Reese, L.C., "Foundation Analysis of off-shore Pile Supported Structure," Proc. 5th Int. Conf. on SMFE, Paris, 1961, Vol. 2, pp. 91-97.
26. Matlock, Hudson and Reese, L.C., "Generalised Solution for Laterally Loaded Piles," Jr. SMFE, ASCE, Vol. 127, No. SM 5, Part I, Oct. 1962, pp. 63-91.
27. Matlock, H. and Grubbs, B.R., Discussion of "Lateral Resistance of Piles in Cohesive Soils," by B.B. Broms, (March, 64, Proc. Paper 3825), ASCE, Jr. SMFE, January 1965, pp. 183-188.

28. McNulty, J.F., "Thrust Loading on Piles," Jr. SMFE, ASCE, Vol. 82, No. SM 2, Proc. Paper 940, April, 1956, pp. 25.
29. Mc. Cammon, G.A., and Ascherman, J.C., "Resistance of Long Hollow Piles to Applied Lateral Loads," Symposium on Lateral Load Test on Piles, ASTM, STP No. 154, July, 1953, pp. 3-9.
30. Newmark, N.M., "Numerical Procedures for Computing Deflections, Moments, and Buckling Loads," Trans. ASCE, Vol. 108, 1943, pp. 1161-1188.
31. Palmer, L.A. and Thompson, J.B., "The Earth Pressure and Deflection Along the Embedded Length of Piles Subjected to Lateral Thrust," Proc. 2nd. Int. Conf. on SMFE, Vo. V, Article VII, b-3, pp. 156-161.
32. Peck, R.B. and Ireland, H.O., "Full Scale Lateral Load Test of a Retaining Wall Foundation," 5th Int. Conf. on SMFE, Paris, France, Vol. II, 1961, pp. 453-458.
33. Prakash, S. and Agarwal, S.L., "Study of a Vertical Pile Under Dynamic Lateral Loads," Proc. 3rd. World Conf. on Earth Quake Engineering, Vol. I, 1965, page, I-215 - I-229.
34. Prakash, S., "Behavior of Pile-Groups Subjected to Lateral Loads," Thesis Submitted in the Univ. of Illinois, in 1962, for Ph.D.
35. Reese, L.C., Discussion of "Soil Modulus for Laterally Loaded Piles," by B. McClelland and J.A. Bocht, Trans. ASCE, Vol. 123, 1958, pp. 1071-1074.
36. Reeves, H.W., "Model Tests on Lateral Bending on Free Head Piles," M.S. Thesis, Rice Institute Houston, Sept. 1955.
37. Roscol, K.H., "A Comparison of Tied and Free Pier Foundation," Proc. 4th Int. Conf. on SMFE, Vo. -I, 1957, pp. 419-423.
38. Rowe, P.W., "The Single Pile Subjected to Horizontal Force," Geotechnique, Inst. of Civil Engineers, Vol. 6, No. 2, London, June, 1956, pp. 70-75.
39. Saul, W.E., "Static and Dynamic Analysis of Pile Foundations Proc. ASCE, Structural Div., Vol. 94, No. ST 5, May 1968, pp. 1077-1100.

40. Shinohara, T. and Kubo, K., "Experimental Study on the Lateral Resistance of Piles (Part I)," Monthly Reports of Transportation Technical Research Institute, Vol. 11, No. 6, July 1961.
41. Siva Reddy, A. and Valsangkar, A.J., "An Analytical Solution for Laterally Loaded piles with Polynomial Variation of Soil Modulus," Indian Concrete Journal, March 1966, pp 91-94.
42. Siva Reddy, A. and Valsangkar, A.J., "Flexural Behavior of Axially and Laterally Loaded Piles," Jr. of the Institution of Engineers (India), Vol 49, No. 7, Part C1 4, March 1969 pp 277-283.
43. Snitko, A.N., "Design of Flexible Supports Embedment in Soil with Variable Sub-grade Co-efficient," Soil Mech. & Found. Engg., (Translated from Russian) No. 3, May-June, 1968. pp 156-158.
44. Subrahmanyam, G., "Resistance of Piles to Lateral Loads," Jr. of the Institution of Engineers (India), Vol 47, Nos. 1&3, Sept. & Nov., 1966, pp 99-110.
45. Teng, W.C., "Foundation Design," Prentice Hall of India (P) Ltd. New Delhi, 1962.
46. Terzaghi, K., "Evaluation of Co-efficient of Sub-grade Reaction, Geotechnique, London, England, Vol. V, 1955, pp 297-326.
47. Timoshenko, S., "Strength of Materials," Part II, D. Van Nostrand Company, Inc., Affiliated East West Press Pvt. Ltd., New Delhi 1953, pp 1-4.
48. Vesic, A.B., "Beams on Elastic Sub-grade and the Winkler's Hypothesis," Proc. 5th Int. Conf. on SMFE, Paris, 1961, Vol. I, pp 845-950.
49. Vesic, A.B., "Bending of Beams Resting on Isotropic Elastic Solid," Jr. of Eng. Mech. Div., ASCE, Vol. 87, No. EM 2, Proc. Paper 2800, April, 1961, pp 35-53.
50. Wiegel, R.L., et al, "Ocean - Wave Forces on Circular Cylindrical Piles," Trans. ASCE, Vol. 124, 1959, pp 89-113.
51. "Symposium on Lateral Load Tests on Piles," ASTM, STP -154, July, 1953.
52. "Supplement to Symposium on Lateral Load Tests on Piles," ASTM, STP No. 154 A, June 1954.